Genetic and phenotypic analysis of complex seed and root traits in oilseed rape (*Brassica napus* L.)

Aysha Kiran

INAUGURAL-DISSERTATION zur Erlangung des **Doktorgrades (Dr. rer. nat.)**

der Naturwissenschaftlichen Fakultät der Justus-Liebig-Universität Giessen

édition scientifique
VVB LAUFERSWEILER VERLAG

1. Auflage 2014

1st Edition 2014

Printed in Germany

édition scientifique
VVB LAUFERSWEILER VERLAG

STAUFENBERGRING 15, D-35396 GIESSEN
Tel: 0641-5599888 Fax: 0641-5599890
email: redaktion@doktorverlag.de

www.doktorverlag.de

Genetic and phenotypic analysis of complex seed and root traits in oilseed rape (*Brassica napus* L.)

INAUGURAL-DISSERTATION
zur Erlangung des Doktorgrades
(Dr. rer. nat.)
der Naturwissenschaftlichen Fakultät
der Justus-Liebig-Universität Giessen

durchgeführt am

Institut für Pflanzenbau und Pflanzenzüchtung I
Professur für Pflanzenzüchtung

vorgelegt von

Aysha Kiran

(M.phil. Biotechnology)

Multan, Pakistan

Gießen 2014

Tag der Disputation: 15. 12. 2014

Dekan FB 09: Prof. Dr. Peter Kämpfer

Gutachter: Prof. Dr. Volker Wissemann
Gutachter: Prof. Dr. Dr. h.c. Wolfgang Friedt

DEDICATED

To my loving parents

who polish my abilities and

from whom I learn A to Z

and

to my husband and sweet sons for their eternal support

List of abbreviations and symbols

AGI	Arabidopsis Genome Initiative,
ANOVA	Analysis of variance
BAT	Bile acid:sodium symporter family protein
BCAT	branched-chain aminotransferase
CAD	Cinnamyl alcohol dehydrogenase
CCR	Cinnamoyl-CoA reductase
CCoAOMT	Caffeoyl CoA 3-O-methyltransferase
CHO	Carbohydrate
CIM	Composite interval mapping
C4H	Cinnamate 4-hydroxylase,
4CL	4-coumarate:CoA ligase
COMT	Caffeic acid/5-hydroxyferulic acid O-methyltransferase
cM	centiMorgan
dap	Days after pollination
DAS	Days after sowing
DGE	Digital gene expression
DH	Doubled haploid
ESP	Epithiospecifier protein
F5H	Ferulate 5-hydroxylase
GLM	General linear model
GSL	Glucosinolates
GWAS	Genome wide association studies
LD	Linkage disequilibrium
LOD	Logarithm of the odds
LRD	Lateral root density
LRL	Lateral root length
LRN	Lateral root number
MAM	methylthioalkyl malate synthase
MLM	Mixed linear model
MUFA	Mono-unsaturated fatty acids

MyAP	Myrosinase associated protein
OSR	Oilseed rape
PAL	Phenylalanine ammonia lyase
PCA	Principle component analysis
PRL	Primary root length
QTL	Quantitative trail loci
r^2	Squared allele frequency correlations
RAD	Restriction site–associated DNA
RNA	Ribonucleic acid
RoG	Primary root rate of growth
RSA	Root system architecture
SNP	Single nucleotide polymorphism
SSR	Simple sequence repeat
TGG	Thioglucoside glucohydrolase
TASSEL	Trait Analysis by Association, Evolution and Linkage
UGs	Unigenes

INTRODUCTION

1.1 *Brassica napus*

Brassica species such as *B. napus* belong to the Brassicaceae (Cruciferae) or mustard family. They play a significant role in world agri- and horticulture due to their economical value as important edible and industrial oilseed, vegetables, condiments and fodder crops. After a wide range adaptations many species have been domesticated as crops, such as oilseed rape/canola and swede (*B. napus*); cabbage, cauliflower, broccoli, Brussels sprouts (*B. oleracea*); Chinese cabbage, *pak choi*, turnip rape (*B. rapa*) and mustards (*B. nigra, B. juncea, B. carinata*). Brassica crops thus make an enormous contribution to public health and economics throughout the world. To ensure the continuity of these benefits, sustained improvement of yield and quality is vital.

The model plant *Arabidopsis thaliana* also belongs to this family and due to this close phylogenetic relationship its thoroughly explored genome information is also advantageous for genetic studies in *Brassica* species. The relationship among the six most important *Brassica* species has also presented a model for understanding the evolutionary processes in polyploidization events at a genomic level (Koch and Kiefer, 2006; Lagercrantz and Lydiate, 1996; Chalhoub et al, 2014)

This “Brassica Triangle” (Fig. 1.1) described by the Korean scientist Nagahara U (1935) demonstrates that three allopolyploid Brassica species *B. napus*, *B. juncea* and *B. carinata* originated from interspecific hybridisations between the three diploid ancestors *B. nigra, B. rapa* and *B. oleracea* (Hong et al., 2008; Snowdon, 2007). *B. napus* originated through spontaneous hybridization between *B. rapa* and *B. oleracea*, resulting in an amphidiploid genome with the full set of chromosomes from its progenitors (Kimber and McGregor 1995; Snowdon et al., 2002). The species *B. napus* is relatively new, having arisen through anthropogenic influence only in the past 500 to 2000 years in the Mediterranean region of south-western Europe. The species is divided into two subspecies, namely *B. napus* ssp. *napobrassica* (swedes) and *B. napus* ssp. napus, which includes spring and winter oilseed, vegetable and fodder. The vegetable forms include the distinct leaf rapes which are used as common winter-annual vegetables (Friedt et al., 2007). Oilseed rape cultivars are grouped into winter and spring types based on their genetic control of vernalization to induce flowering.

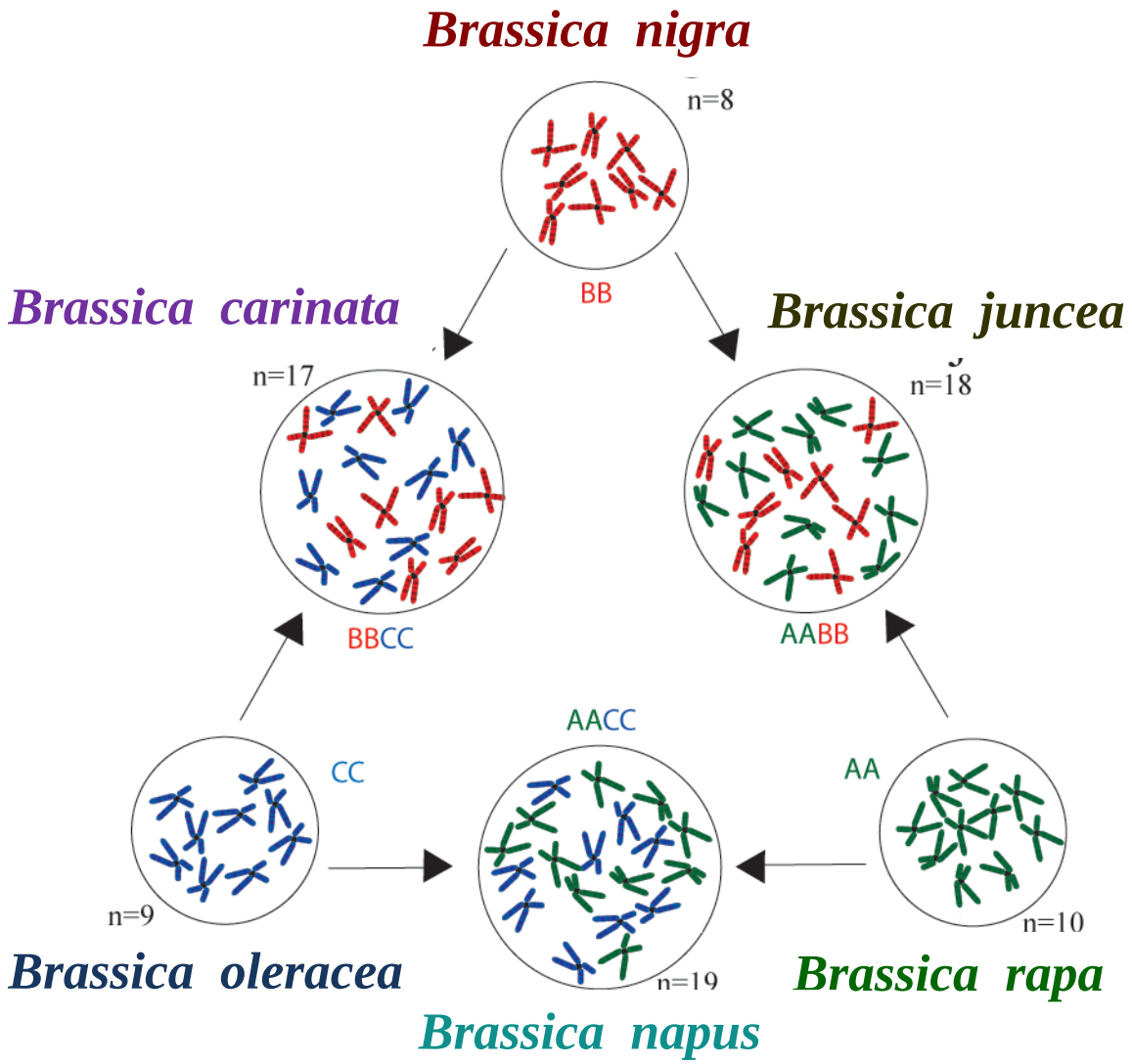

Fig.1.1 The Brassica triangle of Nagahara U (U. Nagahara, 1935) showing genome relationships among cultivated Brassica species. Genomes are represented by the letters A, B, C. n = haploid chromosome numbers. (http://en.wikipedia.org/wiki/Triangle_of_U)

Winter cultivars are predominantly cultivated in Europe and Asia respectively, while spring types are more suitable for the climatic conditions of Canada, Australia, and Northern or Eastern Europe (Friedt and Snowdon, 2009). Winter varieties have a long period of development and seed yield is almost double as compared to spring types, therefore more profitable in the areas where they survive the winter season (Butruille et al., 1999; Ghasemi-Golezani et al., 2011).

1.1.1 Economical importance

Rapeseed/canola (*B. napus* L.) is cultivated all over the world for vegetable oil production. The European Union, China, Canada and Australia are the leading producers. Oilseed rape is the second most important oilseed crop in the world after soybean and a very significant source of vegetable oil in Europe (data from FAOstat: http://faostat.fao.org/). About 40 to 45% oil can be extracted from seeds of modern varieties. Some varieties of rapeseed (high erucic acid rapeseed, HEAR) also provide a raw material for lubricants, hydraulic oils, tensides for detergent and soap production, biodegradable plastics and many other products (Friedt and Snowdon, 2009).

Being an important source of vegetable oil for human nutrition, oilseed rape is a key source of healthy high-calorie mono-unsaturated fatty acids (MUFA) like oleic acid (18:1). These fats constitute about 61% of total fats and help to increase high-density lipoprotein (HDL; so-called "good cholesterol") and reduce low-density lipoprotein (LDL; "bad cholesterol") in the blood. It is comparable to olive oil regarding lower concentrations of saturated fats. It is considered as one of the healthiest cooking oils, even better than olive oil, due to presence of essential fatty acids, α-linolenic acid (omega-3) and linoleic (omega-6) at a better ratio. To fulfill the demand of biodiesel, manufacturers of biodiesel for powering motor vehicles have great demand for rapeseed oil. In Germany biodiesel is mixed with standard diesel in ratios from around 5% to 10%. Rapeseed oil is the favored oil for biodiesel production in most of Europe, because of higher production of oil per unit land as compared to other oil sources, such as soybeans (Cardone et al., 2002).

The first byproduct of oil extraction is the rapeseed cake, which is processed through solvent extraction into rapeseed meal composed of 38-44% protein with a good combination of amino acids. On average, rapeseed meal contains on an as-fed basis (90% dry matter) 10-12% crude fibre, 36-38% crude protein, 1-2% lipids (oil), 6-8% ash, 1.2% total phosphorus and less than 1% calcium. Composition varies widely depending on factors such as origin, growing conditions, the manufacturing process and degree of oil extraction. Primarily, it is used to feed dairy cows due to high fat content which enhances milk production, and because ruminants are insensitive to glucosinolates and especially phenolic fibre compounds in the meal. Poultry, aquaculture and field animals like racehorses can also be fed on rapeseed meal as a protein source. For monogastric animals such as pigs and poultry, however, some anti-nutritive factors particularly glucosinolates, high amount of fibre compounds, phenolic acids,

phytate and low palatability reduce the rapeseed meal ratio that can be used in feed formulations. The glucosinolates have received an extensive attention, because they are very unpalatable and reduce the feed intake and depresses animal performance. High concentrations of glucosinolates act as an inhibitor of the thyroid gland. Rapeseed meal is also relatively high in fibre content, including on average 14.5% cellulose, 5.0% hemi-cellulose and 8.3% of lignin. The amount of protein and energy in canola meal is therefore diluted due to increased fibre component (Enami and Safafar, 2011; Friedman, 1996; Mwachireya et al., 1999). On the other hand, the genetic diversity of *Brassica* crops for beneficial metabolites can also be utilized to maximize the benefits from recent advances in genomics. For effective crop-based studies it is essential to navigate between trait and gene, therefore it is important to integrate information from agronomy, genetics and genomics, breeding, etc. It is a vital key to provide a practical understanding of relevant systems to fortify future crop and its product development within sustainable-ecological framework (http://www.brassica.info/).

1.1.2 Breeding and selection for improved seed quality and seedling development

After its origination by inter-specific hybridization oilseed rape achieved economic importance only in recent decades following an intensive breeding program to improve the oil quality by decreasing nutritionally unwanted components. Initially breeders were focused to reduce erucic acid (22:1, *cis* 13-docosenoic acid) contents in the seed oil and aliphatic glucosinolates to make the meal safer and palatable as livestock feed. Introduction of erucic acid-free ("0-rapeseed") cultivars was a first breakthrough reducing the erucic acid level in the seed oil to less than 1% from natural levels as high as 50% or more (Stefansson and Hougen 1964). The first erucic acid-free variety, derived from a spontaneous mutation of the German spring rapeseed cultivar 'Liho', was released in Canada in early 1970s. However the crop value was still suppressed due to presence of high levels of glucosinolates in the seed. The release of toxic by-products by the digestion of glucosinolates can cause kidney and liver damage along with lymph dysfunction in monogastric animals. The Polish spring rape variety 'Bronowski' was discovered in 1969 to have a low glucosinolate level in seed. It was then used as a base for an international backcrossing program to incorporate this trait into high-yielding erucic acid-free material. In 1974 first "00-rapeseed" variety, 'Tower', was developed with zero erucic acid and low glucosinolate content (Stefansson 1983; Downey

and Röbbelen 1989; Downey 1990). This was the beginning of the advancement of one of the most important oil crops in temperate regions, also named as canola.

Intensive breeding and bottleneck selection of rapeseed for low erucic acid and low glucosinolate content has narrowed down the genetic pool in 00-rapeseed breeding material (Friedt and Snowdon, 2009; Hasan et al., 2006). Today the majority of modern winter and spring oilseed rape varieties have 00 seed quality. However, it is still believed that the residual segments of the "Bronowski" spring genotype reduce yield, winter hardiness, and oil content in newly developed cultivars (Sharpe and Lydiate, 2003). Furthermore, the restricted genetic variability in modern oilseed rape is particularly important regarding the development of genetically diverse heterotic pools of adapted genotypes for hybrid breeding.

Availability of genetic diversity and genetic variation is the heart of any breeding program and plays a critical role in developing well-adapted and improved varieties (Emrani et al., 2011). On the other hand, oilseed rape varieties with high erucic acid, glucosinolates and also high fibre content can provide genetically diverse material for potential breeding programs for heterotic improvement of hybrid varieties, in addition with improved pathogen and pest resistance. Breeding programs are aiming to improve yield, quality and crop pests as important target. Whilst successful, the collateral effect of these improvements has been the production of elite varieties that possess only a fraction of the genetic diversity available in the wider *Brassica* gene pools. It is causing lack of resistance in the crop to various kinds of pests. New alleles have to be transferred into elite breeding lines for sustainable high yield, new disease resistant loci have to be identified for functional and adaptive diseases and improved oil qualities for a variety of industrial and nutritional applications (Allender and King, 2010; Hasan et al., 2006).

1.1.3 Potential importance of root architecture traits

Plant nutrient uptake and water use efficiency are highly dependent on root growth and architecture. Variation in root architecture is essential for the adaptation of plants to target environments since it determines their efficiency in acquiring soil resources. Various crop species and cultivars have different kinds of root systems and different capacities to penetrate into deeper soil layers in search of nutrients and water (Peltonen-Sainio et al., 2011). Nevertheless, soil physical conditions and agricultural management practices can also

influence plant performance, mainly by influencing root depth. The root system of oilseed rape is extremely plastic in both vertical and horizontal distribution depending on water supply (Wang et al., 2009). Some *Brassica* species have demonstrated their potential to reach deep soil layers at the depth to 2.4 m due to their specific taproot system (Thorup-Kristensen, 2006; Lisson et al., 2007). However soil compaction has shown a great impact on the root system of rapeseed (Blake et al., 2006). Measurement of root traits in crop breeding material is complicated and expensive, because mostly it involves a combination of field, laboratory-based screens and glasshouse studies (Clark et al., 2011). High-throughput screens are required to identify germplasm with altered root growth, morphology, root responses to stress and other root architectural traits. Using such techniques to analyse genetic diversity, for example in genome-wide association studies, it might be possible to breed new varieties with improved root phenotypes using genetic loci associated with root architecture traits (Shi et al., 2012).

1.2 High throughput genotyping technologies

Recent scientific discoveries that resulted from the application of ultra-fast DNA sequencing technologies are beginning to revolutionise the fields of polymorphism discovery, genome analysis and molecular breeding (Liu et al., 2012a). New methods finely tuned the resolution of a variety of DNA preparation protocols to single base precision and expanded them to a genome-wide scale. Next-generation-sequencing (NGS) has surprising potential for these technologies to bring massive change in biological and genetic research specifically, and contributes to our important basic biological knowledge quality (Jain, 2012).

Now, that access to genotype information is more or less unlimited due to the power of NGS technologies, the main challenge faced by plant breeders and geneticists today is the understanding of the link between phenotypic variations and the underlying DNA variation. NGS has increased the possibilities by providing high-resolution genetic characterization of crop germplasm through genome-wide assays of allelic variation. Genome-wide analyses of RNA sequences and their quantitative and qualitative measurements have made it possible to look into the complex nature of regulatory networks. Many molecular markers have been originally suggested for the comprehensive analysis of the human genome with respect to the identification of loci which affect the inherited traits quantitatively (Frazer et al., 2007). On the other hand there is a growing gap between our ability to generate genotype data and our

ability to assay phenotype variation for complex traits, especially traits which have strong genotype-environment interactions.

1.2.1 Genome-wide SNP arrays

The NGS technologies have enhanced their quality enormously in the past decade and have made discovery of single-nucleotide polymorphisms (SNP) possible even in complex genomes (Kumar et al., 2012). These are single nucleotide variations between the DNA sequences of individuals in a specific population. Transversions (C/G, A/T, C/A and T/G), transitions (C/T or G/A) and insertions/deletions are three categories of SNPs. Although tri-allelic and tetra-allelic SNPs also exist however most of the SNPs are bi-allelic. SNPs are considered as one of the most suitable markers for the fine mapping of inherited or heritable traits (Chagné et al., 2007). There is a great potential for tremendously fine genetic mapping by SNPs, which are the abundant form of DNA polymorphism. This offers the opportunity to develop haplotypes based on gametic phase disequilibrium for analyses of quantitative traits and unveil allelic variation directly in the sequences of candidate genes.

SNPs have the potential to act as an excellent tool for measurement of heritability, good indicator of genetic diversity and phylogeny in crop species such as *B. napus*. Studies have shown that *B. napus* has a SNP every 600 base pairs of the genome on average (Edwards et al., 2007; Fourmann et al., 2002). Given the ~ 1.2 Gb size of the *B. napus* genome, this would equate to ~ 2 million SNPs. This allows for the construction of high-density genetic maps which can provide a scaffold to map undesirable, as well as agronomically important genetic traits (Duran et al., 2010; Edwards and Batley, 2010). There is great potential to exploit the marker-trait association approaches through SNP markers, and historical recombination is advantageous for population-level surveys to identify trait–marker relationships based on linkage disequilibrium. Thus it has become a preferred genetic approach for many organisms (Cardon and Bell, 2001; Flint-Garcia et al., 2003).

Trick et al. (2009) investigated SNPs in the transcriptome of *B. napus* juvenile leaves by bulk sequencing and approx. 95K putative SNPs were detected between the cultivars. The polyploid nature of *B. napus* genome interferes with both SNP discovery and high throughput SNP marker assay technologies. Most of the detected polymorphisms (87–91%) were

indicative of transcription from homoeologous genes from the two parental genomes within oilseed rape (Trick et al., 2009).

1.2.2 Digital gene expression (DGE) profiling

Digital gene expression profiling by sequenced based methodologies is a superior option to hybridization based methods. The first reported sequencing-based high-throughput methods for gene expression profiling were serial analysis of gene expression (SAGE) (Velculescu et al., 1995) and massively parallel signature sequencing (MPSS) (Brenner et al., 2000). NGS technologies have become a better choice for global gene expression analysis due to their exceptional sensitivity and throughput. Messenger RNA sequencing (e.g. RNAseq) can provide an absolute measurement of gene expression which gives better quantitative and qualitative understanding and precision than the use of microarrays ('t Hoen et al., 2008; Marioni et al., 2008; Ozsolak and Milos, 2011). In combination with suitable bioinformatics tools, RNAseq offers a better methodology to study gene expression dynamics in different biological and cellular frameworks. While profiling gene expression using RNAseq, it is assumed that the depth of coverage of a sequence is proportional to the expression of corresponding gene of interest. In contrast to whole-transcriptome RNAseq approaches, which profile the whole transcriptome but are not always highly quantitative, the use of 3' expressed sequence tag-based digital gene expression (DGE) can accurately quantify gene expression levels even for low-abundance transcripts and provide extremely cost-effective data for differential expression studies (t Hoen et al., 2008; Eveland et al., 2008).

Millions of short sequence tags can be generated by immensely parallel DGE approaches which facilitate a reliable and economical coverage of the transcriptome. However, the short length of the sequence reads (17–36 bases) provides a limited capability for explicit gene assignment, specifically if the genome sequence information is fragmented. Similarly, matching transcripts are hard to detect with short-sequence reads, even if the genome is fully sequenced. Studies from massively parallel sequencing libraries of Arabidopsis and rice have shown that approximately 11% of signature sequences matched multiple target sites in the genome (Nobuta et al., 2007). Nevertheless, the capacity of these massively parallel sequencing approaches to generate millions of short sequence tags can enable reliable, cost-effective coverage of the transcriptome.

Functional diversity within species is linked by differential expression of related, duplicated genes, and furthermore sub-functionalization presents a base for genome evolution. Moreover transcriptome profiling can compare the expression quantitatively to address various questions in functional genomics. The expression of newly identified genes and related transcripts were distinguished in maize by using high-throughput sequencing combined with specificity of 3´-UTRs (Eveland et al., 2008). DGE provides opportunity for gene discovery and clarification of the variations in expression underlying natural variation.

1.2.3 Investigation of genes involved in specific biochemical pathways

High throughput sequencing of tissue-specific transcriptomes from different plants can facilitate the detection of differentially expressed genes in specific metabolic pathways. Expression studies based on cDNA sequencing appears as an extensive reservoir for cloning of candidate genes from explored metabolic pathways, annotation of genomic sequences, the evaluation of tissue-specific gene expression and markers for map-based cloning (White et al., 2000a)

A careful bio-informatics analysis to identify tissue-specific ESTs is a prerequisite to obtain a comprehensive and representative set of cDNAs for gene expression studies. Seed metabolism was studied in Arabidopsis by cloning and sequencing of ESTs encoding seed metabolic enzymes involved in carbohydrate metabolism and fatty acid synthesis. Patterns of expression might reflect the existence of metabolic regulators and groups of genes which are coordinately expressed (White et al., 2000a).

Differentially expressed genes in spring rapeseed were observed by (Dong et al., 2004) at 15 days after flowering (DAF) and 25 DAF, and genes responsible for cell proliferation were observed to be more active during 10-20 DAF. Obermeier et al. (2009) used the LongSAGE technology to study differentially expressed genes in winter *B. napus* genotypes, and 3,094 genes were detected at two time-points of seed development, 23 days and 35 days after pollination (DAP). A shift of gene expression regarding developmental processes from cell proliferation and seed coat formation at 23 DAP to more activity towards seed storage protein at 35 DAP was observed. Detailed studies of regulatory networks, carbohydrate metabolism and fatty acid synthesis in developing seeds of *B. napus* revealed conserved lipid metabolism pathway when compared to the Arabidopsis gene expression patterns (Niu et al., 2009b). Genetic analysis of plant developmental traits has been practically expanded for

characterization and identification of candidate genes, however, knowledge about the behavior of genes, genomics and associated metabolism is still limited due to the amphidiploid nature of *Brassica napus* L.

1.3 Complex trait analysis: Genetic analysis of roots

Genetic variation for complex traits determines fitness in natural environments, as well as the productivity of the crops that sustain all human populations (Mackay et al., 2009). Genetic makeup of crops responsible for this variation as well as the evolutionary factors that maintain quantitative variation in populations were investigated by mapping and cloning of quantitative trait loci (QTLs) to identify the genes. Central to our understanding is to elucidate the genetic architecture of complex traits, which incorporates both the magnitude and the frequency of QTL alleles in a population. Complex-trait analysis in plants is scrutinized by two approaches which both allow QTL identification in samples containing diverse genotypes (Mitchell-Olds, 2010). Conventionally, family-based QTL mapping can be applied to complex pedigrees from crosses among different founding genotypes. Recently, population-based approaches such as genome-wide association studies (GWAS) use populations of unrelated individuals to examine genome-wide associations between single nucleotide polymorphisms (SNPs) and phenotypes. The complex plant root system is greatly influenced by intrinsic developmental and environmental-response pathways.

The major challenge for plant sciences is to help feeding the ever increasing population of the world. Better understanding of root architectural system can confront it under global climatic changes. High population pressure to grow high yielding varieties in exhaustive cropping systems and biotic and abiotic stresses suppress crop yields in many parts of the world, especially developing countries. A number of models predict the continuous increase in these stresses in the future; therefore sustainable and economically viable agricultural developments are required to fulfill the food requirements in a developing world. Improving the root architecture system by identifying the potential genes underlying root characteristics may have great significance for agriculture and food security. The genetic basis of root architecture system can be better understood by 1) cost effective methods for non-invasive imaging of root growth, 2), describing the complex spatial root architectural systems, and 3) understanding and optimizing root physiology adequately.

1.3.1 Root system architecture (RSA)

In a biological sense the term “architecture” indicates the spatial configuration of complex assembled subunits having some functional importance, whereby the term “root architecture” has been used in many perspectives to mention different aspects of the shape of root systems. Uneven distribution of nutrient resources in soil and the limited depletion zone of plants indicate the importance of root architectural systems in crop productivity for exploiting these potential resources. For example, very low mobility of P in the soil retains it in zones of only a few millimeters for many years, so that spatial deployment of the root system required exploiting those resources. Very strong gradients in temperature, oxygen status, water availability, pH, bulk density, and nutrient status commonly occur with soil depth over a scale of centimeters (Lynch, 1995).

Soil exploration for nutrients and its acquisition is determined by root architecture. Genetic variation in root architectural traits is very important for acquisition and uptake of many important nutrients such as P and K. Primary root length, adventitious-root development, basal-root gravitropism, and lateral root length and numbers enhance the ability of plants for topsoil scavenging for a number of elements essential for plant growth and crop productivity. Rhizospheric alterations are critical for nutrient mobility in the soil. Efflux of root exudates such as protons and organic acids are important for rhizospheric modification. There is a great genetic variation for rhizospheric modifications. Ion transporters may contribute in the acquisition of nitrate and improved salt tolerance. Many of these traits are under complex genetic control and genetic variation in these traits is linked with significant yield gains in low-fertility soils. It will be much more productive to breed crops for infertile soils and selection for specific root traits through direct phenotypic evaluation of root variation than by conventional field screening. The use of molecular markers linked to interesting variation for root is also a potentially valuable option. Genotypes with greater yield potentials due to improved root architecture could improve productivity in low-input or low-rainfall systems, which could help to reduce the environmental impact of rigorous fertilization in current high-input agro-systems (Lynch, 2007).

Root development, growth and architecture are major mechanisms for plant nutrient acquisition and water use efficiency especially under changing climate (Manschadi et al., 2008; Ochoa et al., 2006). They are supposed to be one of the leverage for next green

revolution. Additionally, direct or indirect substantial contribution of roots to carbon sequestration is making them key actors in global earth carbon budget. Inter- and intra-species variations in root architectural traits are very useful to breed the crops for root features optimum for diverse environmental conditions (Bouteille et al., 2012; De Deyn et al., 2008; Lynch, 2007). Biomass division between root and shoot may contribute to plant growth and adaptivity to environmental limitations such as nutrient deficiencies, drought or light (de Dorlodot et al., 2007; Hochholdinger and Tuberosa, 2009).

1.3.2 Mapping of quantitative trait loci (QTL) for root traits

The identification of QTL with mapping of large numbers of molecular markers may allow the estimation of parameters of genetic architecture and improve root traits by marker-assisted selection. QTL have been identified which are responsible for different root parameters in a variety of crop and tree species. The important root parameters for which QTL have been reported include primary root length, root biomass, root angle, root branching and ratio of deep and shallow roots (Hund et al., 2009; Kamoshita et al., 2002; Zhang et al., 2001). Evaluation of these traits is difficult in practice since removing intact roots from soil is tedious and root morphological characteristics are complex and easily influenced by environment. To overcome these limitations, new methods are being developed to facilitate visualization of RSA in intact form and to digitalize the RSA contents phenotyping. Several sophisticated image analysis programs have been developed in the past decade to increase the throughput and accuracy of RSA trait measurements and the number and complexity of RSA traits that can be analyzed (Zhu et al., 2011). Various Arabidopsis populations were also evaluated for QTL mapping of either constitutive root-growth traits or environment responding root characteristics such as water deficiency, low availability of P, low nitrogen, and osmotic stress (Clark et al., 2011; Fitz Gerald et al., 2006; Loudet et al., 2005). Such intrinsic and response variables reveal the possible different nature of the molecular mechanism controlling root development. Shi et al. (2012) identified 38 QTL associated with root architectural traits and biomass in *B. napus* in the presence of high and low P level in gel media. Significant QTL for primary root length were identified on chromosomes A07 and C06, while for lateral root number and density a QTL cluster was detected on chromosome A03. These results suggested the feasible use of root traits to be used in crop improvement strategies.

1.3.3 Genome wide association studies in diverse populations

Conventional methods for mapping QTL in plants include the use of bi-parental cross populations. Genetic marker development for the population followed by the phenotypic data collection for the trait(s) of interest enables localization of QTL to specific chromosome regions via linkage mapping. Association mapping is an alternative method for identification of QTL regions based on linkage disequilibrium (LD). Association mapping techniques have been highly explored for mapping genes involved in human disease (Corder et al., 1994; Hawthorne et al., 2013). The underlying principle is the maintenance tendency of LD over many generations for genetically linked loci. The frequency of certain alleles in relation to any phenotypic trait is assessed in a genetically diverse population or collection, and marker to phenotype associations can be detected resulting from ancestral recombination (Buckler and Thornsberry, 2002). Whole genome scans for the presence of SNP markers is currently the method of choice for association analysis. It is being applied in plant sciences since a decade, although it can be somewhat complicated by the complex breeding history of many important crops, confounding effects of population structure, and the lack of knowledge regarding the structure of LD in many plant species (Flint-Garcia et al., 2003).

1.4 Objectives

Seed metabolism and root traits are two important determinants of seed quality and yield, respectively, in *B. napus*. Both are controlled by complex genetic mechanisms. In this study the aim was to develop and use novel digital gene expression (DGE) techniques, on the one hand, to investigate the complex genetics of gene networks responsible for important seed quality traits, and on the other hand to use genome-wide association studies to investigate root architecture as an important determinant of abiotic stress tolerance, nutrient uptake and yield.

The specific objectives of the work were:

- Investigation of differentially expressed gene networks during *B. napus* seed development in relation to the glucosinolate and phenylpropanoid pathways as examples for the regulation of antinutritive seed components.

- Evaluation of genetic variation in root architectural traits through QTL and association mapping in a genetically diverse natural *B. napus* population, to identify markers and germplasm for breeding of useful root traits.

2. MATERIALS AND METHODS

2.1 Digital gene expression profiling during seed development in *B. napus*

For the genome-wide analysis of gene expression in the developing seeds of rapeseed genotypes, this study was planned to examine changes in the transcriptome of seeds at seven developmental points using next-generation-sequencing based Illumina Digital Gene Expression (DGE) tag profiling. Pods were harvested from rapeseed plants from the 2nd day after pollination (dap) till 84 dap to cover the whole duration of seed development in winter rapeseed genotypes.

2.1.1 Plant material

Two *B. napus* L. genotypes were selected for gene expression profiling during seed development. First, V8 is a semi-synthetic breeding line of the Plant Breeding Department (Giessen, Germany) which contains high-erucic acid seed oil and moderate levels of seed glucosinolates (GSL) and lignin. Second, Express617 is an inbred line derived from the winter cultivar Express which was released in 1993 by NPZ-Lembke (Hohenlieth, Germany) characterized by canola quality with stable yield and high oil content; it is known as 00-quality due to zero erucic acid content and low seed GSL, but it has high lignin content.

A pot experiment was conducted at the Institute's research station Rauischholzhausen (Ebsdorfergrund, Germany). Plants were cultivated under controlled growth chamber conditions (16 hours, 20°C day and 8 hours, 16°C night, 60% relative humidity) and self-pollinated. Pods were harvested fortnightly at seven different developmental points from 2 days after pollination (dap) until completely ripe (84 dap) and shock frozen in liquid nitrogen.

2.1.2 Total RNA isolation

Frozen pods were used for total RNA extraction from initial time points (2, 14 and 28 dap) by using TRIZOL reagent (Invitrogen, Carlsbad, USA) according to manufacturer's instructions. Seeds powder was used from 42- 84 dap for total RNA isolation by using plant RNA isolation mini kit (Agilent Technologies, USA). The quality of RNA was checked on agarose gel and quantification was done by Nanodrop ND-1000 spectrophotometer and Agilent 2100 Bioanalyzer (Agilent Technologies, USA).

2.1.3 Digital gene expression library preparation

Digital gene expression (DGE) profiling by tag sequencing (Tag-seq) is an implementation of the LongSAGE protocol on the Illumina sequencing platform that augment effectiveness while reducing both the cost and time required to produce gene expression profiles. The application of next-generation sequencing to SAGE and other tag-based approaches has allowed for the cost-effective sequencing of millions of tags in a given SAGE library. The ultra-high throughput sequencing potential of the Illumina platform allows the generation of libraries containing an average of 20 million tags, a 200-fold improvement over classical LongSAGE. Tag-seq has less sequence composition bias; leading to a better representation of AT-rich tag sequences, and allows a more accurate profiling of a subset of the transcriptome characterized by AT-rich genes expressed at levels below the threshold of detection of LongSAGE. Compared to conventional microarrays, which provide a hybridization-based measure of gene expression, Tag-seq has the advantage of significantly greater dynamic range limited only by sampling depth. This leads to improved accuracy in the quantification of abundant and rare transcripts.

Tag-seq lab protocol (Morrissy et al, 2010) was followed along with Illumina's DGE Tag Profiling Kit for tag libraries preparation according to the manufacturer's instructions. A schematic overview of the procedure is given in Figure 2.1. Similar to conventional SAGE, Tag-seq library construction involves the capture of mRNA molecules via their poly(A)+ tails using magnetic oligo(dT) beads from DNaseI–treated total RNA. DGE starts with reverse transcription of mRNAs purified from biological samples into double stranded cDNAs. The cDNAs are digested with *Dpn*II (or *Nla*III corresponding to the anchoring enzyme in the traditional SAGE protocol). The 3'-cDNA fragments are isolated and ligated with a 5'-adaptor (Adaptor 1) that contains an *Mme*I recognition site. Another round of digestion with *Mme*I (corresponding to the tagging enzyme in the traditional SAGE protocol) generates cDNA tags of 20-nt long when using *Dpn*II (or 21-nt long when using *Nla*III). The tags are then ligated to a 3'-adaptor (Adaptor II). The tag flanked by two adaptors are immobilized onto a solid surface in a flow cell and amplified by bridge PCR. Following purification of tags and dephosphorylation to prevent self-ligation, adapters containing a 2-nucleotide degenerate 3' overhang and sequences compatible with direct sequencing on the Illumina Genome Analyzer are ligated to the random overhang left after *MmeI* digestion. After amplification, the tags are sequenced with an Illumina Genome Analyzer sequencer

(sequencing-by-synthesis) and quantified by the number of times any specific tag sequence is detected ("count"). Tag libraries of all samples were sequenced by GAII Illumina Sequencing commercial facility at ServiceXS B.V., Eindhoven, Netherlands. The tag sequences are then mapped to the unigenes to get the final version of a comprehensive gene expression profile with direct quantitative measurement of gene expression level.

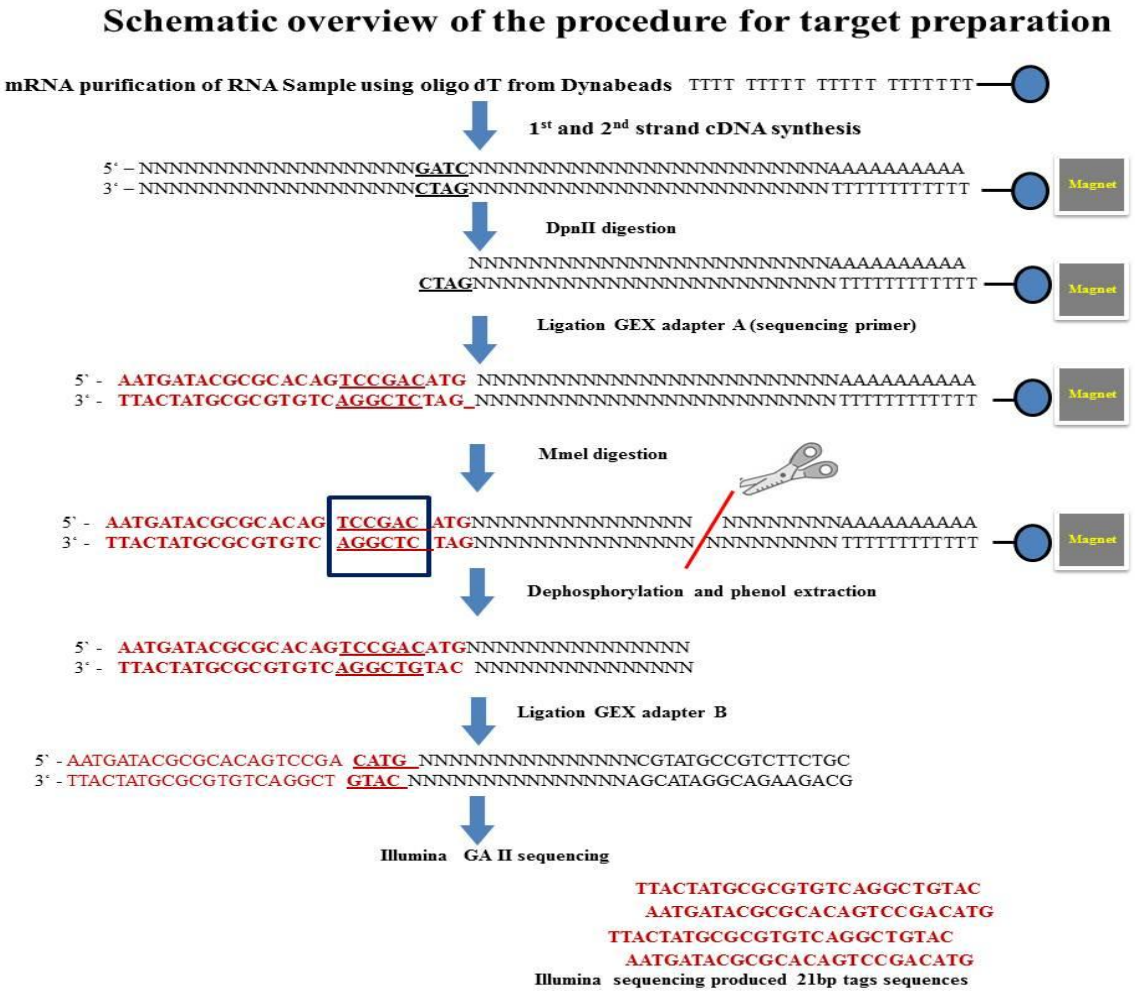

Fig.2.1 Schematic diagram showing the 3'anchored library preparation for digital gene expression by tag profiling for Illumina GAII sequencing (modified from Morrissy et al., 2001).

2.1.4 Bioinformatics and statistical analysis

A set of 189,116 *B. napus* unigenes (UGs) (Bancroft et al., 2011) was used to annotate tag sequences and gene expression was quantified by the number of times any specific tag sequence is detected ("count"). All tags were mapped to the reference sequences, allowing no

more than one nucleotide mismatch per tag. Customized PERL scripts were used to normalize tag distributions per library and determine significance values for differentially expressed genes. CLC genomics software was used for principle component analysis and correlation of developing stages of seeds between two genotypes based on quantitative expression values. BLASTX search was carried out for UGs dataset against the UniProtKB/Swiss-Prot dataset (*Arabidopsis thaliana)* adopting an E-value of 1e-6 and best hit was selected in order to assign the each unigenes an Arabidopsis gene code (AGI). Expression values of unigenes were summed up based on the AGI codes. Log2 transformed ratios were calculated between Express617 and V8 and it was scaled around 0 by subtracting -1.

2.1.5 Differential expression of pathway-specific genes

Expression ratios from all genes expressed differentially between Express617 and V8 during all developmental stages were imported to MapMan Image Annotator version 3.5 (Usadel et al., 2009) to display up and down regulated genes expression in metabolic pathways. The Wilcoxon rank sum test in MapMan program was used to determine the bins which are significantly different from others. MapMan is an open source software which offers a tool to categorize and display expression data based on The Arabidopsis Information Resource (TAIR). It has organized 16,441 AGI genes into 36 functional categories or "BINS" (http://mapman.gabipd.org) (Thimm et al., 2004). The phenylpropanoid and glucosinolate (GSL) metabolic pathways were selected to observe differential expression of their respective genes in detail and viewed in MapMan annotator during seven seed developmental points.

2.2 Evaluation of root development of *B. napus* in mini-rhizotron system

2.2.1 Plant materials

(i) DH-population

A double haploid (DH) population of 250 winter oilseed rape lines (Basunanda et al., 2010) was previously produced from a cross between the German winter oilseed rape inbred line Express 617 (see above) and the genetically diverse semi-synthetic breeding line V8 (see above). For this study 47 best and 47 worse performers in the field due to former yield tests were selected to study root developmental traits in a mini-rhizotron *in vitro* system.

(ii) *B. napus* diversity set

A large *B. napus* diversity set comprising 496 inbred lines representing 187 winter oilseed rape (OSR), 17 winter fodder, 208 spring OSR, one spring fodder, nine semi-winter type OSR, 14 vegetables, 54 swede and six unspecified rapeseed genotypes were analyzed for the development of root traits in the mini-rhizotron system. According to available information selected genotypes originated from Western Europe, Eastern Europe, Asia, Africa, Australia, North America, and some are from unknown origin (Bus et al., 2011).

2.2.2 Mini-rhizotron experiment setup

(i) Gel matrix preparation

Plates were sterilized by gamma rays for seven days to avoid any kind of microbial contamination. Nutrient media were prepared by using recommended amount of MS medium (Murashige and Skoog, 1962) with 0.6 % Gelrite for solidification and mixed with magnet stirrer. Media were autoclaved at standard conditions, cooled until 50^{o}C and poured into the sterilized plates (500 mL per plate). Plates were prepared one day before setting up the experiment and stored overnight in sterile conditions.

(ii) Seed sterilization and sowing

Falcon tubes were labeled with the names of genotypes and 10-15 seeds were added. Seeds were washed with 70% ethanol and rinsed with water in the falcon tubes. Seeds were placed in 6% NaOCl and kept on shaking for five minutes. One drop of liquid detergent was added to reduce the surface tension and tubes were placed in a sterile clean bench (laminar hood). Again seeds were washed five times with autoclaved distilled water to remove liquid detergent and sterilizing agent (6% NaOCl). After sterilization, seeds were sown immediately in gel matrix.

Plates were labeled and the upper 5 cm of media was cut and removed for shoot development (Figure 2.2.1). Fifteen seeds were sown per plate which consists of five seeds per genotype. Plates were tightened with rubber bands and covered with aluminium foil to give dark condition for seed germination and placed in vertical direction in a growth chamber set under controlled conditions (16h day at 20°C and 8h night at 16°C, 60% relative humidity). After

seed germination, aluminium foil was removed from the upper side of plates to allow the penetration of light to the developing seedlings.

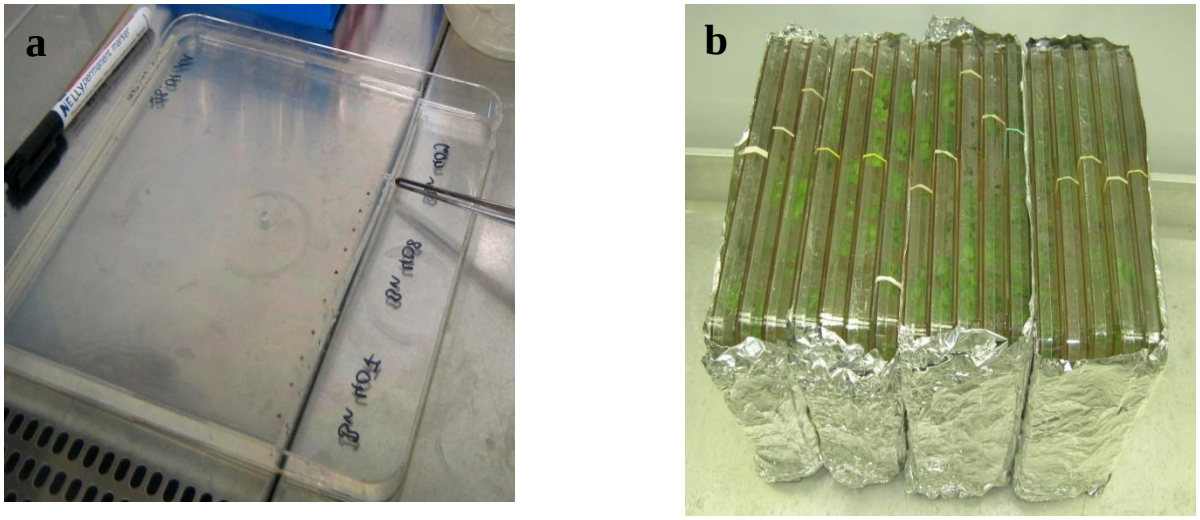

Fig.2.2 Mini-rhizotron experiment setup: (a) Sowing of seeds in gel matrix, (b) Plates containing growing seedlings in the growth chamber under controlled conditions.

2.2.3 Image analysis and data collection

Images of the growing root systems (Figure 2.2.2) were obtained by digitalizing plates from the bottom on the 3rd, 5th and 7th day after sowing (DAS) and were analyzed by using the image analysis software ImageJ (Abramoff, 2007). On the 7th DAS, each visible secondary root was given a registration number. The length of both primary and secondary roots were recorded on the image and then on their images corresponding to earlier days. Data for five root traits were measured which include primary root length (PRL) in cm, rate of primary root growth (RoG) cm per day, lateral root length (LRL) in cm, lateral root number (LRN) and lateral root density (LRD), calculated by using the formula [LRD=LRN/PRL] root/cm. Rate of primary root growth (cm/day) was calculated from records of primary root length at three growth points.

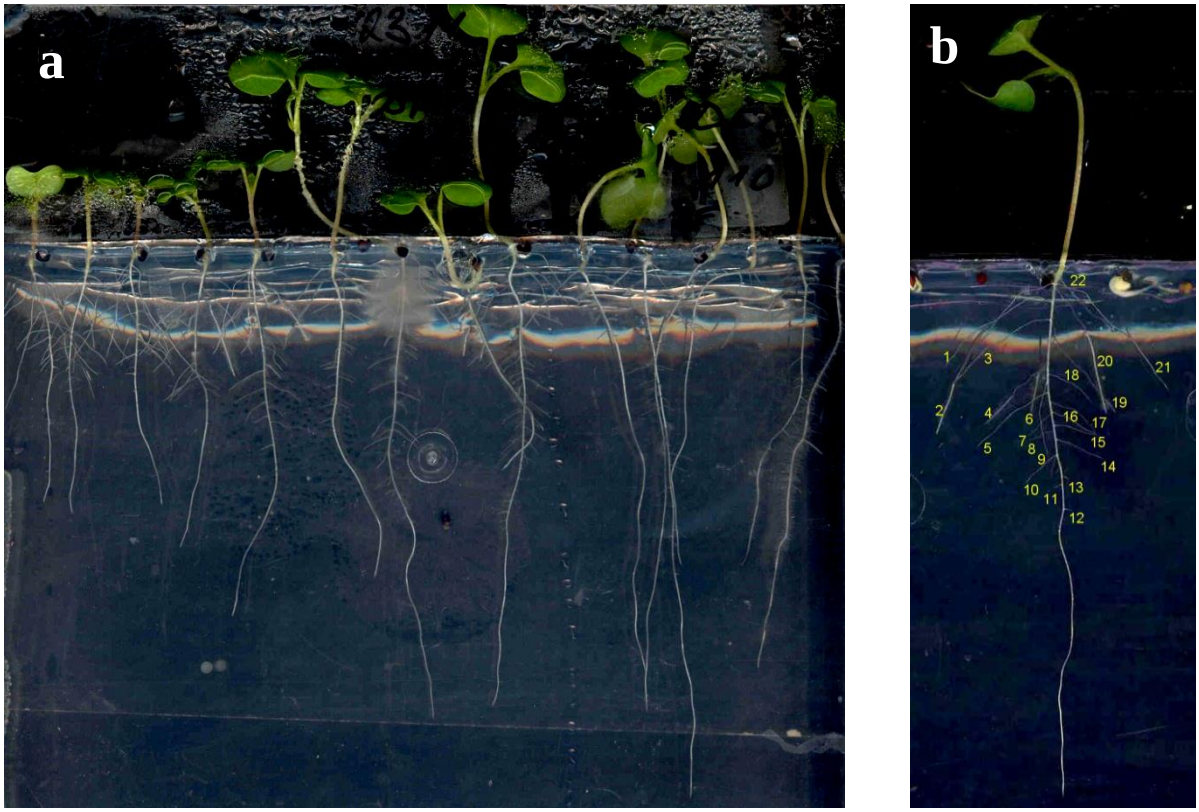

Fig.2.3 Assessment of root development in the *in vitro* rhizotron system. (a) Fifteen plants, five from each inbred line with clear differences in seedling and root development are shown; (b) Secondary roots were labeled with a number at 7th day after sowing.

2.2.4 Data analysis and quantitative trait loci (QTL) mapping

The complete set of data from the DH lines of Express617 x V8 (ExpV8) and the *B. napus* diversity set was subjected to analysis of variance (ANOVA), performed with SAS 8.0 software (SAS Institute 1999) by using PROC GLM based on the trait means for each inbred line. Broad-sense heritability was calculated based on variance components of ANOVA (genetic variance/total phenotypic variance) (Loudet et al., 2005). Pearson correlation coefficients of all combinations of root traits were calculated by using IBM SPSS Statistics Version 18 (IBM Software, Armonk, NY, USA).

A newly generated map from the ExpV8-DH population composed of a large set of simple sequence repeat (SSR) markers, single-nucleotide polymorphism (SNP) markers and restriction site–associated DNA (RAD) markers was used for putative QTL detection (Stein et al., 2013). Distribution of markers on each of the 19 chromosomes is presented in

Appendix A. WinQTL cartographer 2.5 software (Wang et al., 2012) was used to perform QTL analysis based on standard composite interval mapping (CIM) using the ZmapQTL model 6 CIM option. The number of control markers, window size, and walking speed were set to 5, 10 cM, and 1 cM, respectively. The default genetic distance (5 cM) was used to define a QTL in an experiment. Significant QTL-defining logarithms of odds (LOD) values were calculated by 1,000 permutations for each phenotypic trait (Churchill and Doerge, 1994). LOD scores corresponding to P = 0.05 (ranged from 3.2–3.5) were used for identifying significant QTLs associated to different root traits.

2.2.5 Genome wide association mapping

Population structure for the *B. napus* diversity set was investigated for association mapping by using STRUCTURE 2.3.1 (Pritchard et al., 2000). Identification of different sub-populations within a sample of individuals of a population of unknown structure is done by this software. This method assigns individuals to clusters (each cluster corresponding to a different subpopulation) with an associated probability by giving fix number of sub-populations (K). The STRUCTURE software was run by assuming an admixture model, with a burn-in phase of 10,000 iterations which was followed by 10,000 Markov chain Monte Carlo iterations in order to detect the ‘‘true’’ number of K groups in the range of K = 1–20 possible groups. The Q-matrix, which shows the probability that a genotype belongs to a sub-population, was estimated with STRUCTURE. STRUCTURE-HARVESTER was used to calculate delta K (dK) based on the method by Evanno et al. (2005).

SNP marker data were imported into TASSEL version 4.0 (Bradbury et al., 2007). Markers located on unanchored scaffolds and markers having a minor allele frequency (MAF) inferior to 5% were eliminated from the dataset. The remaining SNP markers were used for analysis of linkage disequilibrium and marker-trait associations. LD was estimated as the squared allele frequency correlations (r^2) between all pairs of the SNPs and analyzed for LD decay in this population.

For significant associations between the 6K SNP markers and five root architecture traits, data were subjected to both, General Linear Model (GLM) which is using the percentages of admixture (Q matrix) as fixed effects and mixed linear model (MLM) methods which are more useful for genome-wide association as they also consider population structure and

familial relatedness (Zhang et al., 2010). A kinship matrix was computed with TASSEL 4.0 and used in MLM. Quantile- quantile plots were displayed to assess significance of both models to observ significant results rather than expected by chance. The significance of each marker was tested by setting the false discovery rate (FDR), as described previously in rapeseed association mapping (Cai et al., 2014; Honsdorf et al., 2010) to reduce the probability of false positives caused by multiple testing (Benjamini and Hochberg, 1995). Given the distribution of empirical *P* values of 6K SNP markers, the FDR of 0.2 corresponded to the P value of 0.001, which was employed as threshold of significance of tested markers in the association analysis.

3. RESULTS

3.1 Digital gene expression profiling of seed development

For the genome-wide analysis of gene expression in the developing seeds of rapeseed genotypes, transcriptomic changes were examined at seven developmental points using next-generation sequencing based Illumina Digital Gene Expression (DGE) tag profiling. The seven time points started from the 2nd day after pollination (dap) till 84 dap to cover the whole duration of seed development in winter rapeseed genotypes Express617 and V8. Tags sequenced by Illumina GAII were annotated to 99,284 *B. napus* unigenes (UGs) out of the dataset of 189,116 unigenes. Quantification of expression values of these unigenes by summing up the values based on AGI codes resulted in 16,441 Arabidopsis genes expressed during seven seed developmental stages in both genotypes. The numbers of genes expressed in each developmental stage and up/down regulated genes in Express617 relative to V8 are shown in Table 3.1. Principal component analysis (PCA) showed that gene expression was highly similar between the two genotypes until 28 dap, after which significant differences were observed at later time points (Figure.3.1.1, a). A strong correlation was also observed until 28dap between two genotypes while later developmental stages were significantly different in these two genotypes (Figure.3.1.1, b).

Table 3.1 Number of genes expressed in seven seed developmental points in two *B. napus* genotypes and number of up-/down regulated genes in Express617 relative to V8.

	Developmental time points during seed development						
No. Of Genes	**2 dap**	**14 dap**	**28 dap**	**42 dap**	**56 dap**	**70 dap**	**84 dap**
Expressed in Express617	11072	12602	11526	12901	9940	12644	12178
Expressed in V8	12691	13249	13737	7950	8687	8930	11530
Up-regulated in Express vs V8	5867	6152	5380	9115	6190	9364	5822
Down-regulated in Express vs V8	7370	7790	8488	4197	4794	3599	7434

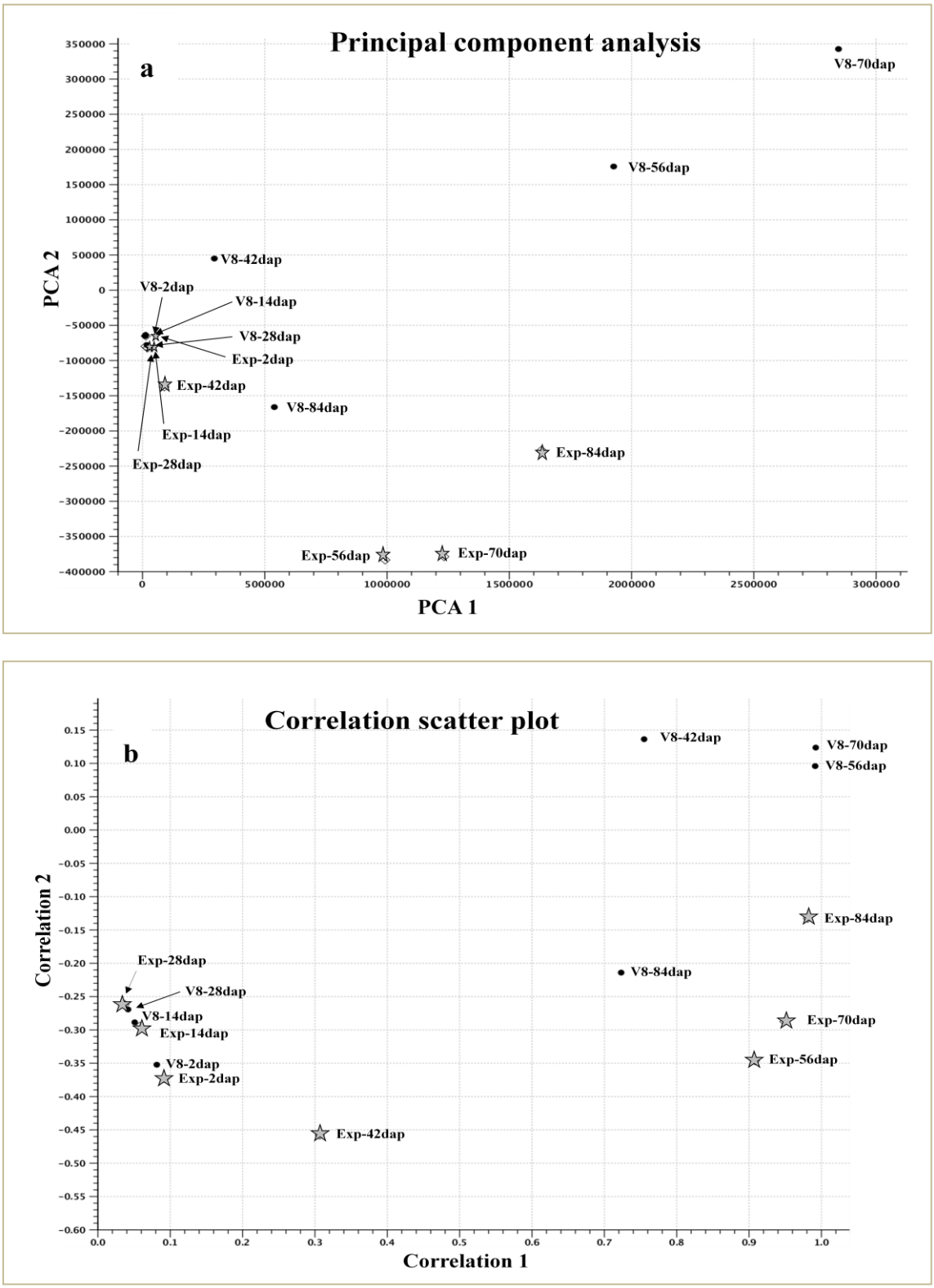

Fig 3.1. a. Principal component analysis (PCA) **b.** Correlation analysis, showing the distribution of seven developmental stages from 2 days after pollination (dap) until 84dap in two *B. napus* genotypes, Express 617 (Exp☆) and V8(●).

3.1.1 Differential expression of genes between *B. napus* genotypes

A large number of differentially expressed genes were observed during whole seed development in both *B. napus* genotypes. The number of up and down regulated genes expressed during seven seed developmental time points in Express617 relative to V8 is presented in Table 3.1. These differentially expressed genes were imported to MapMan metabolic pathway annotator to get insight to the key processes involved in seed development. The whole set contains 16,441 AGI genes which were organized into 36 functional categories (BINS). The Wilcoxon rank sum test showed that some functional categories (BINS) in the overview of all metabolic pathways were substantially different from the others. P-value for the BIN describes how much the data distribution from the genes within that BIN differs from the overall distribution (Table 3.2).

Functional categories found in the whole dataset are photosynthesis, major and minor carbohydrates metabolism, Calvin cycle and glycolysis, cell wall synthesis, amino acid metabolism, lipid metabolism and secondary metabolism associated with phenylpropanoid metabolism, sulfur containing compounds metabolism, hormone metabolism, protein metabolism, signaling, development and transport.

B. napus selected genotypes, Express617 and V8 were crossed previously and their DH-population showed diverse distribution and segregation of quality traits e.g., glucosinolates (GSL) and fiber fractions such as neutral detergent fiber (NDF), acid detergent fiber (ADF), and acid detergent lignin (ADL) (Basunanda et al., 2007; Stein et al., 2013; Wittkop et al., 2012). Based on these facts and differential expression of genes, GSL and phenylpropanoid pathways were selected to observe in detail during seed development in these winter rapeseed genotypes. Table 3.3 and 3.4 showed the differential expression of genes involved in phenylpropanoid and GSL pathway genes in each seed developmental time point respectively.

Table 3.2 Wilcoxon rank sum test in MapMan ranked differentially expressed genes between Express617 and V8 at each seed development time point, p-value shows the differential expression of the functional categories (BINS) from overall data distribution. Red color to blue color show low to high P-values.

BinCode	Name of Bin	Number of Genes	2 dap	14 dap	28 dap	42 dap	56 dap	70 dap	84 dap
1	Photosynthesis	169	0.444	0.264	0.001	0.843	0.135	0.244	0.002
10	Cell wall	337	0.761	0.165	0.829	0.401	0.058	0.528	0.001
11	Lipid metabolism	324	0.056	0.047	0.933	0.832	0.618	0.698	0.001
12	N-metabolism	23	0.811	0.634	0.069	0.973	0.998	0.831	0.660
13	Amino acid metabolism	225	0.069	0.366	0.511	0.908	0.484	0.570	0.858
14	S-assimilation	12	0.478	0.326	0.576	0.317	0.649	0.961	0.482
15	Metal handling	52	0.837	0.764	0.052	0.459	0.124	0.917	0.670
16	Secondary metabolism	273	0.168	0.083	0.198	0.706	0.867	0.689	0.001
17	Hormone metabolism	344	0.297	0.482	0.403	0.002	0.640	0.196	0.001
18	Co-factor and vitamin metabolism	64	0.293	0.636	0.837	0.698	0.267	0.243	0.330
19	Tetrapyrrole synthesis	38	0.936	0.737	0.948	1.000	0.001	0.864	0.899
2	Major CHO metabolism	87	0.320	0.336	0.253	0.166	0.305	0.087	0.032
20	Stress	577	0.122	0.227	0.240	0.001	0.022	0.001	0.129
21	Redox	165	0.100	0.225	0.014	0.824	0.316	0.143	0.086
22	Polyamine metabolism	10	0.506	0.115	0.119	0.421	0.702	0.753	0.075
23	Nucleotide metabolism	141	0.566	0.671	0.282	0.266	0.398	0.216	0.545
24	Biodegradation of Xenobiotics	23	0.800	0.242	0.873	0.638	0.589	0.634	0.250
25	C1-metabolism	31	0.456	0.316	0.607	0.713	0.809	0.295	0.885
26	Miscellaneous	940	0.025	0.163	0.006	0.001	0.565	0.989	0.001
27	RNA	1947	0.080	0.625	0.010	0.102	0.025	0.146	0.001
28	DNA	324	0.217	0.145	0.001	0.044	0.109	0.772	0.097
29	Protein	2473	0.575	0.266	0.548	0.077	0.079	0.001	0.001
3	Minor CHO metabolism	98	0.135	0.247	0.307	0.103	0.973	0.608	0.117
30	Signalling	810	0.227	0.709	0.067	0.031	0.413	0.111	0.539
31	Cell	601	0.894	0.994	0.277	0.051	0.442	0.671	0.183
32	Micro RNA	2	0.368	0.841	0.248	0.425	0.232	0.448	0.372
33	Development	519	0.183	0.951	0.025	0.375	0.885	0.293	0.451
34	Transport	688	0.054	0.742	0.860	0.856	0.949	0.230	0.804
35	not assigned	5048	0.005	0.335	0.447	0.158	0.090	0.019	0.111
4	Glycolysis	58	0.110	0.806	0.232	0.222	0.138	0.221	0.396
5	Fermentation	14	0.448	0.240	0.768	0.130	0.359	0.282	0.202
6	Gluconeogenesis / glyoxylate cycle	10	0.201	0.945	0.443	0.245	0.420	0.612	0.006
7	Oxidative phosphorylation	28	0.693	0.786	0.894	0.105	0.277	0.728	0.419
8	TCA	64	0.025	0.985	0.420	0.892	0.026	0.472	0.440
9	Mitochondrial electron transport/ ATP synthesis	101	0.881	0.532	0.002	0.533	0.634	0.854	0.164

Table 3.3 Expression of genes involved in phenylpropanoid pathway. Expression value is log2 transformed and ratio was calculated between Express617 and V8 at each seed development time point. Red color show higher expression of genes and blue means down-regulation of gene expression in Express617

BinCode	AGI-Code	Gene	2 dap	14 dap	28 dap	42 dap	56 dap	70 dap	84 dap
16.2.1.1	at2g37040	PAL1	0.422	-0.659	0.633	1.041	-0.005	0.939	-0.453
16.2.1.1	at3g10340	PAL4	0.800	-7.635	2.793	1.061	0.453	1.781	-0.488
16.2.1.1	at3g53260	PAL2	0.707	0.188	0.369	0.455	0.706	0.388	-2.530
16.2.1.2	at2g30490	C4H	-0.362	-0.847	0.899	9.947	0.088	1.399	-1.590
16.2.1.3	at1g51680	4CL1	1.260	-0.234	1.793	1.052	-0.435	0.422	-1.418
16.2.1.3	at1g65060	4CL3	-3.706	-0.267	-1.822	5.562	7.132	-0.482	-0.455
16.2.1.3	at3g21230	4CL5	0.800	-0.622	0.424	-0.985	1.085	2.662	2.025
16.2.1.3	at3g21240	4CL2	0.000	0.000	0.000	0.000	0.000	0.000	-3.256
16.2.1.3	at4g05160	4CL-like1	0.000	0.000	0.000	4.392	5.547	3.967	0.000
16.2.1.3	at4g19010	4CL-like2	-0.784	0.899	-0.430	4.392	-6.747	5.552	-1.181
16.2.1.3	at5g63380	4CL4	-6.443	-0.423	-0.130	6.562	0.000	0.896	1.440
16.2.1.4	at5g48930	HCT	0.498	0.279	0.985	0.640	-0.352	0.122	-1.637
16.2.1.5	at2g40890	C3H	0.656	-0.411	1.189	1.346	0.766	0.769	-1.404
16.2.1.9	at5g54160	COMT	-0.076	0.129	0.150	-1.127	-0.172	0.328	2.166
16.2.1.6	at1g24735	CCoAOMT-like1	-0.410	-0.711	-0.491	1.652	-0.831	0.434	0.520
16.2.1.6	at1g67980	CCoAOMT-like2	0.319	0.296	-0.604	-0.662	0.159	-0.386	-0.357
16.2.1.6	at4g26220	CCoAOMT-like3	-0.017	-0.093	-0.647	-0.804	0.306	-0.007	2.051
16.2.1.6	at4g34050	CCoAOMT1	1.453	0.404	-0.135	2.315	0.643	0.280	3.702
16.2.1.8	at4g36220	F5H	-0.439	-0.388	0.788	2.377	-0.015	0.366	0.043
16.2.1.7	at1g15950	CCR1	0.834	0.981	0.101	-0.567	0.145	0.286	-0.760
16.2.1.7	at1g80820	CCR2	-7.208	4.890	0.000	0.000	0.000	1.256	-2.293
16.2.1.7	at4g30470	CCR-like1	-1.659	-6.729	0.137	7.852	1.028	2.415	2.798
16.2.1.7	at5g14700	CCR-like2	-1.784	0.354	-6.474	-0.032	-0.937	0.989	0.000
16.2.1.7	at5g58490	CCR-like3	-0.685	-0.916	0.162	-0.166	-0.200	-0.619	-0.560
16.2.1.10	at1g72680	CAD1	0.000	0.000	0.000	0.000	6.132	3.967	0.000
16.2.1.10	at3g19450	CAD4	-0.521	-0.086	0.583	8.884	0.192	0.616	5.017
16.2.1.10	at4g34230	CAD5	-5.121	-1.646	1.816	5.392	0.000	7.359	-0.560
16.2.1.10	at4g37980	CAD7	-0.278	-1.160	-0.304	0.000	0.000	0.000	0.000
16.2.1.10	at4g37990	CAD8	-0.822	-1.768	-1.653	8.562	0.969	-0.490	1.440
16.2.1.10	at4g39330	CAD9	-0.108	-0.306	-0.050	7.093	0.000	0.000	0.000

Differential expression of 58 genes involved in phenylpropanoid pathway were detected, out of which 30 genes are from the pathway directed to the lignin biosynthesis specific genes. These genes belong to the ten enzymes families which are Phenylalanine ammonia-lyase (PAL), Cinnamate 4-hydroxylase (C4H), 4-coumarate:CoA ligase (4CL), Hydroxycinnamoyl-coenzyme A shikimate:quinate hydroxycinnamoyl-transferase (HCT), P-coumaroyl shikimate 3' hydroxylase (C3'H), Caffeoyl CoA 3-O-methyltransferase (CCoAOMT), Cinnamoyl-CoA reductase (CCR), Ferulate 5-hydroxylase (F5H), Caffeic acid/5-hydroxyferulic acid O-methyltransfer-ase (COMT) and Cinnamyl alcohol dehydrogenase (CAD) were differentially expressed in both genotypes during seed development. Log ratio of these all genes is presented in Table 3.1.3 and these ratios were viewed in Mapman during whole seed developmental period from 2dap to 84dap.

Diffenetial expression of 30 genes involved in GSL metabolic pathway were detected and their log ratios are presented in Table 3.1.4). Those genes are belong to Bile acid:sodium symporter family protein 5 (BAT5), methylthioalkyl malate synthase (MAM), branched-chain aminotransferase (BCAT), Isopropylmalate isomerase (IPMI), Cytochromes CYP79 and CYP83, CYP81, C-S lyase (SUR1), glycosyltransferase (UGT74B1 & UGT74C1), sulfortransferase (ST5a,b,c), Oxidoreductase AOP1, AOP3, GSL-OH and Flavin-Monooxygenases FMO GS-OX. Ten genes which are responsible for GSL degradation include Epithiospecifier protein (ESP), EPITHIOSPECIFIER MODIFIER1 (ESM1), Myrosinase associated protein MyAP1 and MyAP2, MYROSINASE-BINDING PROTEIN (MBP1), NITRILE SPECIFIER PROTEINS NSP2 and NSP5, S-glycosyl hydrolase PEN2 (PENETRATION 2) and β-thioglucoside glucohydrolase TGG1 & TGG2.

Digital gene expression profiling by tag sequencing also enables to detect low level expression of transcription factors. Differential expression of six MYB family transcription factors, MYB32, MYB4, MYB58, MYB61, MYB63 and MYB85 was detected which play their role in phenylpropanoid pathway regulation. Expression of three MYB family transcription factors, MYB28, MYB34 and MYB51 and OBP2/DOF1.1 were detected which are regulating GSL metabolic pathway. Significant differential expression of these genes at specific developmental time point is discussed in further sections in detail.

Table 3.4 Expression of genes involved in GSL metabolic pathway. Expression value is log2 transformed and ratio was calculated between Express617 and V8 at each seed development time point. Red color show higher expression of genes and blue means down-regulation of genes expression in Express617

BinCode	AGI_Code	Gene	2dap	14dap	28dap	42dap	56dap	70dap	84dap
16.5.1.1.1.4	at2g43100	IPMI SSU2	-8.121	-1.726	-0.082	6.392	6.132	5.289	-2.882
16.5.1.1.1.8	at2g31790	UGT74C1	-6.928	-3.196	-8.428	-0.691	-1.031	-2.748	-2.297
16.5.1.3.1	at2g44490	PEN2	1.152	1.319	-2.015	-2.132	-6.747	4.552	-1.882
16.5.1.3.2	at5g48180	NSP5	-0.832	-0.709	-0.015	-2.906	0.568	0.901	-1.634
16.5.1.3.3	at3g44300	NIT2	-1.788	-1.512	0.101	-0.110	-1.179	0.381	-0.846
16.5.1.1.1.13	at2g25450	GSL-OH	0.000	-1.713	0.500	1.231	-1.200	-0.168	-0.801
16.5.1.3.2	at2g33070	NSP2	-0.773	-1.167	-0.256	0.304	0.766	2.542	-0.743
16.5.1.3.3	at5g22300	NIT4	-5.706	1.162	0.400	0.000	0.000	3.967	-0.730
16.5.1.3.3	at3g44320	NIT3	-1.287	-0.974	-1.002	5.392	-0.825	1.089	-0.252
16.5.1.1.1.10	at1g12140	FMO GS-OX5	-0.818	-0.450	0.134	-1.394	-0.352	-0.961	-0.224
16.5.1.1.1.1	at3g49680	BCAT3	-1.521	1.484	-6.059	0.131	-0.294	5.289	-0.197
16.5.1.1.1.9	at1g74090	SOT18	0.000	-6.314	-2.184	-1.588	-1.423	1.268	-0.120
16.5.1.1.1.2	at5g23010	MAM1	-8.028	-1.068	-0.288	0.000	-6.162	0.000	0.000
16.5.1.2.1	at5g61420	MYB28	-5.121	0.747	-6.059	0.000	0.000	0.000	0.000
16.5.1.1.3.2	at2g22330	CYP79B3	0.000	0.162	0.985	0.000	0.000	0.000	0.000
16.5.1.1.3.1	at4g39950	CYP79B2	0.000	0.162	0.985	0.000	0.000	1.382	0.000
16.5.1.1.1.3	at4g13430	IPMI LSU1	-0.852	-1.370	0.263	7.038	-0.440	1.415	0.020
16.5.1.2.3	at1g18570	MYB51	0.755	1.370	-0.320	-0.864	-7.410	-1.426	0.025
16.5.1.3.1.1	at5g26000	TGG1	-0.097	0.147	-2.683	-0.782	1.804	-0.069	0.267
16.5.1.3.1.1	at5g25980	TGG2	-0.422	-0.160	0.000	6.852	3.626	1.184	0.527
16.5.1.3.2.1	at1g54040	ESP	0.035	-1.733	0.769	2.427	1.008	1.512	0.555
16.5.1	at4g03070	AOP1	0.000	-2.075	0.995	0.479	0.567	3.609	0.753
16.5.1.1.4.3	at1g24100	UGT74B1	-2.485	0.065	-0.218	-0.769	0.000	0.000	0.762
16.5.1.1.4.2	at2g20610	SUR1	-0.065	-0.101	-1.079	-1.319	-1.570	-0.326	0.954
16.5.1.1.3.3	at1g74100	SOT16	0.396	2.109	0.531	-0.933	-0.101	0.110	1.440
16.5.1.1.1.7	at4g13770	CYP83A1	-4.007	-1.211	-0.366	-5.746	0.000	0.000	1.984
16.5.1.1.4.1	at4g31500	CYP83B1	1.624	0.093	0.453	6.392	0.000	5.552	2.057
16.5.1.1.1.1	at3g19710	BCAT4	-8.580	-0.587	-0.489	-3.053	-1.435	-0.317	2.152
16.5.1.3.1	at1g54010	MAP1	-1.422	0.000	-5.059	6.852	0.000	1.159	2.270
16.5.1.2.3	at1g07640	OBP2/DOF1.1	0.064	-1.101	0.623	5.714	4.547	5.289	2.696
16.5.1.3.1	at1g54020	MAP2	-1.101	-2.509	-1.461	0.898	0.291	0.368	2.860
16.5.1.3.1	at1g52040	MBP1	-0.274	-1.050	-2.211	0.000	0.000	0.000	2.959
16.5.1.3.1	at3g14210	ESM1	0.000	0.000	3.460	0.000	1.344	0.102	3.112
16.5.1.1.3.4	at5g57220	CYP81F2	0.000	0.000	0.000	0.000	0.000	0.000	4.281
16.5.1.1.1.9	at1g18590	SOT17	0.000	-0.423	1.570	0.000	0.000	0.000	4.281
16.5.1.4.1	at4g12030	BAT5	0.000	-1.061	-7.059	4.392	-0.031	6.137	5.503
16.5.1.2.3	at5g60890	MYB34	6.921	0.000	0.000	5.977	0.000	0.000	5.696
16.5.1.1.1.11	at4g03050	AOP3	0.000	-0.838	1.107	0.424	1.908	1.966	6.017

3.1.2 Investigation of genes involved in phenylpropanoid pathway

The phenylpropanoid pathway was investigated with a focus on lignin biosynthesis by DGE profiling in *B. napus* genotypes, Express617, which has high lignin content and V8, with a moderate level of lignin. Mapman assisted the visualization of differential expression of phenylpropanoid pathway genes during whole seed development period in these *B. napus* winter genotypes at seven developing time points. Over view of genes expression at selected time points showed that at early stages of seed development most of genes have similar expression level in both genotypes. The highest up-regulation of genes were observed at 42 and 70 dap which is in fact seed maturation period (Fig 3.2 a-g).

Phenylalanine ammonia-lyase (PAL) catalyzes the first step of the phenylpropanoid pathway, and is responsible for the deamination of phenylalanine to yield trans-cinnamic acid and ammonia. PAL1, PAL2 and PAL4 genes were found in UGs which shows low level of expression during early seed developmental points and highest expression was observed at 70 dap in both genotypes while these genes show down regulation in Express617 relative to V8 at 84dap (Fig 3.2 a-g). Three hydroxylation steps in lignin biosynthesis are controlled by cytochrome P450s and they also play their role to determine the contribution of guaiacyl and syringyl monomers. Three P450s Cytochromes are Cinnamate 4-hydroxylase (C4H), p-Coumarate 3-hydroxylase (C3H) and Ferulate 5-hydroxylase (F5H). C4H is responsible for the conversion of cinnamate into p-coumarate and C3H catalyzes the hydroxylation of p-coumaroyl shikimate to yield caffeoyl shikimate. Expression level of C4H and C3H was higher in late developing time points while F5H show high expression in early time points. C4H and C3H are up-regulated in Express617 compare to the V8 from 28 to 70 dap and down-regulated at 84dap. F5H is the third P450cytochrome, catalyzing the NADPH- and O_2-dependent hydroxylation of both coniferaldehyde and coniferyl alcohol to yield 5-hydroxy-coniferaldehyde and 5-hydroxyconiferyl alcohol, respectively which are required for S-lignin production. F5H showed a high expression during the whole developmental period and relatively shows up-regulation in Express617 at 42dap (Fig 3.2 a-g).

4-coumarate: CoA ligase (4CL) catalyzes the formation of CoA esters of p-coumaric acid, caffeic acid, ferulic acid, 5-hydroxyferulic acid, and sinapic acid. Seven 4CL putative genes were detected in UGs dataset which shows up-regulation in Express617 at 42 and 70dap (Fig 3.2 a-g). HCT catalyzes two steps in phenylpropanoid metabolism. First is its involvement to

convert p-coumaroyl CoA to coumaroyl shikimate/quinate and secondly it catalyze caffeoyl shikimate/quinate conversion to caffeoyl CoA. Single HCT gene in known in Arabidopsis and *B. napus* six unigenes were annotated as HCT and show lower to higher expression level from early to late development points of seeds in both genotypes. HCT was up-regulated in Express617 at 28 and 42 dap and down-regulated at 84dap.

Two necessary methylation steps invoved in biosynthesis of monolignols are catalyzed by CCoAOMT and COMT. CCoAOMT catalyzes the methylation of caffeoyl-CoA to feruloyl-CoA and 5-hydroxyferuloyl-CoA to sinapoyl-CoA and is, together with COMT, responsible for the methylation of the monolignol precursors. COMT has a dominating role for methylation of 5-hydroxyconiferaldehyde and/or 5-hydroxyconiferyl alcohol to sinapaldehyde and/or sinapyl alcohol, respectively. Single COMT and four CCoAOMT genes were found in UGs dataset. CCoAOMT1 (side block in Fig 3.2 a-g) is mainly recognized to involve in methylation step of monolignols precursors and showed higher expression in Express617 relative to V8 during seed development. COMT shows almost constant level of expression in both genotypes during seed development; only slight down-regulation at 42dap and higher expression at 84dap in Express617 was observed (Fig 3.2 a-g).

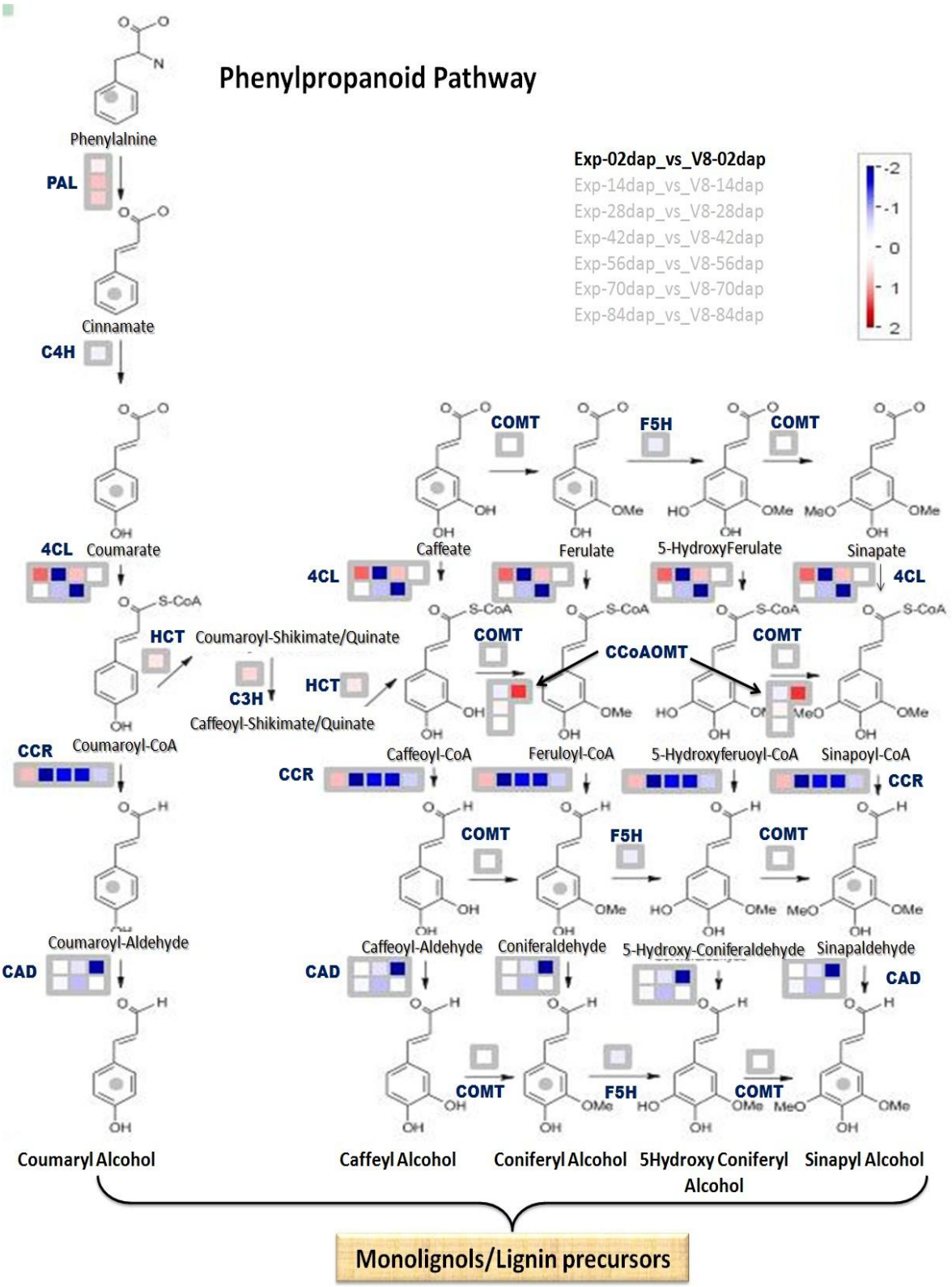

Fig 3.2 a. Phenylpropanoid pathway for lignin biosynthesis visualized in Mapman. Expression of genes at 2nd dap in *B. napus* genotypes, Express617 relative to V8. Red color show higher expression of genes and blue means down-regulation of genes expression in Express617.

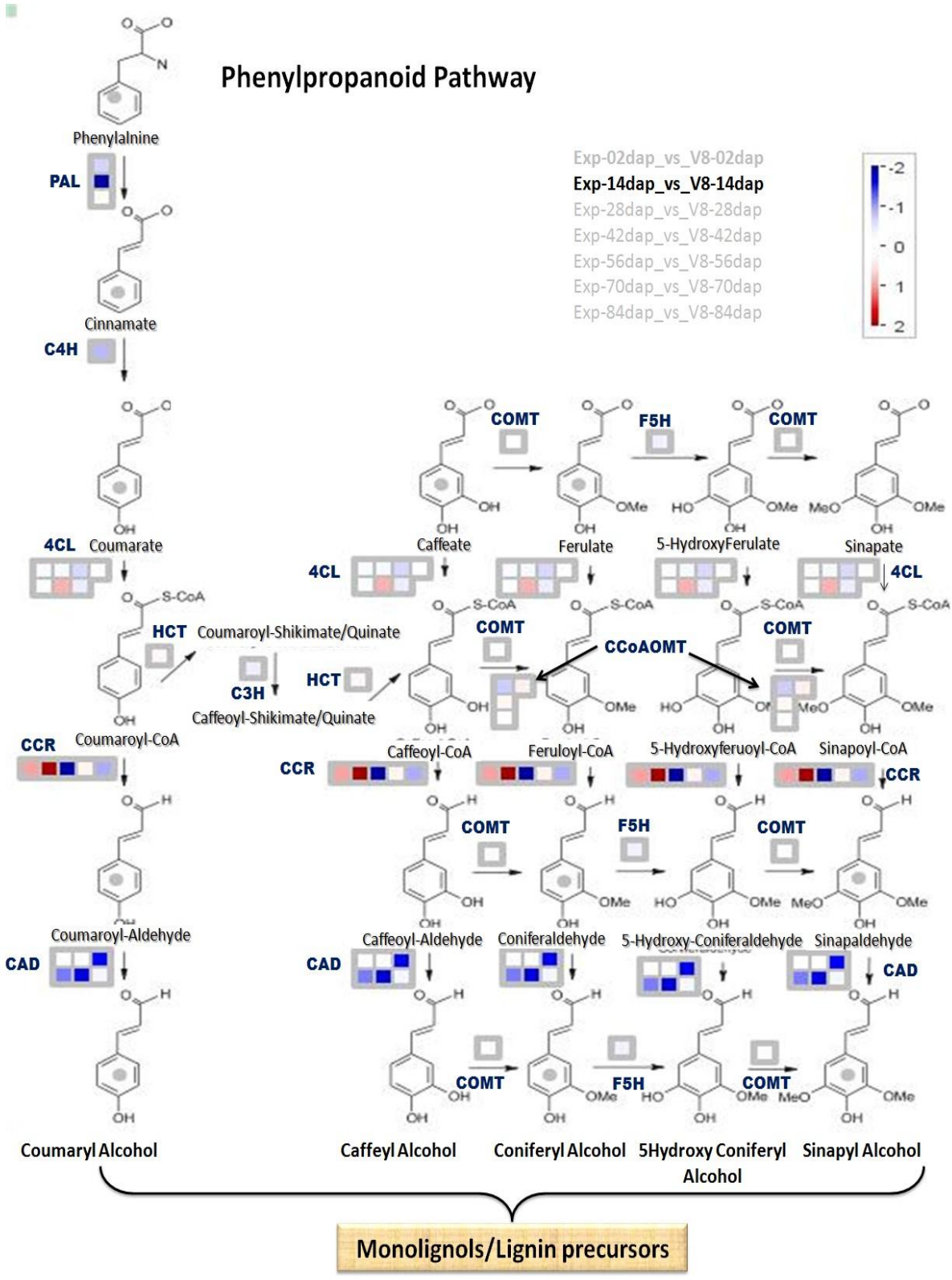

Fig 3.2 b. Phenylpropanoid pathway for lignin biosynthesis visualized in Mapman. Expression of genes at 14 dap in *B. napus* genotypes, Express617 relative to V8. Red color show higher expression of genes and blue means down-regulation of genes‘ expression in Express617.

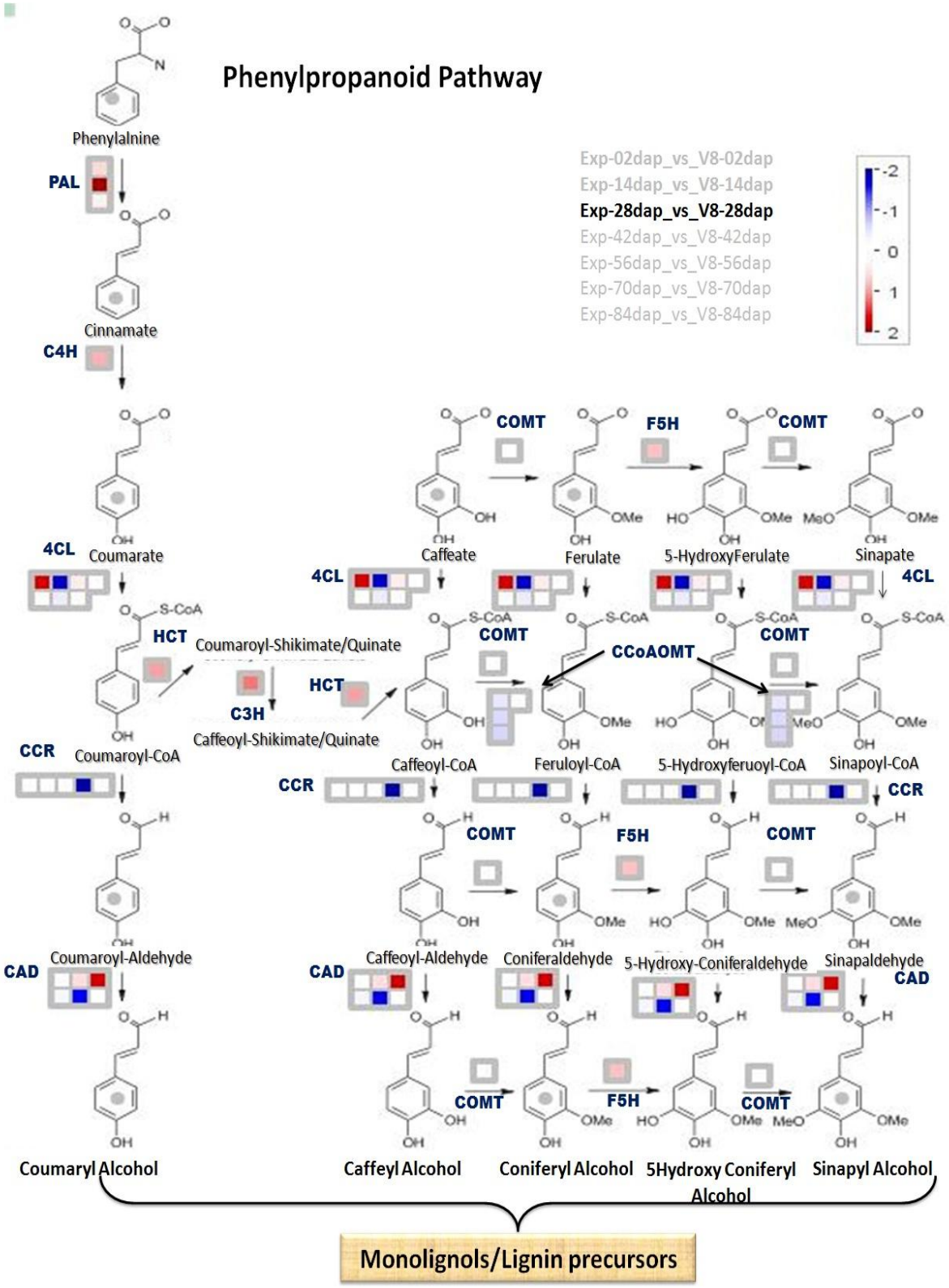

Fig 3.2 c. Phenylpropanoid pathway for lignin biosynthesis visualized in Mapman. Expression of genes at 28 dap in *B. napus* genotypes, Express617 relative to V8. Red color show higher expression of genes and blue means down-regulation of genes expression in Express617

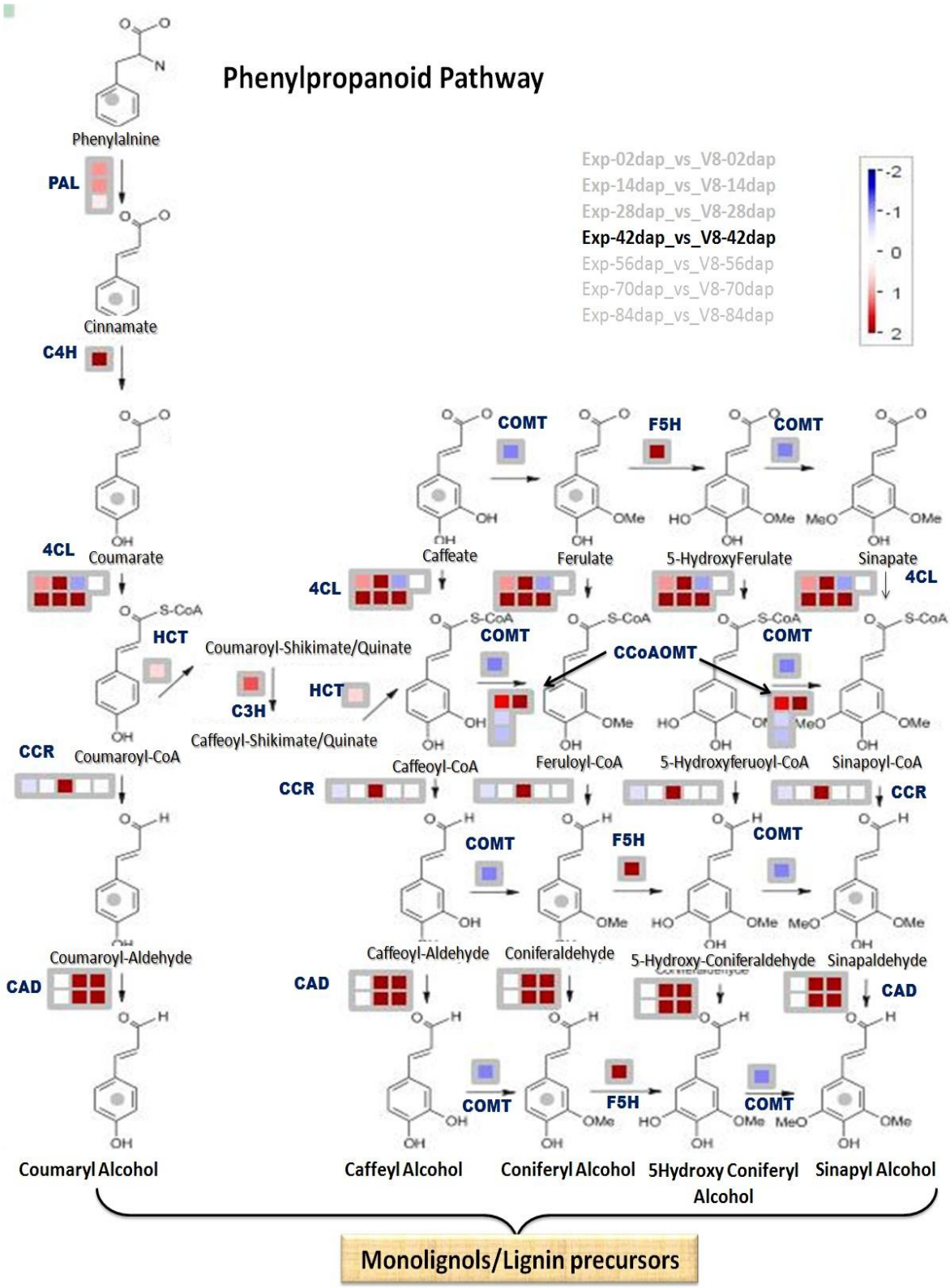

Fig 3.2 d. Phenylpropanoid pathway for lignin biosynthesis visualized in Mapman. Expression of genes at 42 dap in *B. napus* genotypes, Express617 relative to V8. Red color indicates higher expression of genes and blue means down-regulation of genes expression in Express617

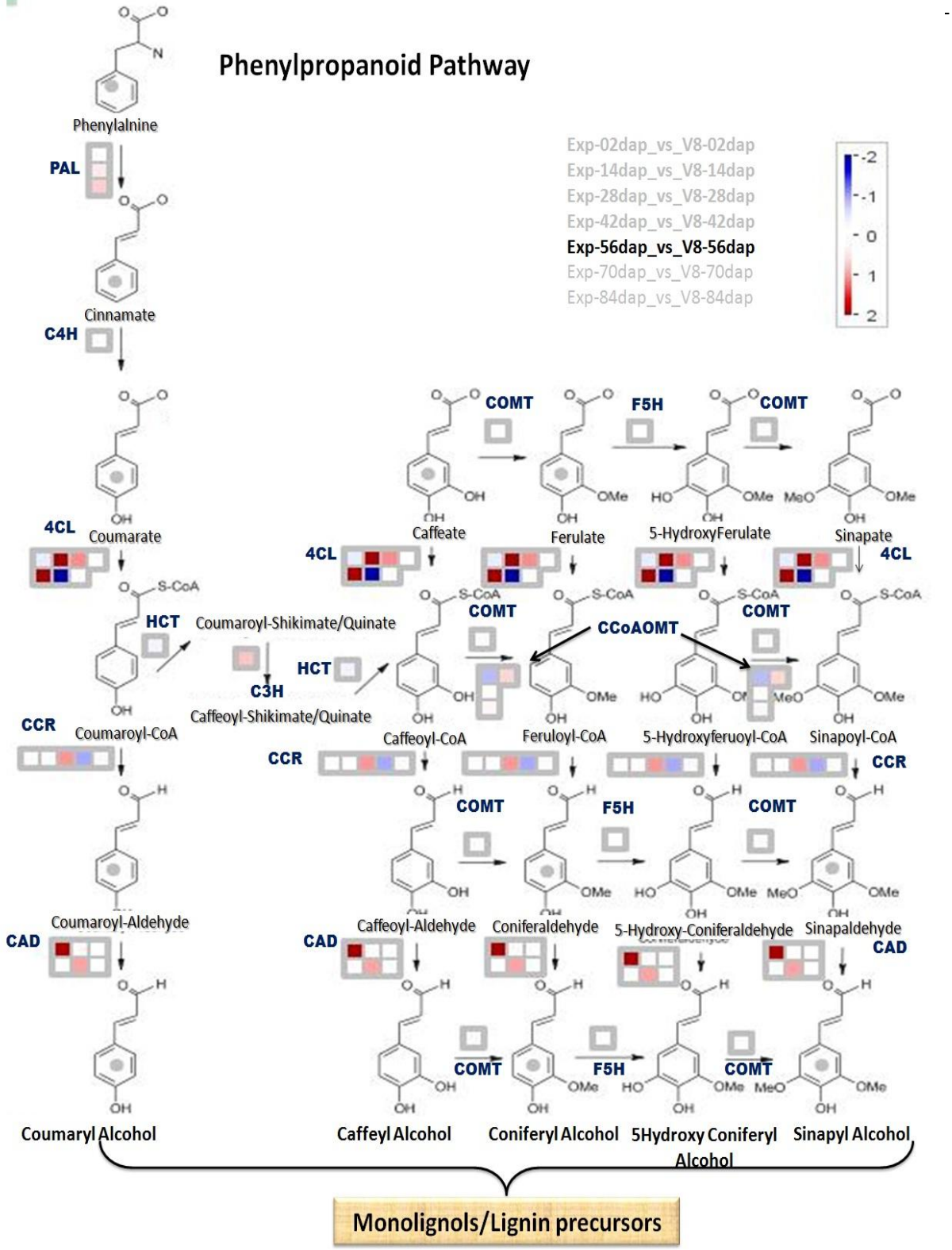

Fig 3.2 e. Phenylpropanoid pathway for lignin biosynthesis visualized in Mapman. Expression of genes at 56 dap in *B. napus* genotypes, Express617 relative to V8. Red color show higher expression of genes and blue means down-regulation of genes‘ expression in Express617.

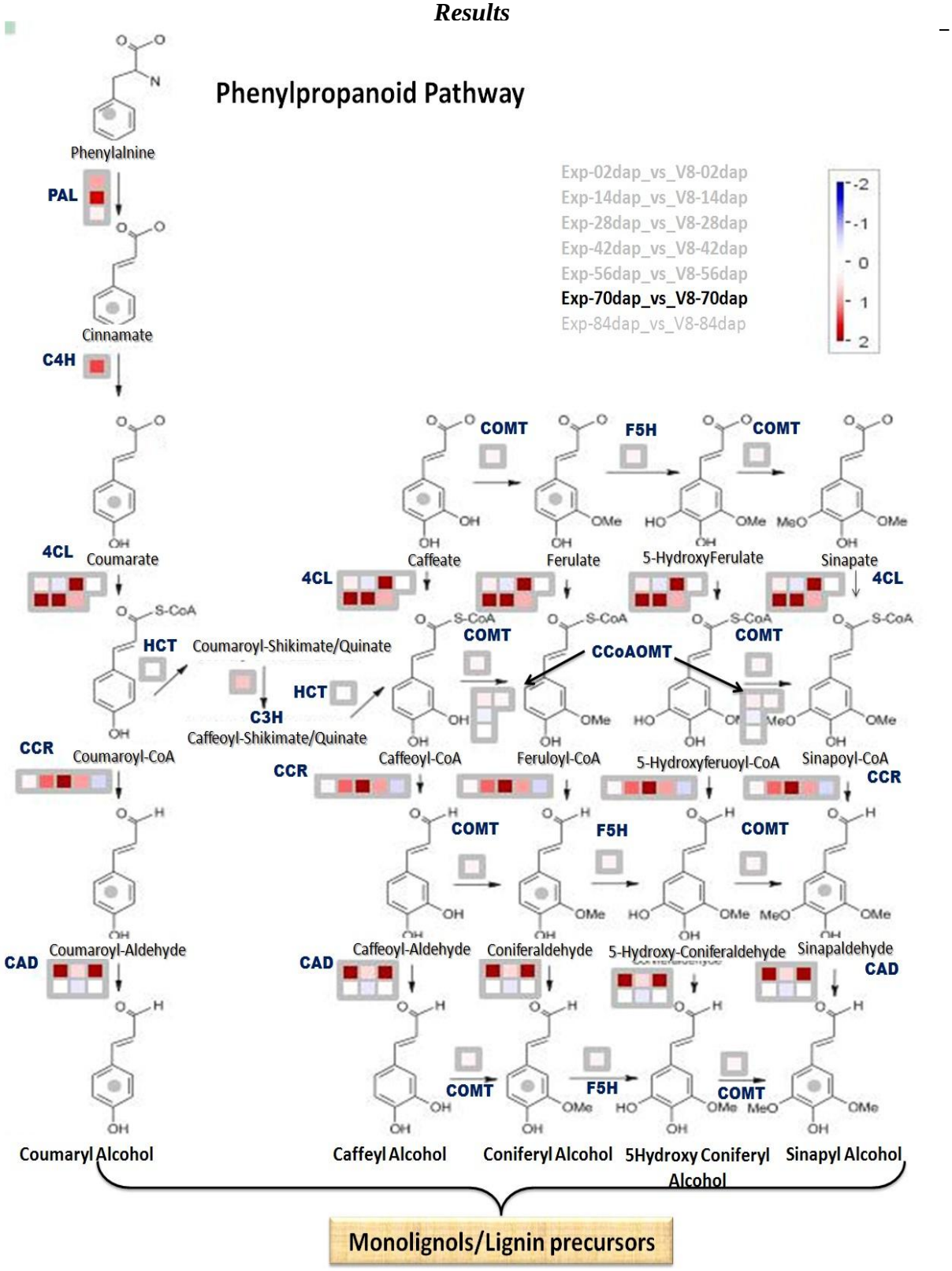

Fig. 3.2 f. Phenylpropanoid pathway for lignin biosynthesis visualized in Mapman. Expression of genes at 70 dap in *B. napus* genotypes, Express617 relative to V8. Red color show higher expression of genes and blue means down-regulation of genes expression in Express617

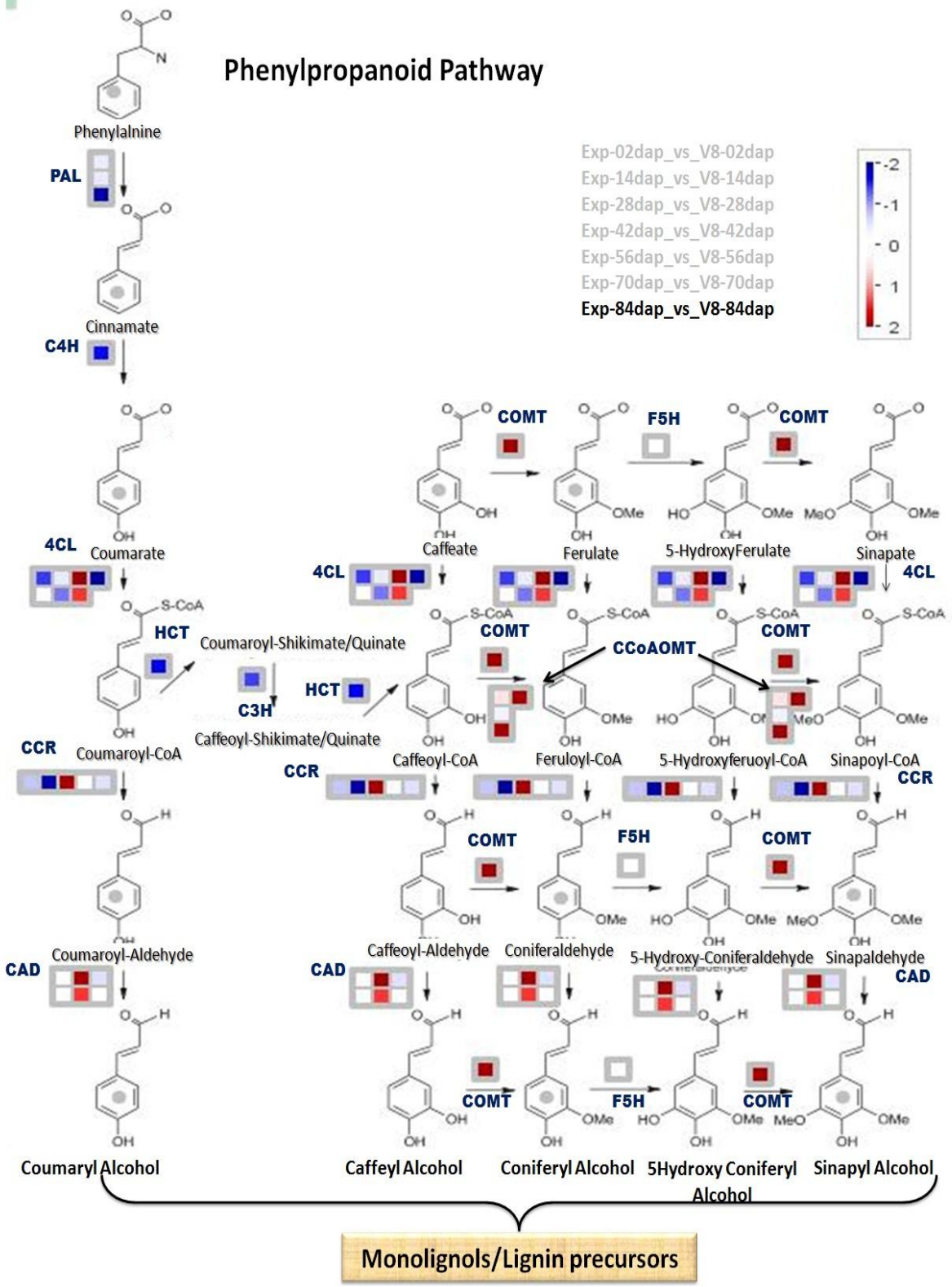

Fig. 3.2 g. Phenylpropanoid pathway for lignin biosynthesis visualized in Mapman. Expression of genes at 84 dap in *B. napus* genotypes, Express617 relative to V8. Red color show higher expression of genes and blue means down-regulation of genes‘ expression in Express617.

CCR is the first enzyme of the monolignol specific part of the lignin biosynthetic pathway which catalyzes the conversion of cinnamoyl-CoA esters to their respective cinnamaldehydes. Three CCR related genes along with CCR1 and CCR2 genes were found in UGs set. CCR1 show high expression in both genotypes during seed development and higher expression in Express617 compared to V8. Expression of CCR2 was not detected in both genotypes from 28-56dap while down-regulation was observed in Express617 at 84dap.

CAD genes are catalyzing the last step in monolignol biosynthesis, and are responsible for final reduction of cinnamyl aldehydes into their corresponding alcohols which are final precursors of monolignols. Six CAD genes were found in whole UGs set. Expression of CAD1 was not detected and CAD5 appeared only at 84dap in V8. CAD4 showed higher level of expression in Express617 and in V8 no expression was found at 42 and 84dap. CAD7 and CAD9 genes expression was detected only until 28dap in V8 while in Express617 CAD9 expression was detected until 56dap. In V8, at 42dap no expression was detected from all CAD genes (Fig. 3.3).

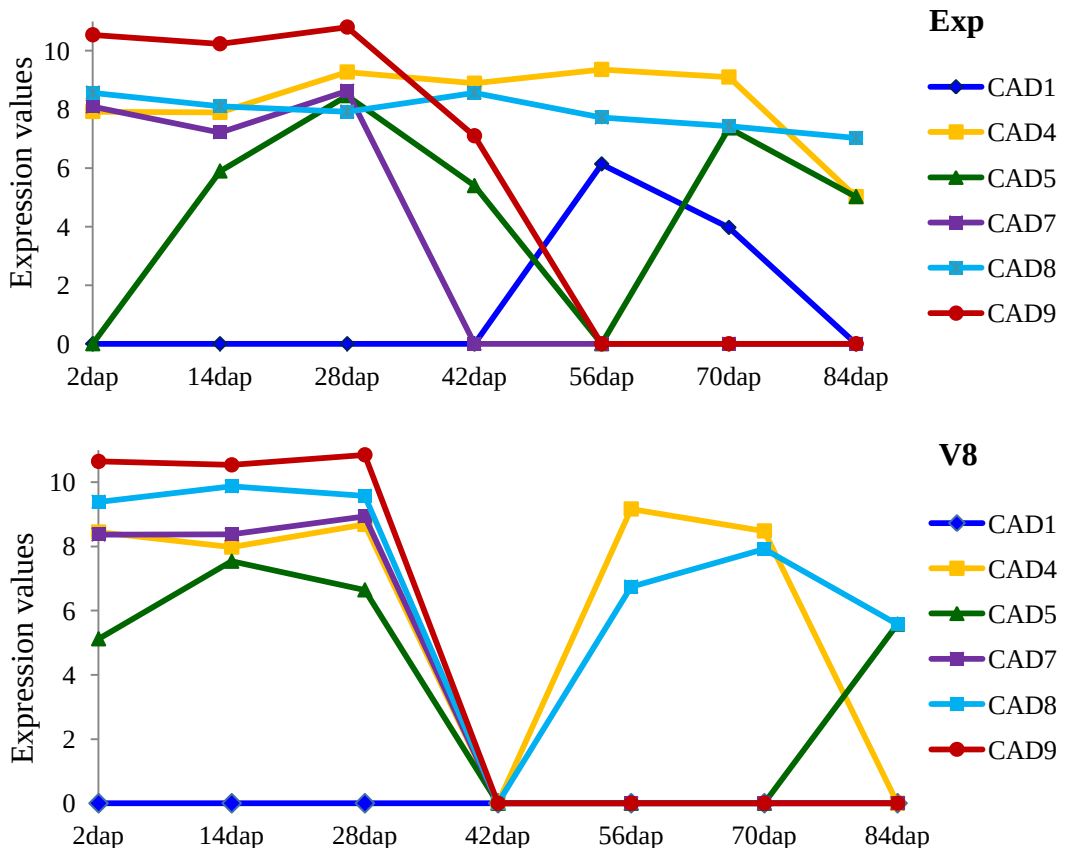

Fig.3.3 Expression of CAD genes in Express617 (Exp) and V8 during seed development from 2nd day after pollination (dap) to 84 dap

3.1.3 Transcription factors involved in phenylpropanoid pathway regulation

Expression of six MYB family transcription factors (TFs) was detected which are involved in phenylpropanoid pathway regulation. All of these TFs appeared to show higher expression level at 70dap in Express617 compare to other developing time points. MYB61 showed high level of expression in both genotypes with a slightly down-regulation in V8 compared to Express617.

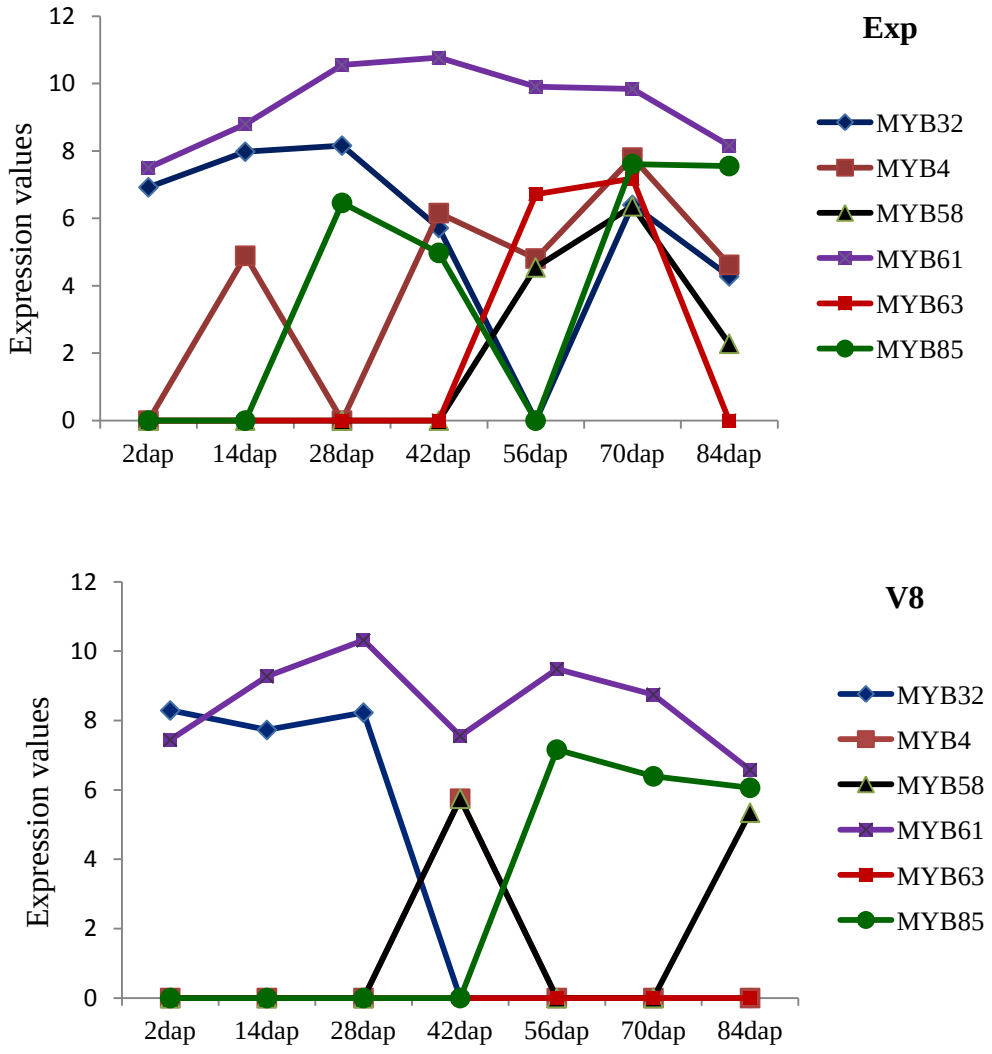

Fig.3.4 Expression of transcription factors involved in phenylpropanoid pathway regulation in Express617 and V8 during seed development from 2nd day after pollination (dap) to 84 dap

Expression of MYB63 was not detected in V8 and MYB4 was only detectable at 42dap. MYB32 appeared only from 2-28dap and MYB85 expression was detected only from 56-84dap. In Express617, MYB32 expression was detectable from 2-42dap and MYB85 appeared from 42-56 and 70-84dap, MYB63 expression was found only from 56-70dap and

MYB4 expression was detected at 14dap and then from 42-84dap. MYB58 expression was detectable from 56-84dap in Express617 and in V8 it appeared only at 42 and 84dap (Fig3.4).

3.1.4 Investigation of genes involved in glucosinolate metabolism

Rapeseed meal is highly regarded as a component of animal feed with high protein content and a desirable amino acid profile. Glucosinolate (GSL) concentration in seeds affects the value of the meal and reduces the amount that can be used in animal feed formulations. Express617 is 00 quality cultivar of *B. napus* which has 20.63 uMol/g seed dry weight total GSL cotent while V8 has very high amount of total GSL content (48.75 uMol/g seed dry weight) (Basunanda et al., 2007). Genes annotated to GSL biosynthesis and degradation pathway were visualized in Mapman. Detailed pathway with genes specific to different stepsin GSL pathway are not available in Mapman genes annotated to this pathway were exported and their up and down (red to blue color) regulation is presented in in Tables.

Biosynthesis of GSL can be divided into three phases:

(i) amino acid side chain elongation

(ii) Glucosinolate core structure formation from amino acid moiety

(iii) secondary modification

(iv) GSL degradation enzymes

(i) Amino acid side chain elongation

Bile acid:sodium symporter family protein 5 (BAT5), methylthioalkylmalate synthase (MAM), and branched-chain aminotransferase (BCAT), are involved in elongation of methionine. Isopropylmalate isomerase (IPMI) genes are also involved in Leu biosynthetic pathway and the Met chain elongation cycle for glucosinolate formation. IPMI LSU1 is the large subunit of enzyme and three sub units IPMI SSU1, SSU2 and SSU3 are reported for their role in amino acid elongation. All these genes show down regulation in Express617 until 28dap Table 3.5.1. BAT5 is up-regulated at 70 and 84dap. BCAT4 and MAM1 show very strong down regulation in Express617 during all developing time points. BCAT4 has slight up-regulation at 84dap. IPMI LSU1 and SSU2 have lower expression level until 28dap and SSU2 has high expression from 42 to 70dap.

Table 3.5.1 Expression of GSL pathway genes involved in amino acid chain elongation. Expression value is log2 transformed and ratio was calculated between Express617 and V8 at each seed development time point. Red color show higher expression of genes and blue means down-regulation of genes expression in Express617

Side Chain Elongation

BinCode	AGI	Gene	2dap	14dap	28dap	42dap	56dap	70dap	84dap
16.5.1.4.1	at4g12030	BAT5	0.000	-1.061	-7.059	4.392	-0.031	6.137	5.503
16.5.1.1.1.1	at3g49680	BCAT3	-1.521	1.484	-6.059	0.131	-0.294	5.289	-0.197
16.5.1.1.1.1	at3g19710	BCAT4	-8.580	-0.587	-0.489	-3.053	-1.435	-0.317	2.152
16.5.1.1.1.2	at5g23010	MAM1	-8.028	-1.068	-0.288	0.000	-6.162	0.000	0.000
16.5.1.1.1.3	at4g13430	IPMI LSU1	-0.852	-1.370	0.263	7.038	-0.440	1.415	0.020
16.5.1.1.1.4	at2g43100	IPMI SSU2	-8.121	-1.726	-0.082	6.392	6.132	5.289	-2.882

(ii) Glucosinolate core structure formation from amino acid moiety

Ten genes were annotated as group of genes responsible for GSL core structure formation. Core structure formation is accomplished via oxidation by cytochromes P450, CYP79 and CYP83 which are followed by C-S lyase (*SUR1*), glycosyltransferase (*UGT74B1* & *UGT74C1*) and sulfortransferase (*SOT16, SOT17, SOT18*) in five steps. CYP79 cytochromes expression was detected only in early time points 14 & 28dap with slight up-regulation, *CYP79B2* expression was also appeared at 70dap. *CYP83A1* show lower expression from 2-42 dap while CYP83B1 show slight up-regulation from 2-28dap and at 84 dap and strong up-regulation at 42 and 70 dap in Express617. Sulfotransferase family members *SOT16, SOT17, SOT18* also showed differential expression during seed developmental points. *SOT16* has a bit higher expression from 2-28dap and at 70 -84 dap and lower expression at 42 and 56dap. Expression of *SOT17* was only detectable at 14, 28 and at 84 dap its show highest expression in Express617 relative to V8. *SOT18* was strongly down regulated at 14dap and show only slight higher expression at 70dap. *SUR1* gene showed down-regulation from 2-70dap and a minor up-regulation at 84dap. *UGT74B1* & *UGT74C1* showed down regulation during whole seed development period in Express617 with a slight higher expression of *UGT74B1* at 84dap (Table3.5.2).

Table 3.5.2 Expression of GSL pathway genes involved in core structure formation. Expression value is log2 transformed and ratio was calculated between Express617 and V8 at each seed development time point. Red color show higher expression of genes and blue means down-regulation of genes expression in Express617

Core Structure Formation

BinCode	AGI	Gene	2dap	14dap	28dap	42dap	56dap	70dap	84dap
16.5.1.1.3.1	at4g39950	CYP79B2	0.000	0.162	0.985	0.000	0.000	1.382	0.000
16.5.1.1.3.2	at2g22330	CYP79B3	0.000	0.162	0.985	0.000	0.000	0.000	0.000
16.5.1.1.1.7	at4g13770	CYP83A1	-4.007	-1.211	-0.366	-5.746	0.000	0.000	1.984
16.5.1.1.4.1	at4g31500	CYP83B1	1.624	0.093	0.453	6.392	0.000	5.552	2.057
16.5.1.1.3.3	at1g74100	SOT16	0.396	2.109	0.531	-0.933	-0.101	0.110	1.440
16.5.1.1.1.9	at1g18590	SOT17	0.000	-0.423	1.570	0.000	0.000	0.000	4.281
16.5.1.1.1.9	at1g74090	SOT18ST5b	0.000	-6.314	-2.184	-1.588	-1.423	1.268	-0.120
16.5.1.1.4.2	at2g20610	SUR1	-0.065	-0.101	-1.079	-1.319	-1.570	-0.326	0.954
16.5.1.1.4.3	at1g24100	UGT74B1	-2.485	0.065	-0.218	-0.769	0.000	0.000	0.762
16.5.1.1.1.8	at2g31790	UGT74C1	-6.928	-3.196	-8.428	-0.691	-1.031	-2.748	-2.297

(iii) Secondary modification

Last crucial enzymatic reactions on intact GSL are their secondary modification, before their transportation to sink or degradation by myrosinases. Side chain modification begins with the oxidation of sulphur in the methylthio-precursor to produce methylsulfinyl and then methylsulfonyl moieties which is catalyzed by flavin monooxygenase FMO GS-OX. GSL-OH dependent hydroxylation is responsible for conversion of alkenyl to hydroxy aliphatic GSL (Table3.5.3). FMO GS-OX5 and GSL-OH showed down regulation during seed developmental time points in Express617 relative V8. A binary reaction controlled by AOP genes changes methylsulfinyl to alkenyl- and to hydroxyl- aliphatic GSL. AOP1 and AOP3 expression was down-regulated at 14 dap and up-regulation was observed from 28 to 84 dap. AOP3 showed strong up-regulation at 84dap in Express617.CYP81F2 encoding a cytochrome P450 monooxygenase, catalyzes the conversion of tryptophan derived indole-3-yl-methyl to 4-hydroxy-indole-3-yl-methyl glucosinolate. Expression of CYP81F2 was only detected at 84 dap with a significant up-regulation in Express617 relative V8.

Table 3.5.3. Expression of GSL metabolic pathway genes involved in secondary modifications. Expression value is log2 transformed and ratio was calculated between Express617 and V8 at each seed development time point. Red color show higher expression of genes and blue means down-regulation of genes expression in Express617

Secondary modification									
BinCode	**AGI**	**Gene**	**2dap**	**14dap**	**28dap**	**42dap**	**56dap**	**70dap**	**84dap**
16.5.1	at4g03070	AOP1	0.000	-2.075	0.995	0.479	0.567	3.609	0.753
16.5.1.1.1.11	at4g03050	AOP3	0.000	-0.838	1.107	0.424	1.908	1.966	6.017
16.5.1.1.3.4	at5g57220	CYP81F2	0.000	0.000	0.000	0.000	0.000	0.000	4.281
16.5.1.1.1.10	at1g12140	FMO GS-OX5	-0.818	-0.450	0.134	-1.394	-0.352	-0.961	-0.224
16.5.1.1.1.13	at2g25450	GSL-OH	0.000	-1.713	0.500	1.231	-1.200	-0.168	-0.801

(iv) GSL degradation enzymes

Ten genes were annotated in UGs dataset as putative myrosinases or myrosinases associated proteins involved in hydrolysis of GSL (Table3.5.4). *EPITHIOSPECIFIER MODIFIER1* (ESM1) showed higher expression in Express617 relative to V8 at 28dap and from 56 to 84dap. Epithiospecifier protein (ESP) has low expression only at 14dap and up-regulation was detected in Express617 at all other developing time points. Myrosinase associated protein MyAP1 and MyAP2 showed down-regulation from 2-28dap and then up-regulated in Express617 until the 84dap, MyAP1 showed strong up-regulation at 42dap. *MYROSINASE-BINDING PROTEIN (MBP1)* was down-regulated from 2-28dap and no expression was detected from 42-70dap and up-regulation was found at 84dap in Express617. *NITRILE SPECIFIER PROTEINS,* NSP2 and NSP5 showed low level of expression at early time points from 2-42dap and at 84dap while from 56-70dap higher level of expression was observed in Express617. S-glycosyl hydrolase PEN2 (*PENETRATION* 2) showed up-regulation from 2-14dap and at 70dap and strong down-regulation was observed at 56dap. Expression of β-thioglucoside glucohydrolase TGG1 and TGG2 was detected with a strong up-regulation of TGG2 at 42dap while TGG1 was down-regulated at 42dap.

Table 3.5.4. Expression of genes in GSL degradation. Expression value is log2 transformed and ratio was calculated between Express617 and V8 at each seed development time point. Red color show higher expression of genes and blue means down-regulation of genes expression in Express617

Glucosinolates Degradation									
BinCode	**AGI**	**Gene**	**2dap**	**14dap**	**28dap**	**42dap**	**56dap**	**70dap**	**84dap**
16.5.1.3.1	at3g14210	ESM1	0.000	0.000	3.460	0.000	1.344	0.102	3.112
16.5.1.3.2.1	at1g54040	ESP	0.035	-1.733	0.769	2.427	1.008	1.512	0.555
16.5.1.3.1	at1g54010	MyAP1	-1.422	0.000	-5.059	6.852	0.000	1.159	2.270
16.5.1.3.1	at1g54020	MyAP2	-1.101	-2.509	-1.461	0.898	0.291	0.368	2.860
16.5.1.3.1	at1g52040	MBP1	-0.274	-1.050	-2.211	0.000	0.000	0.000	2.959
16.5.1.3.3	at3g44300	NIT2	-1.788	-1.512	0.101	-0.110	-1.179	0.381	-0.846
16.5.1.3.3	at3g44320	NIT3	-1.287	-0.974	-1.002	5.392	-0.825	1.089	-0.252
16.5.1.3.3	at5g22300	NIT4	-5.706	1.162	0.400	0.000	0.000	3.967	-0.730
16.5.1.3.2	at2g33070	NSP2	-0.773	-1.167	-0.256	0.304	0.766	2.542	-0.743
16.5.1.3.2	at5g48180	NSP5	-0.832	-0.709	-0.015	-2.906	0.568	0.901	-1.634
16.5.1.3.1	at2g44490	PEN2	1.152	1.319	-2.015	-2.132	-6.747	4.552	-1.882
16.5.1.3.1.1	at5g26000	TGG1	-0.097	0.147	-2.683	-0.782	1.804	-0.069	0.267
16.5.1.3.1.1	at5g25980	TGG2	-0.422	-0.160	0.000	6.852	3.626	1.184	0.527

3.1.5 Transcription factors regulating GSL metabolic pathway

Expression of three MYB family transcription factors, MYB28, MYB34 and MYB51 and OBP2/DOF1.1 were detected. MYB28 expression was at 14dap in Express617 and in V8 it was from 2-28dap. MYB34 expression was not detected in V8 while in Express617 it appeared at 2, 28 and 84 (Fig3.1.5). MYB51 was appeared from 2-42dap and no expression was detected at 56dap in Express617. In V8 higher expression of MYB51 was found at 42 dap compared to the other time points. OBP2/DOF1.1 expression was detected during whole seed developmental stages in Express617 while its expression was only detected from 2-28dap in V8.

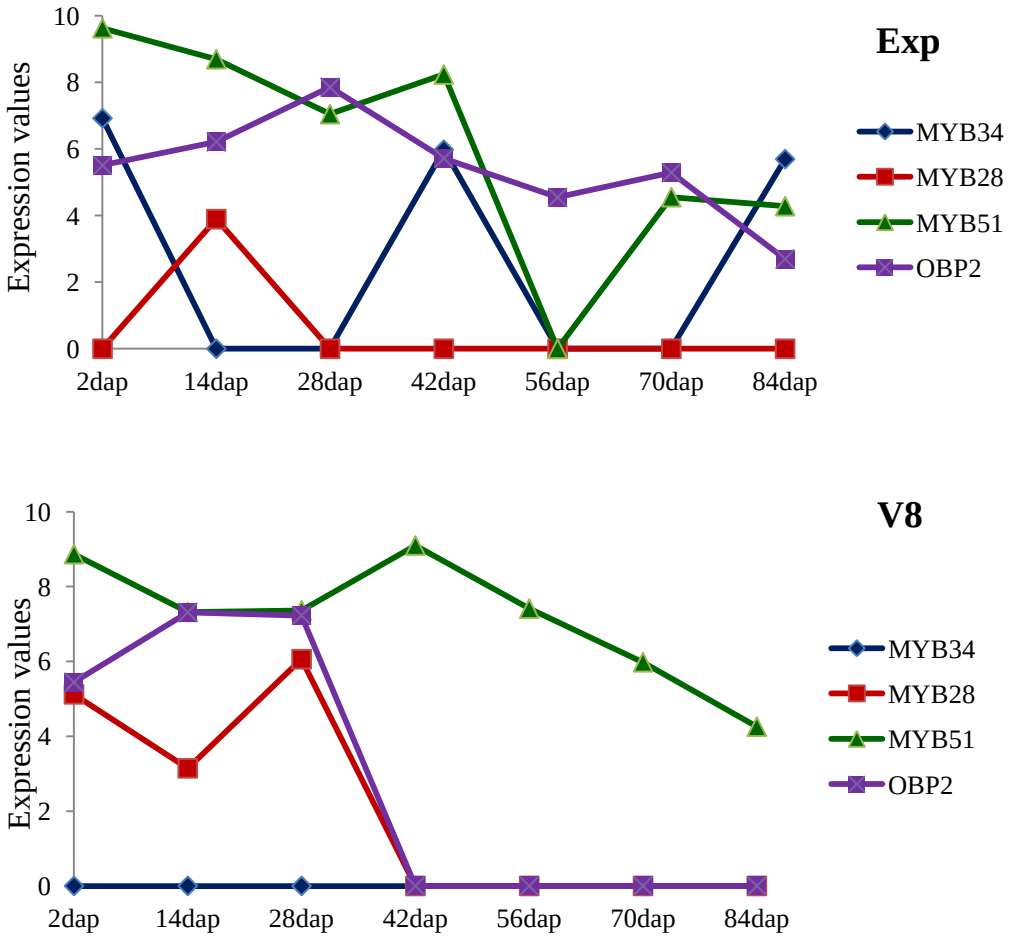

Fig.3.5 Expression of transcription factors involved in GSL pathway regulation in Express617 (Exp) and V8 during seed development from 2nd day after pollination (dap) to 84 dap

3.2 Root architectural traits

Root architectural traits were studied in two sets of *B. napus* genotypes, Express617 x V8 DH population (94 lines) and diversity set include winter, spring, vegetable and swede type. Five root traits were selected for phenotypic analysis which includes primary root length (PRL), rate of primary root growth (RoG), lateral root length (LRL), lateral root number (LRN) and lateral root density (LRD).

3.2.1 Phenotypic variation and correlations among root architectural traits

Whole data set for root traits from Express 617 x V8 DH population and diversity set accessions was subjected to analysis of variance and correlation among root traits. *B. napus* diversity set approx. 500 inbred lines was subjected to STRUCTURE software to get its distribution in sub-population sets. Diverse rapeseed genotypes were distributed into three sub population set; winter oilseed rape (WOSR), spring oilseed rape (SOSR) and swede type with some vegetables. Broad sense heritability was calculated from genotypic and phenotypic variance in bi-parental DH population from Express617 x V8. Lateral root traits showed higher heritability, LRN (25%), LRL (36%) and LRD (26%) as compared to primary root length (20%) and primary root growth rate (13%).

(i) Primary root length (PRL)

The primary root length in Express 617 x V8 DH population was normally distributed (Fig. 3.6 a). Minimum value of PRL was 5.778cm in DH78 and maximum was 13.567cm in DH34. Parental lines are lying almost around the mean value (10.11cm) in which V8 had 9.708 cm and Express 617 had 10.172 cm. PRL showed strong correlation to rate of primary root growth, lateral root length and number, but negative correlation was observed with lateral root density in this population (Fig 3.11). In three sub-populations of diversity set, normal distribution was observed for primary root length (Fig. 3.6 b). Winter genotypes showed a range from 4.204 cm (minimum) to 13.373 cm maximum length of primary roots while minimum value was 3.408 cm in SOSR with maximum value of 11.227 cm. In Swede and vegetables type rapeseed genotypes, minimum primary root length was 3.629 cm and maximum length was 10.519 cm. In three sub populations this trait showed significant positive correlation with primary root rate of growth (RoG), lateral root number (LRN) and length (LRL) and a negative correlation was observed with lateral root density (LRD) (Table 3.6).

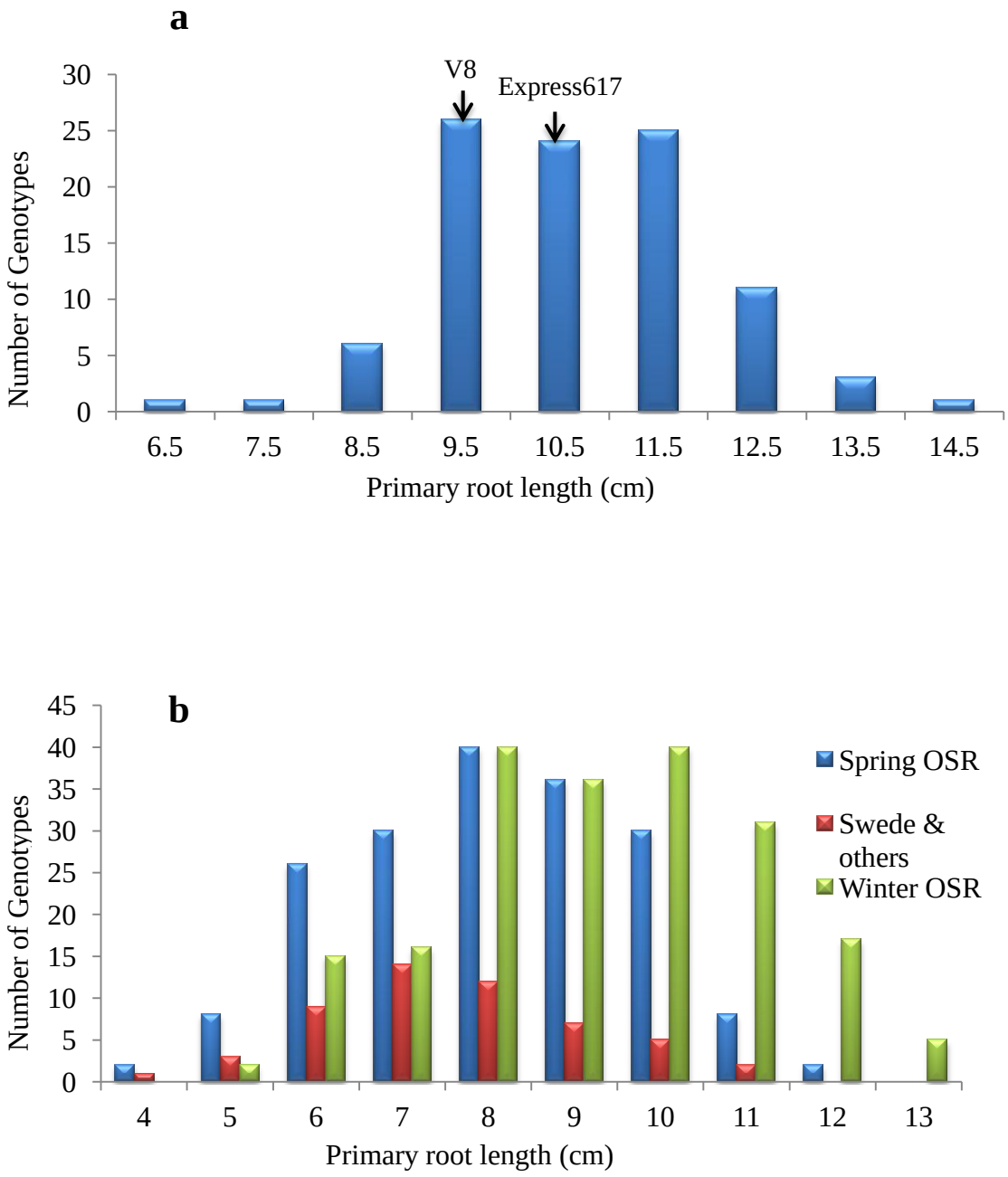

Fig 3.6 Distribution of primary root length (PRL) in (**a**) 94 DH lines from the population of Express 617× V8. PRL values for cross parents are marked by arrows on respective columns and (**b**) *B. napus* diversity set showed distribution of PRL in three sub-populations which are composed of winter, spring and swede with some vegetable rapeseed genotypes.

(ii) Rate of primary root growth (RoG)

Primary root length was recorded at three growth time points (3, 5 and 7 DAS) for the calculation of rate of growth per day for each plant from each line. The distribution of rate of primary root growth was slightly skewed to the right in the DH population (Fig. 3.7 a). Lowest rate was 0.981cm per day observed in DH78 while highest rate of primary root growth was observed in DH203 which was 2.336cm per day. DH34 which showed the greatest PRL in DH population showed the RoG of 2.328cm per day, approximately equal to maximum rate of growth. Parental genotypes of this population had 1.836 and 2.030 cm per day for V8 and Express617 respectively. RoG also showed similar pattern of correlation as it was observed for PRL in this DH population (Fig 3.11).

Winter, spring and other rapeseed genotypes in diversity set showed normal distribution of rate of primary root growth in three sub-populations (Fig. 3.7, b). Minimum rate of growth was similar in three sub-populations (0.637 cm/day) while winter rapeseed genotypes showed maximum RoG of 2.419 cm/day and in spring rapeseed and swede group maximum rate was 2.26 and 1.83 cm/day respectively. RoG also showed negative correlation with LRD in these three sub-populations, but significant positive correlation was observed with other root traits (Table 3.6).

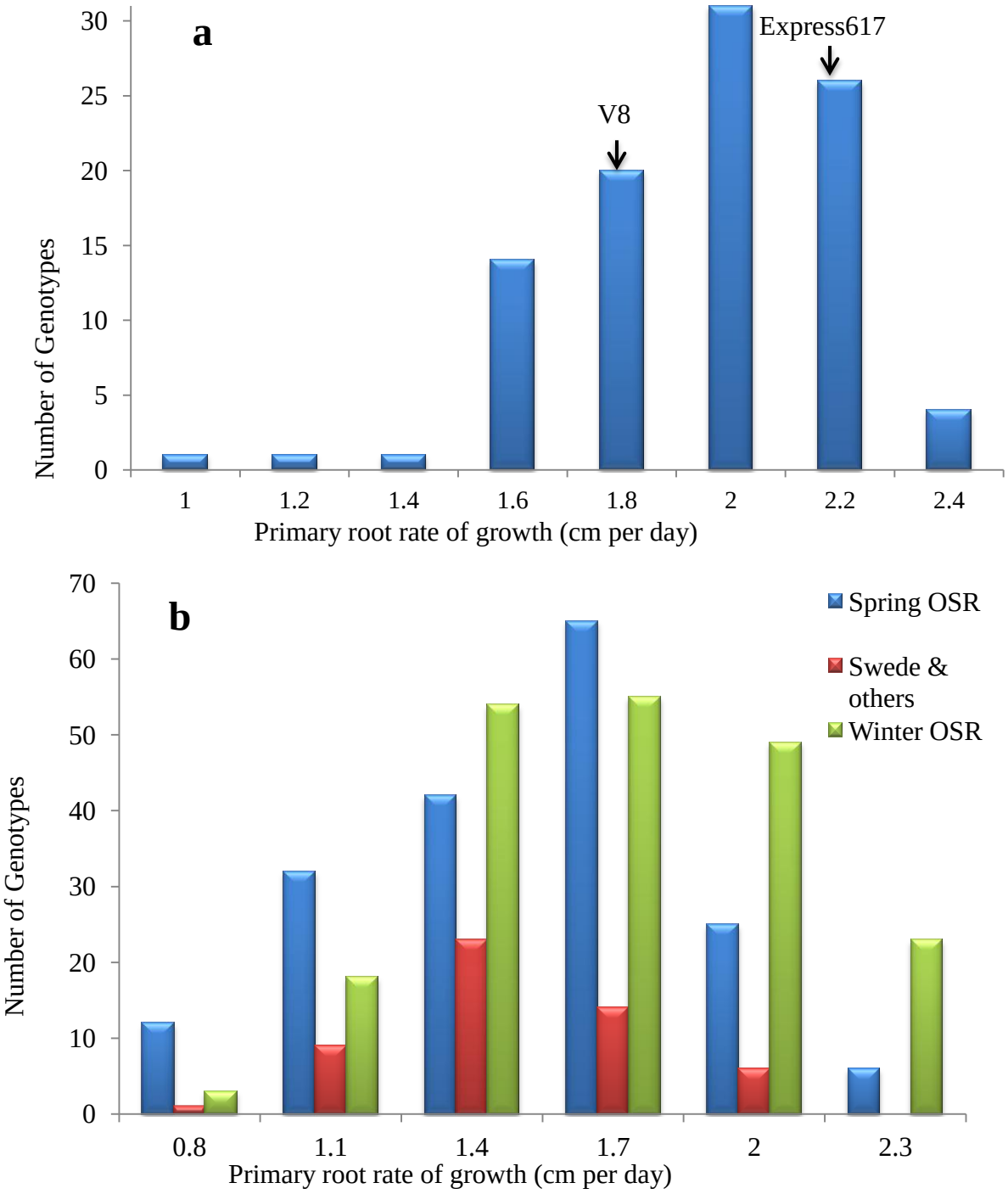

Fig 3.7 Distribution of Primary root rate of growth (RoG) in (a) 94 DH lines from the population of "Express 617"× "V8". RoG values for cross parents are marked by arrows on respective bars and (b) *B. napus* diversity set showed distribution of RoG in three sub-populations which composed of winter, spring and swede with some vegetable rapeseed genotypes.

.

(iii) Lateral root number (LRN)

Lateral root number was ranged from 3(DH2) to 17(DH593) lateral roots in DH population where in parental genotypes 11 LR were observed in V8 and Express617 had 9 lateral roots per plant. Distribution of LRN in DH population is also relatively normal (Fig. 3.8 a). LRN showed strong positive correlation with all other observed root architecture traits in DH population (Fig. 3.11). Distribution of LRN is slightly skewed to left side in all three sub-populations of rapeseed genotypes diversity set (Fig. 3.8 b). Minimum two lateral roots were observed in three sub sets and maximum 22 lateral roots were observed in SOSR. WOSR and Swedes showed maximum 18 lateral roots. LRN showed significantly positive correlation with all other root traits in all these three sub-populations (Table 3.6).

(iv) Lateral root length (LRL)

Total lateral root length per plant showed a wide range from 3.2 cm (DH2) to 22.39cm (DH605) with a skewed distribution to the left side as many DH lines showed greater LRL compared to their parental genotypes (Fig. 3.9, a). Greater LRL was observed in V8 (16.92cm) compared to Express617 (10.21cm). LRL also showed positive correlation to all other observed root traits similar to LRN (Fig. 3.11).

Similar pattern of skewed distribution was observed in three sub-population of diversity set as showed by DH population (Fig. 3.9 b). Maximum lateral root length was observed in WOSR (31.387cm), SOSR, swede and other vegetable rapeseed genotypes showed 24.74 and 20.245 cm maximum total lateral root length per plant respectively. Minimum LRL was observed in swede type rapeseed (0.862cm) while minimum LRL is similar in WOSR and SOSR (1.26 and 1.06cm respectively). LRL showed significant positive correlation with all observed root traits in WOSR, SOSR and Swedes (Table 3.6).

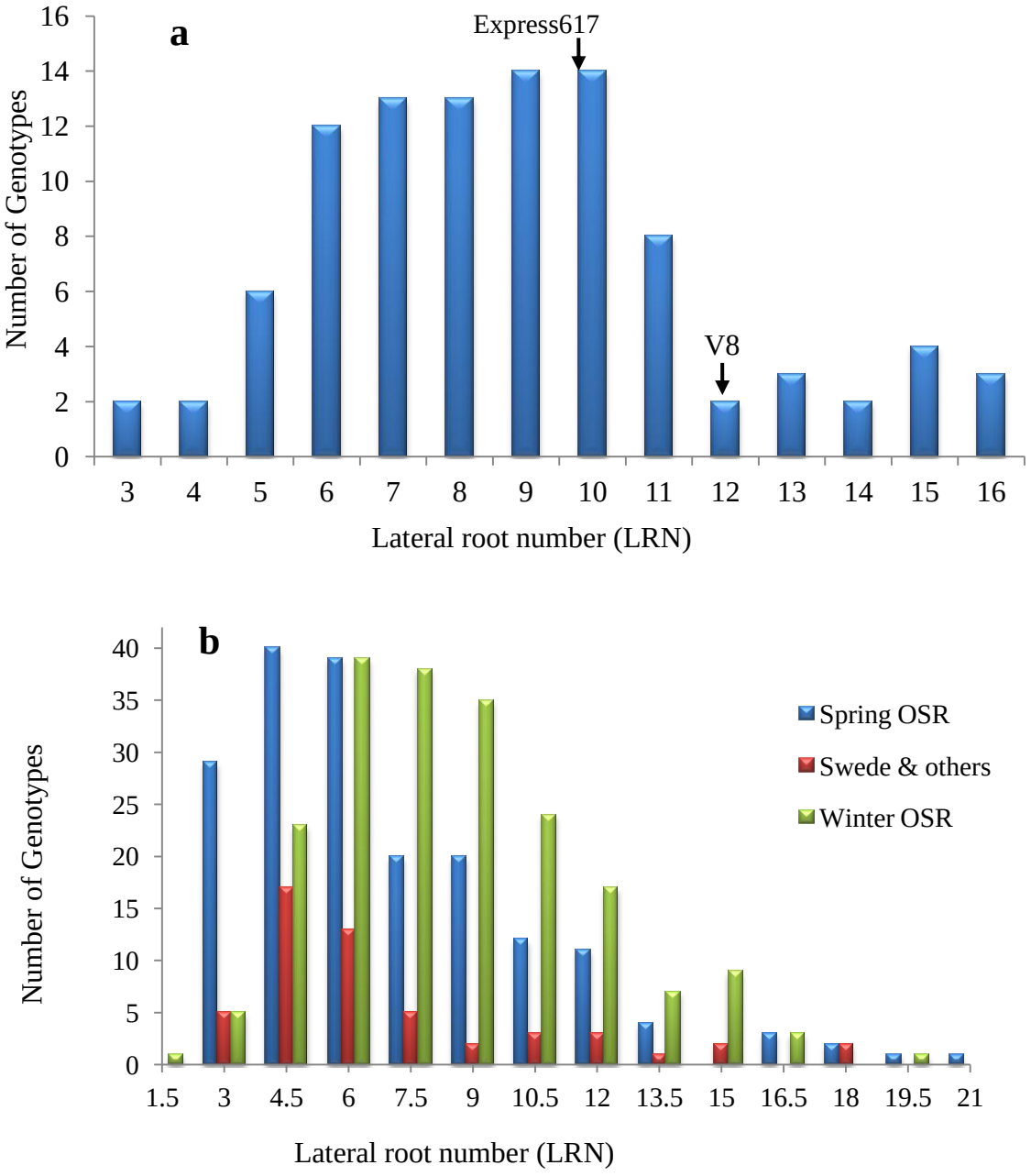

Fig 3.8 Distribution of lateral root number (LRN) in (a) 94 DH lines from the population of "Express 617"× "V8". LRN values for cross parents is marked by arrows on respective bars and (b) *B. napus* diversity set showed distribution of LRN in three sub-populations which composed of winter, spring and swede with some vegetable rapeseed genotypes.

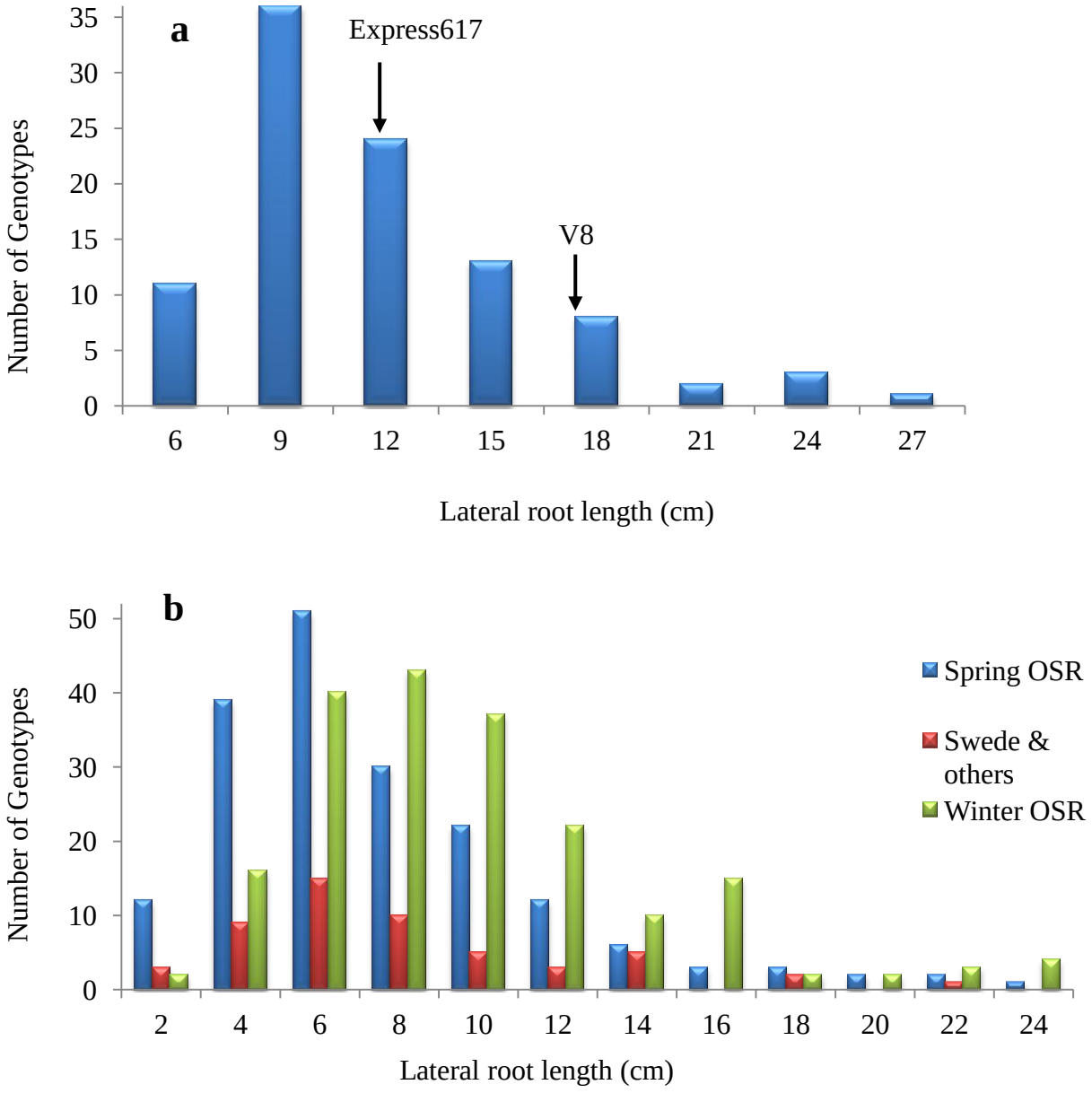

Fig 3.9 Distribution of lateral root length (LRL) in (a) 94 DH lines from the population of "Express 617"× "V8". LRN values for cross parents is marked by arrows on respective bars and (b) *B. napus* diversity set showed distribution of LRL in three sub-populations which composed of winter, spring and swede-type with some vegetable rapeseed genotypes.

(v) Lateral root density (LRD)

Lateral root density is a relative value calculated as a function of lateral root number divided by primary root length (root/cm) to get idea about strength of root architecture. Normally distributed LRD showed variation in DH population from 1.6 cm^{-1} (DH98) to 0.38 cm^{-1} (DH2) in which parental genotypes showed similar LRD (1.1 cm^{-1}) and be positioned approximately in the mean value of whole population (Fig.3.10, a). LRD showed significant positive correlation with other recorded lateral roots traits but a negative correlation was observed with the PRL and primary root rate of growth in DH population (Fig.3.11).

Distribution of LRD is skewed to left side in all three sub-population of rapeseed diversity set (Fig.3.10, b). Swede type rapeseed showed highest LRD of 3.364 cm^{-1}, in WOSR highest LRD observed was 3.15 cm^{-1} and in SOSR highest LRD was 2.42 cm^{-1}. Minimum LRD in swedes was 0.334 cm^{-1} while WOSR and SOSR showed minimum 0.252 cm^{-1} and 0.212 cm^{-1} LRD respectively. Similar to the DH population, WOSR, SOSR and swedes inbred lines also showed significant negative correlation to the primary root traits. Strong positive correlation of LRD was observed in all three sub-populations with LRL and LRN (Table 3.6).

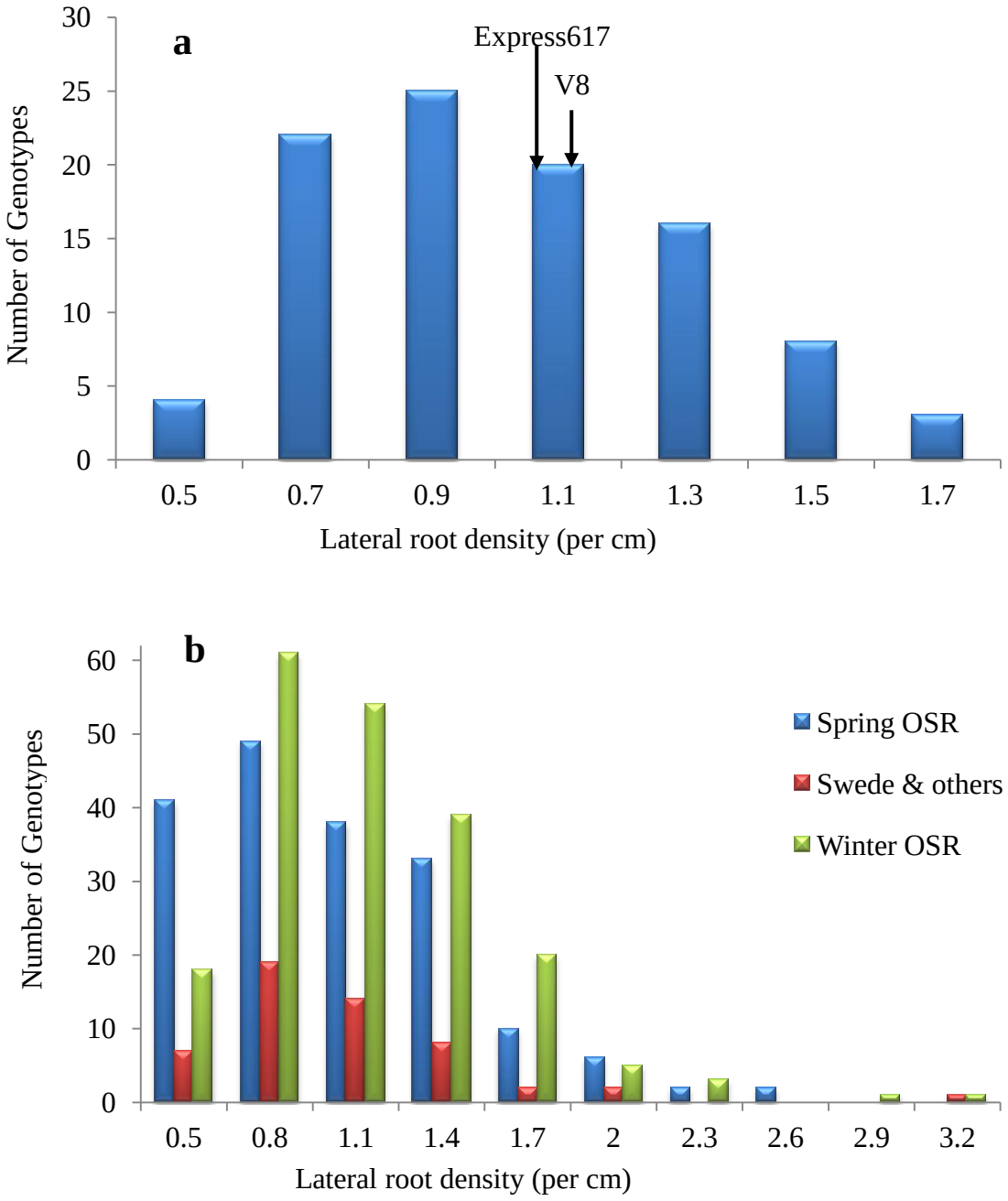

Fig 3.10 Distribution of Lateral root density (LRD) in (a) 94 DH lines from the population of "Express 617"× "V8". LRD values for cross parents is marked by arrows on respective bars and (b) *B. napus* diversity set showed distribution of LRD in three sub-populations which composed of winter, spring and swede-type with some vegetable rapeseed genotypes.

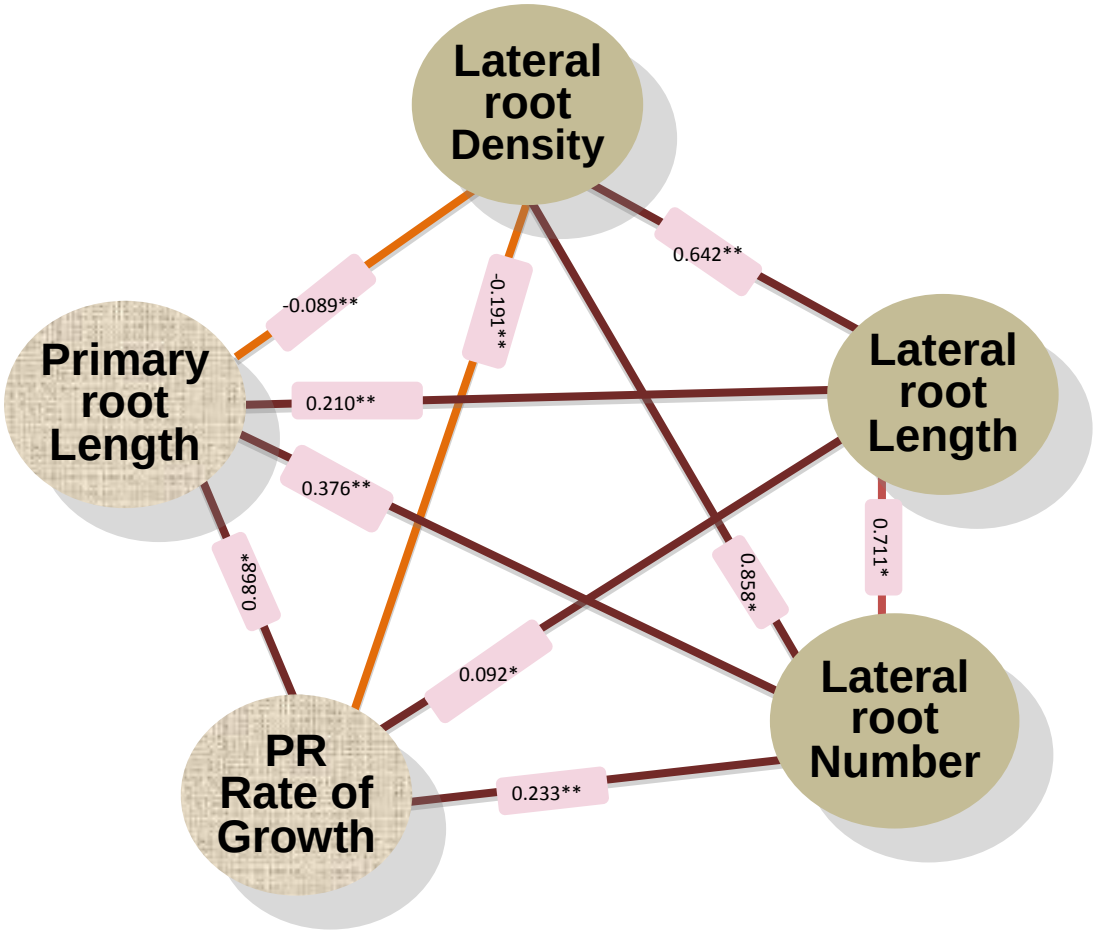

Fig. 3.11 Pearson Correlation analysis among root architecture traits in 94DH lines from "Express617" x "V8". Correlation values showed on connecting lines. ** means significant at 0.01 and * means significance at 0.05 level. Negative sign showed negative correlation among traits.

Table. 3.6 Pearson Correlation analysis among root architectural traits in *B. napus* diversity set. Correlation with ** means significant at 1% probability level. Negative sign showed negative correlation among traits.

Root traits	**PRL**	**RoG**	**LRN**	**LRL**	**LRD**
PRL	1	0-920**	0.321**	0.236**	-0.223**
RoG	0.920**	1	0.196**	0.095**	-0.301**
LRN	0.321**	0.196**	1	0.839**	0.704**
LRL	0.236**	0.950**	0.839**	1	0.618**
LRD	-0.223**	-0.301**	0.704**	0.618**	1

3.2.2 Quantitative trait loci (QTL) mapping in the bi-parental population

A total of 11 QTLs associated to root architecture traits were detected across five of the 19 chromosomes by composite interval mapping (CIM) in WinQTL cartographer (Wang et al., 2012). The position of QTLs on chromosomes for respective trait, LOD scores, 2LOD support intervals, additive effects and proportion of phenotypic variance (R^2) and heritability of trait is presented in Table 3.7. Summary of positions of QTLs related to lateral root traits is presented in figure 3.12a and QTLs linked to primary root traits are presented in figure 3.12b.

Individual QTL contribution (R^2) ranged from 11.5% to 25.5%. On chromosome A03, two Significant QTLs associated to lateral root traits (LRN and LRD) was co-localized to 269.81cM and very near to this at 267.81cM one other QTL region was detected which is significantly linked to LRL trait. These QTLs showed highest trait variance of 25.566% for LRN, 24.868% for LRD and 21.718% for LRL. Four markers between 102.2 and 130.9cM on A03 also showed association with LRD. Three more significant QTL regions associated with LRL were identified; one on chromosome A07 between 71.4-95.1cM and two were on chromosome C01 between 106.1-127.9cM and 127.9-135.6cM respectively

For primary root traits, one unique QTL was detected on C03 between 118.6cM and 129.3cM with a proportion of 13.187% phenotypic variance. Three QTLs associated to primary root rate of growth were identified on chromosome C04. Two of them are co-located between 94.8cM and 112.5cM contributing 15.5% and 19.59% of trait variance. Third QTL region with four markers was between 121.5cM and 141.8cM showed 11.5% R^2 .

Table 3.7 Results of QTL analysis for root architecture traits in the mapping population Express617 x V8 (94 DH lines). QTL positions associated to phenotypic trait were estimated by using zmapQTL composite interval mapping function.

Trait	Chromosome	Markers Name	Position (cM)	LOD score	2 LOD support interval (cM)	Additive effect	R2 (%)
LRN	A03	E42M55_125 E31M61_305	269.81	5.492	266.4-271.4	1.9018	25.5656
LRL	A03	E42M55_125 E31M61_305 Bn-Scaffold000 013-p2361675	267.81	4.349	265-275	2.1224	21.7179
LRD	A03	E42M55_125 E31M61_305 Bn-Scaffold000013-p2361675	269.81	5.702	266.1-275.7	0.173	24.8682
LRD	A03	BRMs043 RAD3862 UQ03A0022413 HMR443	116.41	3.318	102.2-130.9	-0.1029	11.082
LRL	A07	Na12E11 RAD1530 Bn-Scaffold000 012-p430018 Ni2D03	84.41	3.164	71.4-95.1	-1.5219	10.7016
LRL	C01	Bn-ctg71800 14734674-p4604 UQ10C0272604 RAD1176 RAD5014	107.01	4.098	106.1-127.9	-1.7846	14.0719
LRL	C01	RAD5014 RAD5115 RAD4042	131.31	3.561	127.9-135.6	-1.6838	12.4195
PRL	C03	RAD1335 RAD3813 RAD1602 RAD5363 Bn-ctg71800 14759848-p17449	122.41	3.850	118.6-129.3	-0.8015	13.1872
RoG	C04	RAD5167 RAD2834 RAD3056	97.11	3.924	94.8-100.1	-0.1699	15.4999
RoG	C04	RAD3056 Bn-ctg71800 14712950-p2504 Bn-ctg71800 14755177-p1784 RAD4045	106.21	5.040	100-112.5	-0.1782	19.5915
RoG	C04	RAD4153 RAD983 CB10159 Ol13D02A	130.71	3.196	121.5-141.8	0.1406	11.555

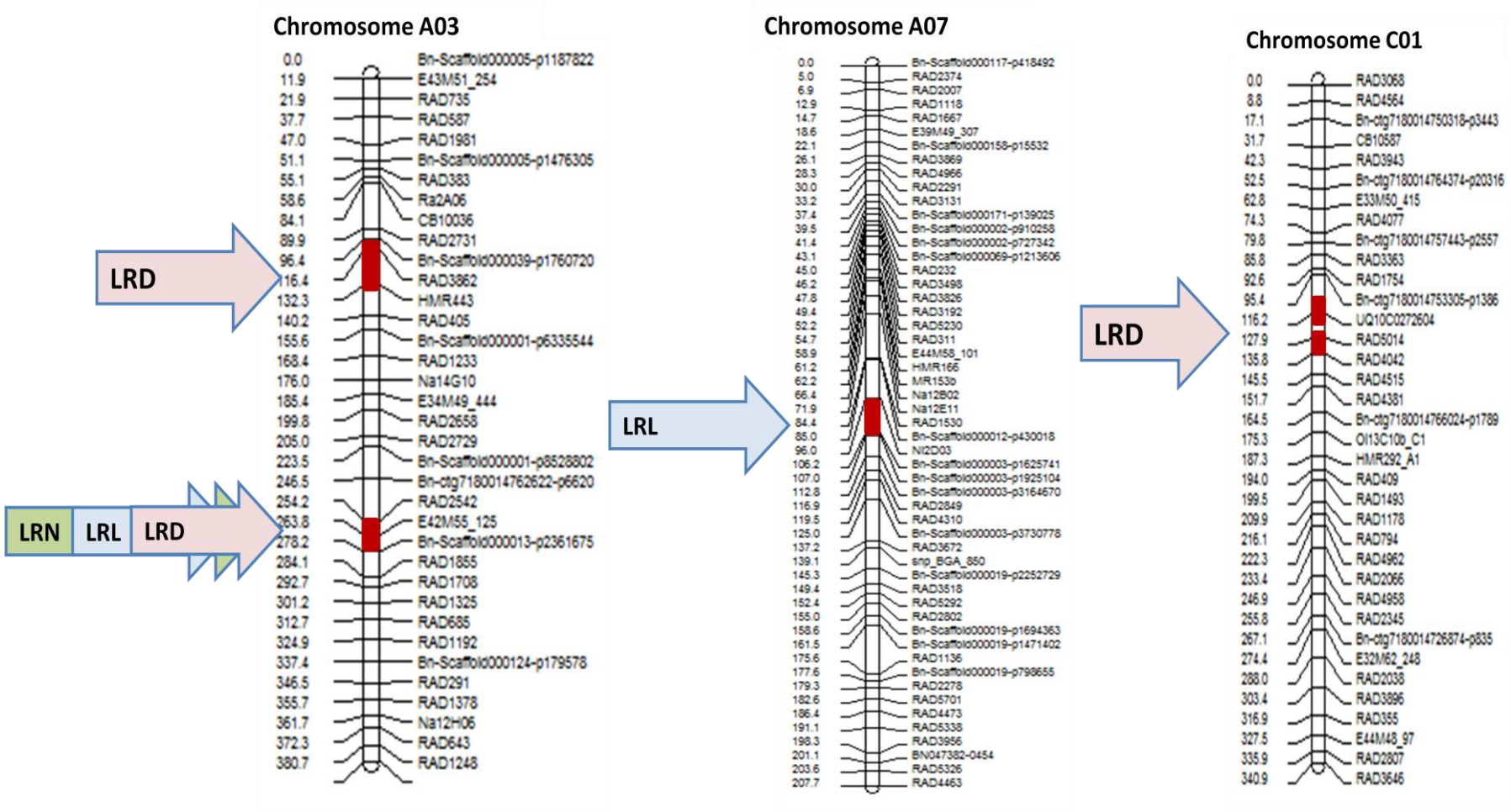

Fig.3.12 a. QTLs detected in 94DH lines from "Express617" x "V8" for lateral root traits, lateral root number (LRN), lateral root length (LRL), lateral root density (LRD). QTL positions in cM (2LOD support interval) are marked as red bar and markers name are presented on chromosome to their respective distance in cM along whole chromosome.

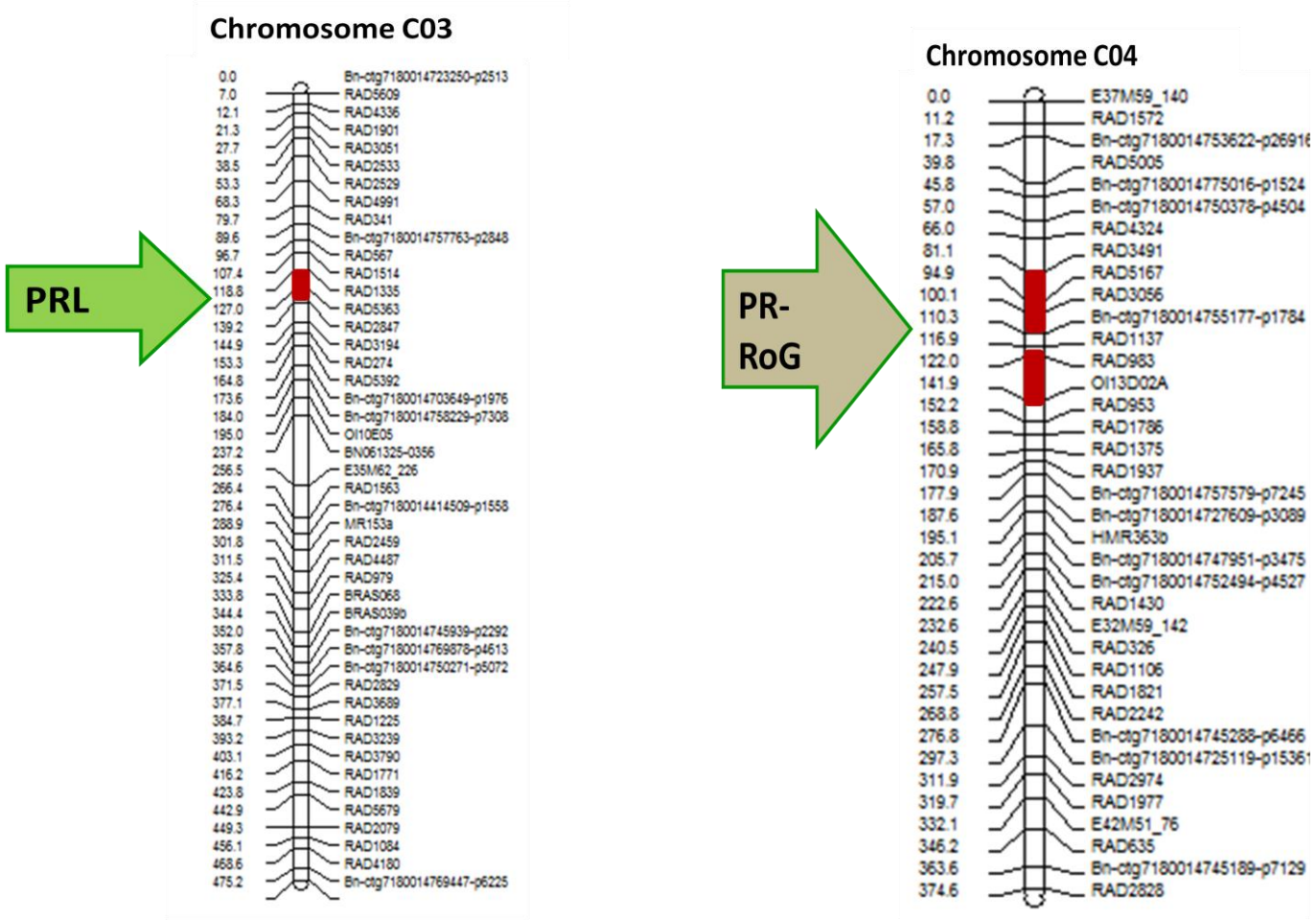

Fig 3.12 b. QTLs detected in 94DH lines from "Express617" x "V8" for primary root traits, primary root length (PRL) and primary root rate of growth (PR-RogG). QTL positions in cM (2LOD support interval) are marked as red bar and markers name are presented on chromosome to their respective distance in cM along whole chromosome.

3.2.3 Population structure and linkage disequilibrium (LD) in *B. napus* diversity set

The prerequisite for all association analysis was the characterization of population structure within *B. napus* diversity set of inbred lines by using the software package STRUCTURE 3.2.1 (Pritchard et al., 2000). STRUCTURE data was subjected to Structure-Harvester (Earl & vonHoldt, 2012) for Evanno test (Evanno et al., 2005) which showed two consecutive peaks for deltaK (Fig. 3.13b). Highest likelihood value was at K=2 but there is a consecutive peak at K=3 which suggest that in a broad sense this set can be divided in to two sub sets while three sub-populations are preferable for more precise results. Results are presented in Table 3.8 and figure 3.13a represents Q-matrix from K results which were used as covariates in the models to correct the association tests for false positives. Structure analysis divided the whole diversity set into three sub-populations mainly composed winter, spring and vegetables with swede type rapeseed genotypes. Similar clusters were found in this diversity set based on MCLUST by Bus et al. (2011).

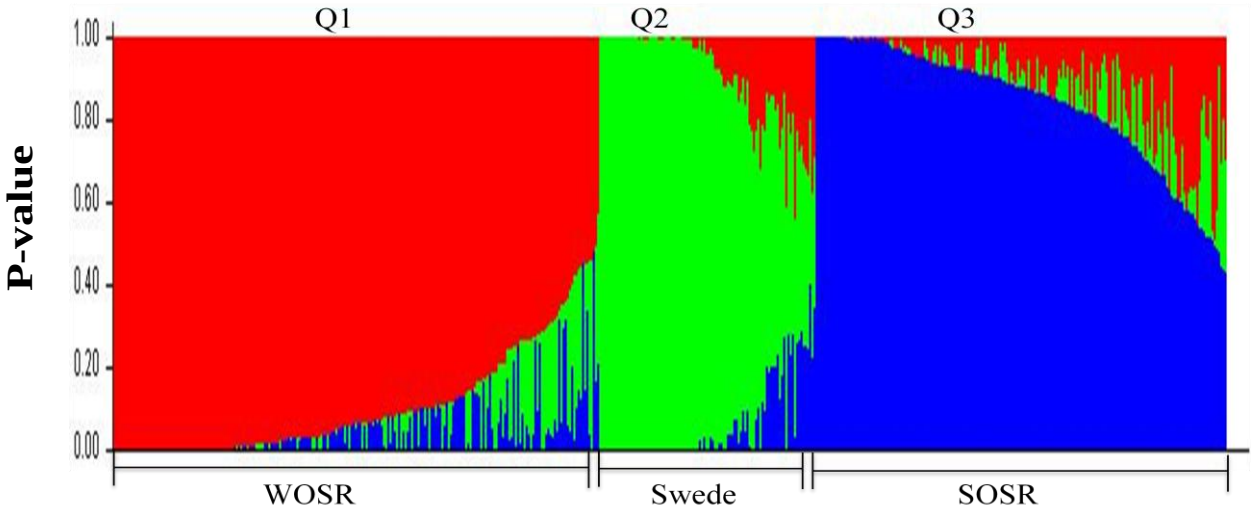

Fig 3.13. a Population structure analyses of *B. napus* diversity set using a Bayesian approach implemented by STRUCTURE. Colors define three Genetic Group (Q-matrix): Group 1 in red is winter oilseed rape genotypes (WOSR), Group 2 in green is mainly composed of swede-type rapeseed genotypes with some vegetables and Group 3 in blue is spring oilseed rape (SOSR).

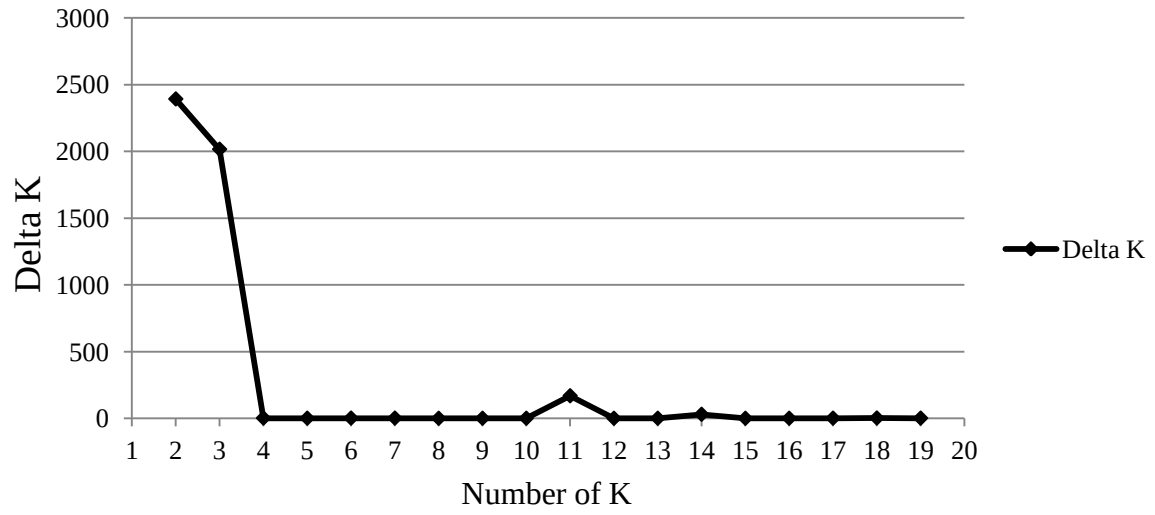

.

Fig. 3.13. b. The plot of Delta K (ΔK) for STRUCTURE analysis to determine the sub-population groups within a set of 515 diverse *B. napus* genotypes

Table. 3.8 Summary of the average logarithm of the probability of data likelihoods (LnP(D)) for diversity set of genetically diverse *B. napus* genotypes

No. of K	L(K)	StDev	Delta K
1	-2587790	11.97622	
2	-2267719	40.04901	2391.726
3	-2043434	86.77866	2015.288
4	-1994033	6908.453	1.968575
5	-1958232	4682.509	0.943778
6	-1926850	2814.096	1.698492
7	-1900247	2527.571	1.645156
8	-1877803	3880.096	0.14235
9	-1855911	4863.031	0.385033
10	-1835892	6097.82	0.426254
11	-1818472	7568.589	168.6382
12	-3077405	4022773	0.018237
13	-4262974	7803348	0.465225
14	-1818226	100736.7	30.03828
15	-2399436	1973038	0.038452
16	-2904781	2092247	0.482204
17	-2401235	1351285	1.044286
18	-3308819	2951709	2.380212
19	-11242096	13540013	1.196114
20	-35370777	34588560	0.608541

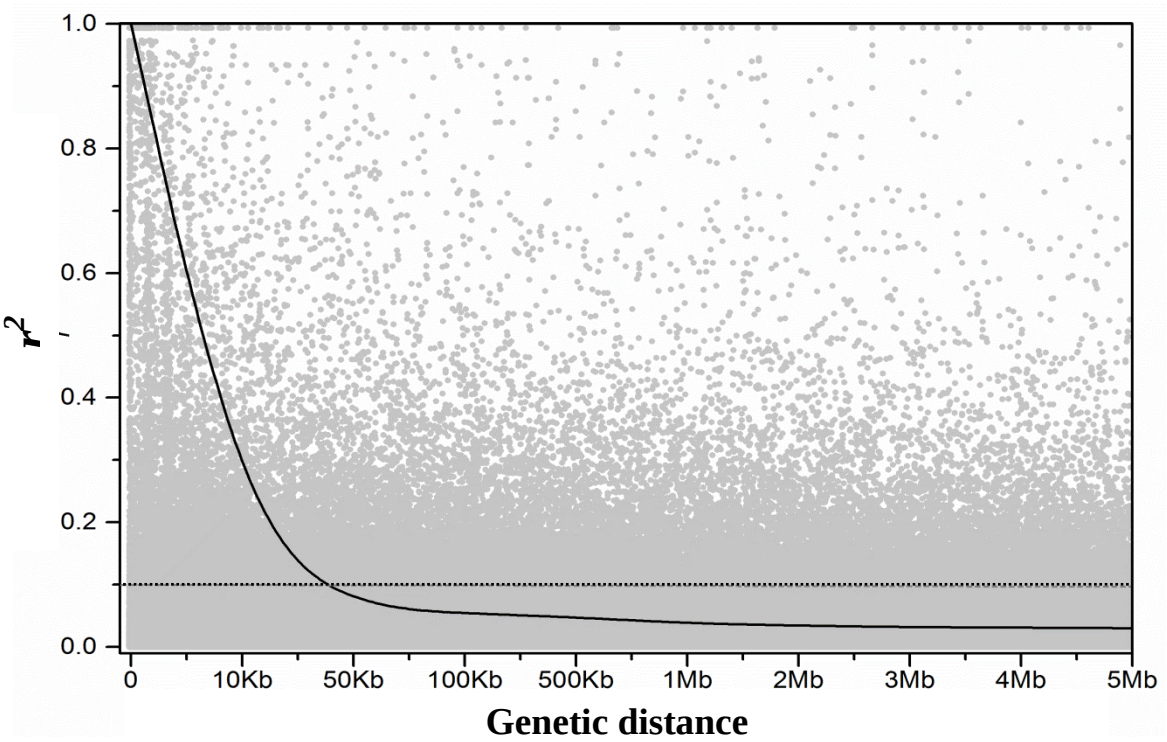

Fig.3.14. Linkage disequilibrium (LD) determined by squared allele frequency correlations (r^2) against genetic distance between 6K SNP markers. Inner fitted curve illustrates LD (r^2) decay of marker pairs over all chromosomes on genetic distance. Horizontal line fixed at 0.1 r^2 indicates the extent of LD.

Linkage disequilibrium (LD) was determined by squared allele frequency correlations (r^2) against distance between 6K SNP markers. Pattern of linkage disequilibrium (LD) was observed among the whole panel of markers distributed across all nineteen rapeseed chromosomes (Fig.3.14). Value of r^2 (range 0-1) decreased as the genetic distance between the pairs of loci increased which indicates that the probability of LD was low between distant locus pairs. The mean pair-wise r^2 is 0.035 for whole rapeseed population. A fixed value of r^2 is 0.1 beyond which LD is assumed to be caused by genetic linkage. The point at which the curve intercepts the 0.1 r^2 is determined as the average LD decay of the population. Based on these criteria average LD decay of the whole genome was observed to be from 10-50Kb.

3.2.4. Marker-trait association mapping in *B. napus* diversity set

The marker-trait association mapping between five root architecture traits was performed by using general linear model (GLM) which considered population structure (Q-matrix), and with mixed linear model (MLM) model, considering both kinship (K) and population structure (Q), implemented in TASSEL 4 software. GLM model is taking into account admixture percentage of population structure (Q) as a fixed factor for association analysis. GLM and MLM were compared in quantile-quantile plot (Fig. 3.15) for distribution of observed *P*-value and relative to expected *P*-value for these five root traits. Based on great deviation of observed *P* –value in GLM in comparison to MLM, results of MLM were studied in detail to analyze trait-marker association.

Manhattan plots (Fig. 3.16 a-e) presenting the markers showed significant association for root traits. Level of significance was tested against a 20% false discovery rate ($P \leq 0.001$) recommended for rapeseed previously by (Cai et al., 2014; Honsdorf et al., 2010)). A total of 38 significant associations were detected between SNP markers and phenotypic root traits. These 38 markers were distributed across 16 chromosomes out of total 19 chromosomes. Information about markers names their respective chromosomes with physical position, percentage of phenotypic variance (R^2), *P* and –log*P* values showed significance of association and effect of markers with respect to phenotypic differences are presented in Table 3.9.

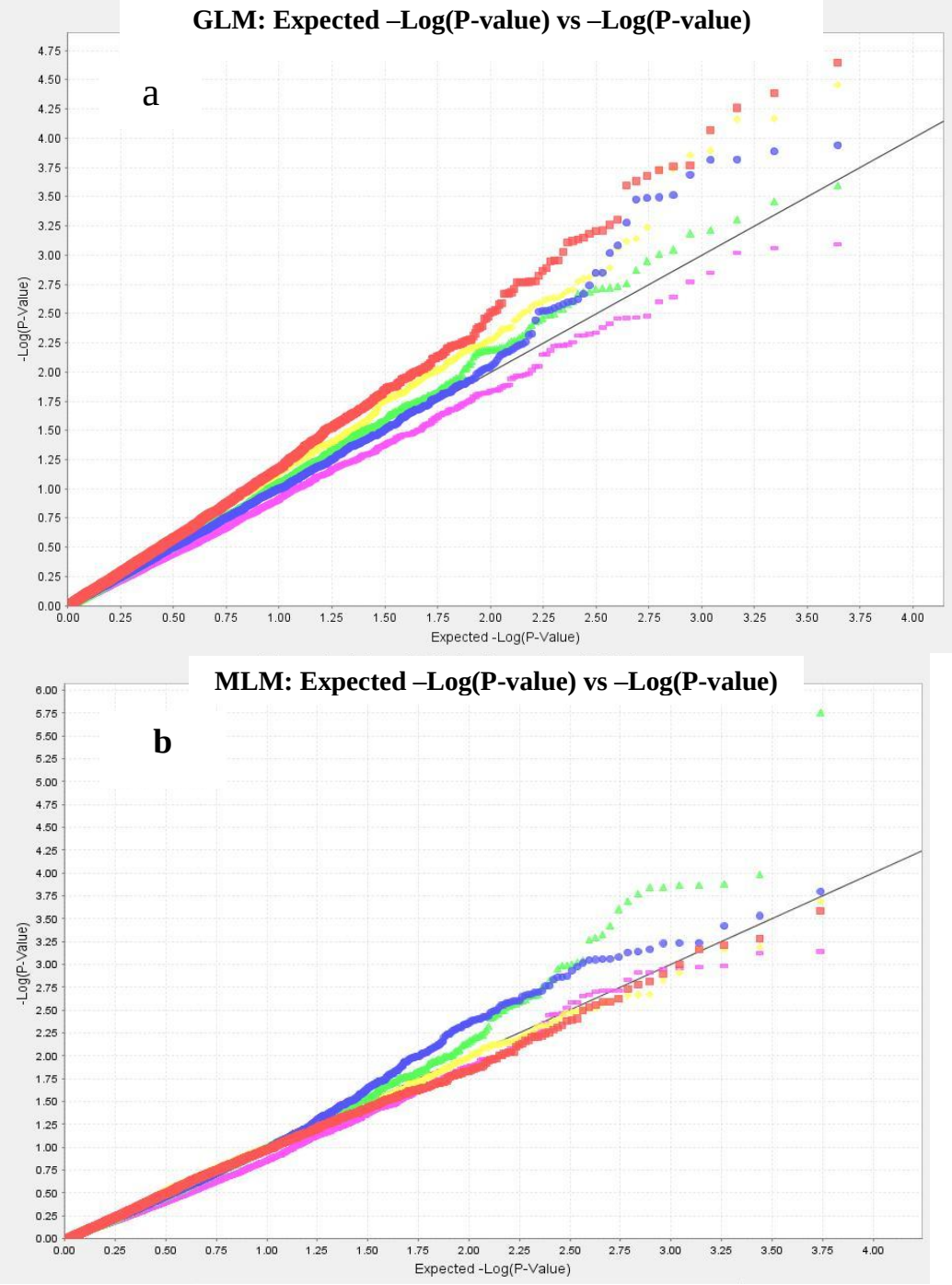

Fig. 3.15. Quantile-quantile plots of estimated –log10 (*P*) for two models used for association analysis of five selected root architecture traits in *B. napus*. a. GLM (traits data + Q-matrix from population structure). b. MLM (trait data + Q-matrix + kinship). Primary root length (red); primary root rate of growth (blue) lateral root number (blue); lateral root length (yellow) lateral root density (green); Black line represents the expected *P*-values with no existed association.

Seven markers located across six chromosomes were significantly associated with primary root length (PRL) (Fig. 3.16 a). Of which three markers are also showed significant association with primary root rate of growth (RoG). Bn-ctg7180014758221-p10306 on chromosome C05 had largest effect on both primary root traits with R^2 = 7.32% and 6.76% for RoG and PRL respectively. Two markers Bn-ctg7180014744438-p3846 and Bn-ctg7180014771544-p5387 positioned on chromosome A08 were also co-associated with PRL and RoG. Total nine markers are significantly associated with primary root rate of growth across seven chromosomes (Fig. 3.16 b). Phenotypic variance (R^2) for RoG ranged from 2.9% to 7.6 % for these nine markers Table. Lateral root traits were clustered to the markers on chromosome A06, Bn-Scaffold000009-p3611341was significantly associated to LRN and LRL, while Bn-Scaffold000009-p2084204 showed significant association with LRN and LRD. Twelve markers were detected to be significantly associated with lateral root number (LRN) with a phenotypic variance (R^2) ranged from 2.7% to 3.6% (Fig. 3.16 c). Bn-ctg7180014724170-p12006 on chromosome C03 is also found to be significantly associated to LRN and LRL. Total four markers showed significant association with LRL were detected (Fig. 3.16 d). Two other markers were located on chromosome A09 and C05. Five markers were significantly associated to LRD on four chromosomes, two were on A06, one on each A05, A07 and C08 chromosomes (Fig. 3.16 e).

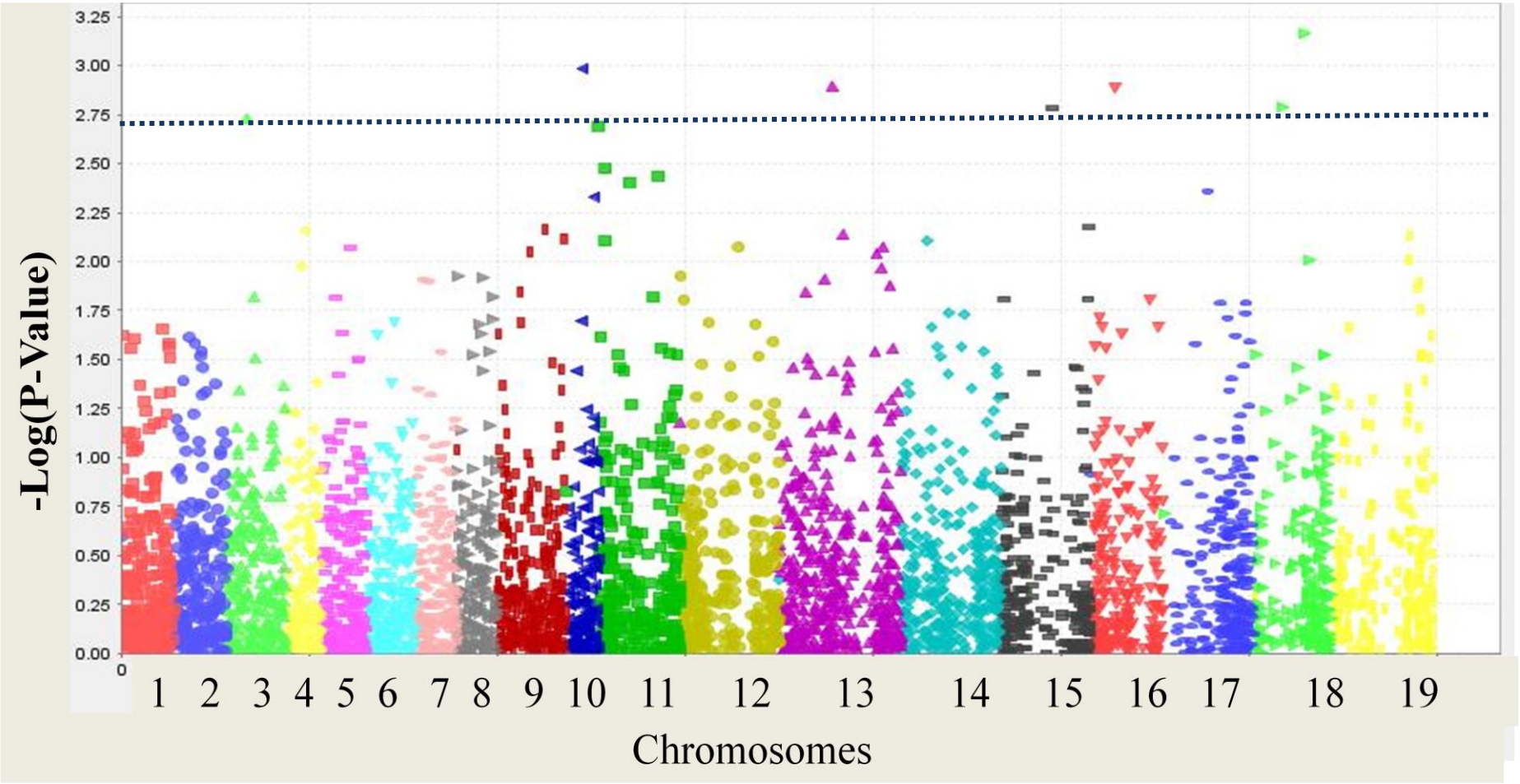

Fig 3.16 a Genome wide association scan for primary root length (PRL) in *B. napus* diversity set. Negative log10-transformed *P* values from a genome-wide scan are plotted against physical position on each of 19 chromosomes. These plots are based on the association results in 496 lines using 6K SNPs. Each dot represents a SNP. Blue horizontal dashed line indicates the significance threshold.

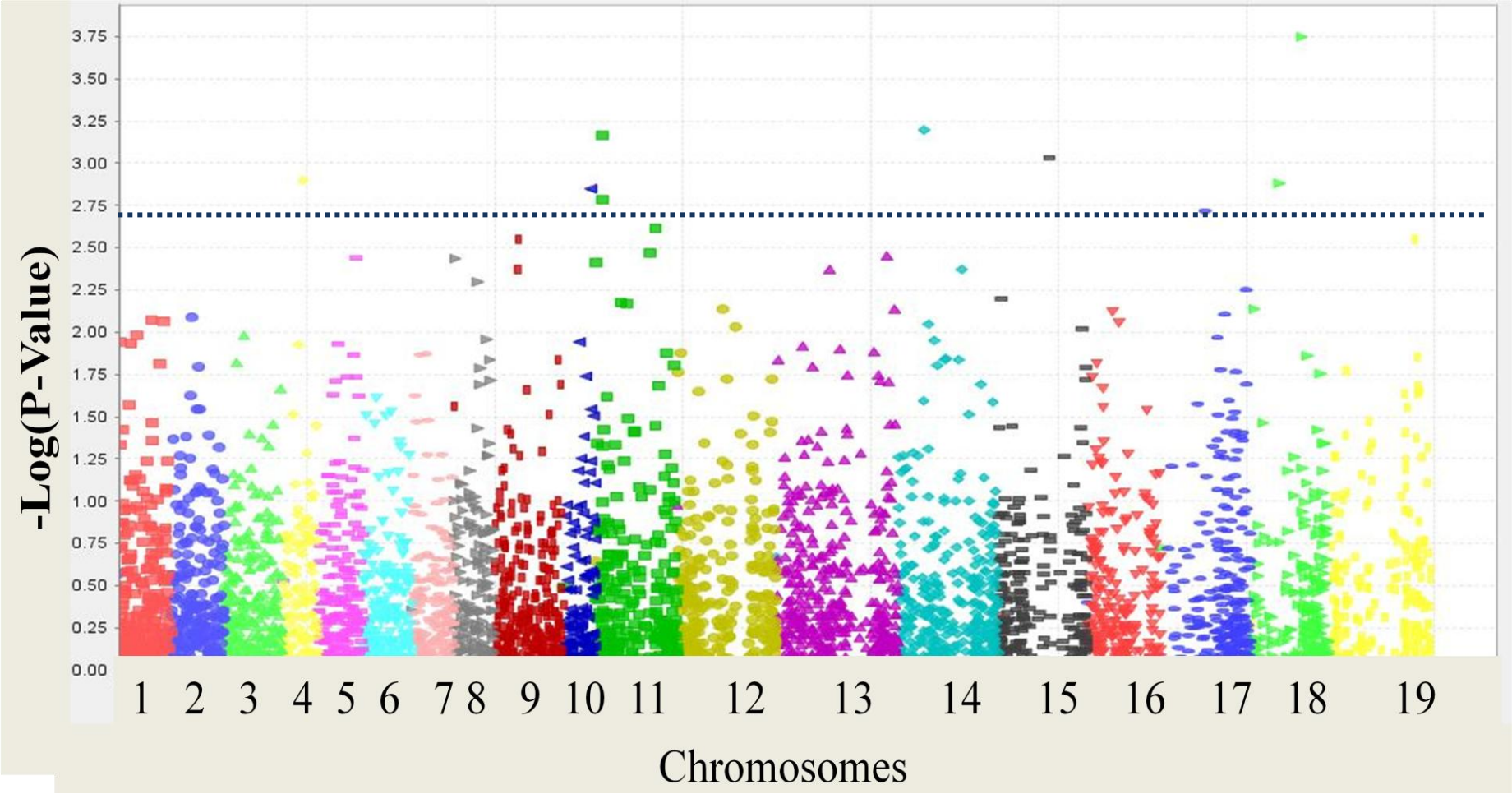

Fig 3.16 b Genome wide association scan for primary root rate of growth (RoG) in *B. napus* diversity set. Negative log10-transformed *P* values from a genome-wide scan are plotted against physical position on each of 19 chromosomes. These plots are based on the association results in 496 lines using 6K SNPs. Each dot represents a SNP. Blue horizontal dashed line indicates the significance threshold.

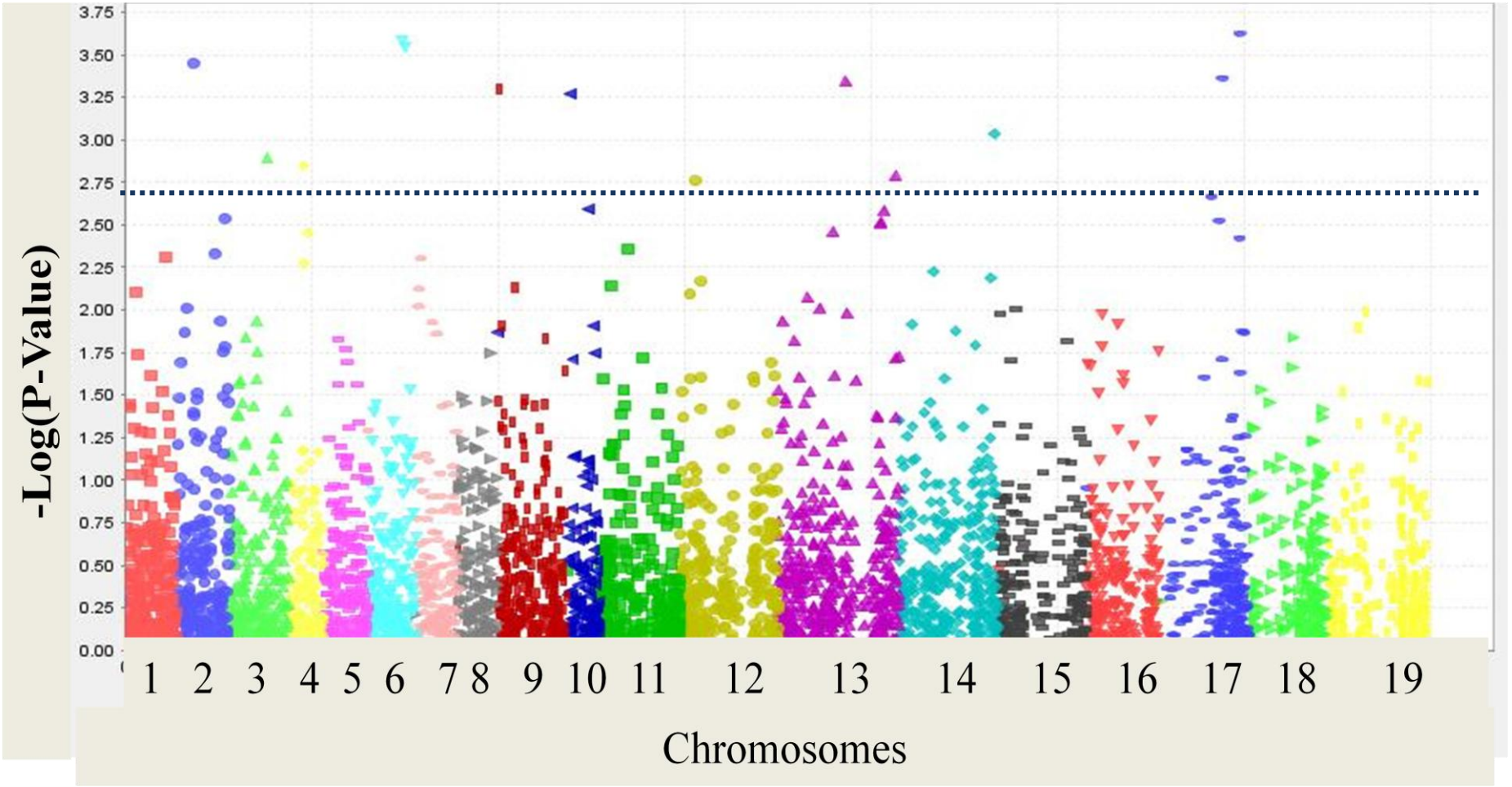

Fig 3.16 c .Genome wide association scan for lateral toot number (LRN) in *B. napus* diversity set. Negative log10-transformed *P* values from a genome-wide scan are plotted against physical position on each of 19 chromosomes. These plots are based on the association results in 496 lines using 6K SNPs. Each dot represents a SNP. Blue horizontal dashed line indicates the significance threshold.

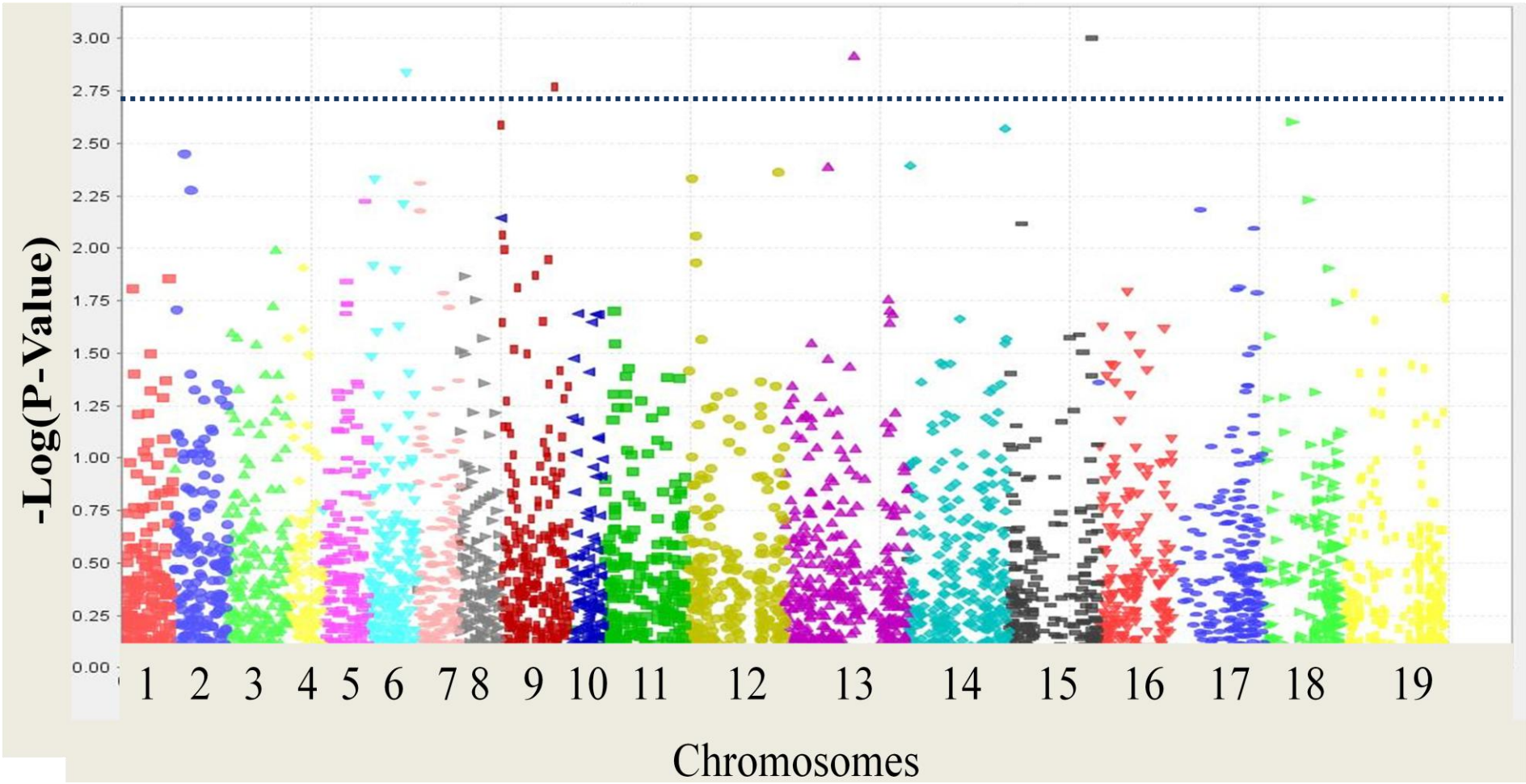

Fig 3.16 d Genome wide association scan for lateral root length (LRL) in *B. napus* diversity set. Negative log10-transformed *P* values from a genome-wide scan are plotted against physical position on each of 19 chromosomes. These plots are based on the association results in 496 lines using 6K SNPs. Each dot represents a SNP. Blue horizontal dashed line indicates the significance threshold.

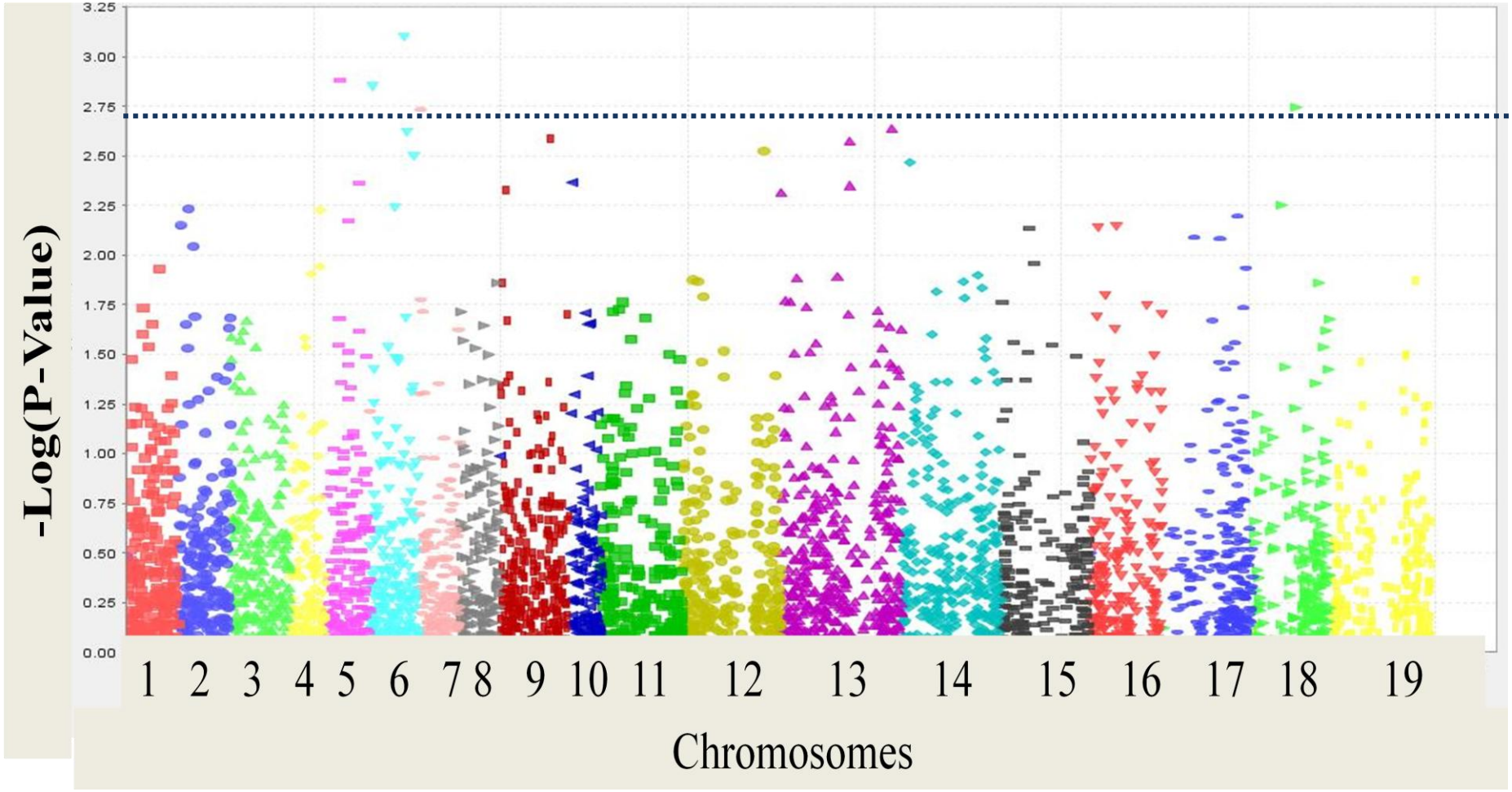

Fig 3.16 e. Genome wide association scan for lateral root density (LRD) in *B. napus* diversity set. Negative log10-transformed *P* values from a genome-wide scan are plotted against physical position on each of 19 chromosomes. These plots are based on the association results in 496 lines using 6K SNPs. Each dot represents a SNP. Blue horizontal dashed line indicates the significance threshold.

Table: 3.9. Results from genome wide association analysis for five root architecture traits in *B. napus* diversity set. Markers with bold names are common between more than traits.

Trait	Marker	Choromosome	Physical position (bp)	*P*-value	-LogP	R2 (%)	Effects
PRL	Bn-ctg7180014732800-p7852	16	13751224	0.0013	2.88	3.14	-0.075
PRL	**Bn-ctg7180014744438-p3846**	18	15538723	0.0012	2.79	3.15	-0.543
PRL	Bn-ctg7180014744657-p695	13	28272074	0.0012	2.89	3.33	-0.335
PRL	**Bn-ctg7180014758221-p10306**	15	26991993	0.0015	2.78	6.76	0.0344
PRL	**Bn-ctg7180014771544-p5387**	18	27262657	0.0001	3.16	3.44	1.211
PRL	Bn-Scaffold000001-p2025747	3	10797406	0.0015	2.73	3.05	0.625
PRL	Bn-Scaffold000002-p4464378	10	8335340	0.00103	2.98	2.53	0.416
RoG	Bn-ctg7180014729156-p492	14	13849623	0.0006	3.19	3.49	1.214
RoG	**Bn-ctg7180014744438-p3846**	18	15538723	0.0013	2.88	3.26	-0.543
RoG	Bn-ctg7180014753064-p3702	11	3820466	0.0012	2.78	3.07	-0.012
RoG	Bn-ctg7180014753064-p3935	11	3820233	0.0006	3.17	3.46	0.0799
RoG	**Bn-ctg7180014758221-p10306**	15	26991993	0.001	3.03	7.31	0.0344
RoG	Bn-ctg7180014769003-p8702	17	23881203	0.0011	2.71	2.96	-0.345
RoG	**Bn-ctg7180014771544-p5387**	18	27262657	0.0001	3.75	4.11	1.211
RoG	Bn-Scaffold000008-p1736198	10	14536015	0.0014	2.89	3.11	0.184
RoG	Bn-Scaffold000079-p733903	4	10649599	0.0012	2.91	3.17	1.890

Trait	Marker	Choromosome	Physical position (bp)	*P*-value	-LogP	R2 (%)	Effects
LRN	**Bn-ctg7180014724170-p12006**	13	36371606	0.0004	3.34	2.95	-1.117
LRN	Bn-ctg7180014727094-p3245	17	43365813	0.0002	3.62	4.04	1.196
LRN	Bn-ctg7180014745270-p2499	13	62976733	0.0013	2.78	3.06	-2.278
LRN	Bn-ctg7180014747147-p10093	14	51321756	0.0009	3.03	3.51	-1.498
LRN	Bn-ctg7180014775494-p1264	17	34032058	0.0004	3.36	3.76	0.882
LRN	**Bn-Scaffold000009-p2084204**	6	18454525	0.0007	3.58	3.95	-1.283
LRN	**Bn-Scaffold000009-p3611341**	6	19981662	2.85E-04	3.54	3.99	-1.511
LRN	Bn-Scaffold000013-p3645554	3	20266449	0.0012	2.89	7.66	-4.575
LRN	Bn-Scaffold000018-p2001991	10	1762681	5.39E-04	3.26	3.63	-2.267
LRN	Bn-Scaffold000030-p1733969	12	8575743	0.0013	2.75	3.01	-0.497
LRN	Bn-Scaffold000038-p1053013	2	8567589	3.55E-04	3.44	3.84	-1.334
LRN	Bn-Scaffold000048-p683458	4	8158537	0.0014	2.84	3.11	-0.617
LRN	Bn-Scaffold000128-p457982	9	688895	5.04E-04	3.29	3.64	-2.419
LRD	**Bn-Scaffold000009-p2084204**	6	18454525	0.0007	3.09	3.41	-1.283
LRD	Bn-Scaffold000020-p649204	18	23533364	0.001	2.74	3.03	-1.128
LRD	Bn-Scaffold000025-p1146347	5	7965136	0.0013	2.88	3.29	-0.514
LRD	Bn-Scaffold000026-p1533569	6	1659690	0.0014	2.84	4.23	0.482
LRD	Bn-Scaffold000153-p245403	7	1097121	0.0014	2.73	3.16	0.442
LRL	**Bn-ctg7180014724170-p12006**	13	36371606	0.0012	2.91	2.52	-1.117
LRL	Bn-ctg7180014758607-p7246	15	43664102	9.97E-04	3.001	5.86	-1.549
LRL	Bn-Scaffold000006-p2769741	9	28675597	0.0012	2.76	3.08	-2.139
LRL	**Bn-Scaffold000009-p3611341**	6	19981662	0.0014	2.83	3.20	-1.511

4. DISCUSSION

Genomic sequences and development of advanced genetic markers system greatly improve the potential for accelerated marker assisted selection to improve seed quality and yield-related traits in oilseed *B. napus*. Molecular markers can be particularly interesting to further reduce total glucosinolates in rapeseed meal, and also for the selection of breeding lines with low seed fibre content. Cosegregating or tightly linked molecular markers linked to important genes or QTL can be reliable, efficient, cost effective and time saving tools that may enhance the capacity of conventional breeding for improving agronomic, quality and yield related traits of crop species without adverse effects.

A number of potential candidate genes involved in metabolic pathways including glucosinolate (GSL) biosynthesis and phenylpropanoid pathway have been identified based on QTL mapping in *B. napus*. Molecular maps of diverse populations developed using various marker systems support marker assisted selection in plant breeding, provided the markers are linked to QTL with major effects on the trait of interest. Additional knowledge of gene expression patterns can provide important functional information to help identify important candidate genes for major QTL. In this project the differential expression of genes involved in the GSL biosynthesis and phenylpropanoid (lignin) biosynthesis pathways was investigated in winter rapeseed genotypes Express617 (low glucosinolate, high fibre) and V8 (low glucosinolate, high fibre) during seed development, in order to determine fundamental differences related to expression of these important antinutritive compounds.

Root system architecture (RSA) is another genetically complex agronomic trait encoded by the combined effect of multiple loci. RSA refers to the spatial configuration of a root system with implications for nutrient uptake, overall plant architecture, growth rate and yield, developmental plasticity in response to environmental changes and abiotic stress resistance. Novel root system phenotyping technologies and the availability of genomic resources have opened the way to elucidate the genetic control of root development in plants. A double-haploid (DH) population derived from a cross between Express617 and V8 was examined along with a rapeseed diversity set of 496 inbred lines for root traits phenotypes in a gel rhizotrons system. QTL mapping in the biparental population and marker trait association mapping in the diversity set provided first fundamental information towards understanding the complex genetic mechanisms behind root architecture in *B. napus*.

4.1 Transcriptomic networks involved in seed quality parameters

A better understanding of expression networks during seed development is essential for further breeding progress, specifically in valuable seed plants like cereals or oilseed crops. Substantial improvements of yield and quality of seeds were achieved by successful breeding in rapeseed based on selection for zero erucic acid and low GSL content, in combination with high oil content and desireable fatty acid composition. Transcriptional profiles of high and low erucic acid rapeseed cultivars were compared previously to get insight into the structure of the primary transcriptional networks coordinating the metabolic responses to *Brassica* seed developmental programs (Hu et al., 2009). Their results demonstrated that genes responsible for lipid profile show differential expression from 10-45 dap in developing seeds.

In the present study, gene expression profile was observed in two black seeded *B. napus* winter genotypes: Express617, a 00-quality cultivar with a high lignin content, and V8, with high erucic acid and GSL contents but moderate level of lignin. A DH population from these two lines was explored previously for metabolites, seed and seedling developmental traits (Basunanda et al., 2010; Basunanda et al., 2007; Wittkop et al., 2012; Stein et al., 2013). The DGE based transcriptomic profiling of the two parental genotypes aimed at obtained information about the expression of genes responsible for the differential phenotypes for total seed GSL and fiber content. A similar transcriptional profile was observed for major metabolic pathways in both genotypes. Early stages of seed development from 2-28 dap are highly correlated. As expected these early developmental stages exhibited a high expression of genes involved in embryonic development, photosynthesis pathway, cell proliferation and seed coat formation. Increased expression of photosynthesis related genes is also indicative of the connection and importance of seeds' photosynthetic efficiency, an important contributing factor to the synthesis of oil reserves in the seeds (Schwender et al., 2004). Later time points showed very low correlation between the two genotypes. Genes involved in lipid and storage protein accumulation showed higher expression during this seed maturation phase (from 42 dap until 84 dap) in both genotypes, corresponding to studies reported previously in *B. napus* (Hajduch et al., 2006; Obermeier et al., 2009). Obermeier et al. (2009) found a high abundance of transcripts encoding napin, cruciferin and oleosin storage proteins at 35 dap in winter rapeseed.

Arabidopsis, a close relative of *Brassica* crop species, provides an important model system to explore gene expression networks and get insight to the developmental processes from embryogenesis till seed maturation, including the accumulation of proteins and lipids reserves, dormancy induction and the acquisition of desiccation tolerance (Vicente-Carbajosa and Carbonero, 2005). White et al. (2000b) performed transcriptomic studies in developing seeds of Arabidopsis by genome wide analysis of gene expression by tag sequencing, to understand regulatory networks governing metabolic pathway from carbohydrate to oil. Recently, gene expression profiling of seed development was reported in *B. napus* from 2-40 dap (Venglat et al., 2013). In comparison to Arabidopsis, a very similar pattern and developmental aspects were observed in both species during embryogenesis. The *B. napus* embryo is up to 1000 times larger than Arabidopsis, however, the ultimate result of considerably higher cell growth and division during seed development in rapeseed. Conservation of fatty acid biosynthesis and regulation, carbon flux and lipid metabolism was also reported between *B. napus* and Arabidopsis by analysis of genes expression profiles (Niu et al., 2009a). By the advent of new genetic technologies and bioinformatics tools, whole transcriptome profiling gives the possibility to interrogate gene expression on a global scale at the tissue specific level (Wang et al., 2010). In comparison to array-based expression analyses, digital gene expression (DGE) methods offer the advantage that expression levels can be quantified even for low-abundance transcripts or previously unknown genes by sequencing at sufficient depth (Edwards et al., 2013).

4.1.1 Differential expression of genes during seed development

Seed development is an intricate process relying on all genetic information for coordinated growth of seed specific tissues to allow successful propagation of the species. Production of a viable embryo requires the developing seed to pass through a genetically determined and conserved developmental program. *B. napus* has its importance mainly due to edible oil extracted from the seeds. The oil synthesized during the seed maturation phase is the major energy reserve for later growth and development prior to the full establishment of photosynthetic capacity of the seedling (Tan et al., 2011).

In this study the differential expression of genes responsible for phenotypic differences in seed meal quality parameters, particularly total GSL and fiber contents, was observed. For housekeeping genes both genotypes showed similar expression profiles during early seed

developmental points. For example, the higher observed expression of genes responsible for embryogenesis and photosynthesis corresponds to other studies in *B. napus* (e.g. Hua et al., 2012). Similarly, genes responsible for accumulation of storage components (proteins and fatty acids) showed higher expression during the seed maturation period (Hajduch et al., 2006). An overall view of differentially expressed genes, by Wilcoxon test ranking in the software Mapman, showed significant difference of functional categories (BINS) relevant to RNA, DNA, proteins and carbohydrate metabolism, along with genes responsible for stress responses and secondary metabolism (flavonoids, carotenoids, phenylpropanoids, GSL and sulfur containing compounds). Differentially expressed genes for a specific phenotypic trait or specific metabolite accumulation during seed development are fascinating in terms of genetic understanding of their respective pathways. In developing seeds of *B. napus*, up-regulation of genes responsible for erucic acid content in oil was studied to evaluate their role in high and low erucic acid content in oil (Hu et al., 2009). The present study found significant up and down regulation of GSL and phenylpropanoid pathway genes, along with transcription factors involved in the regulation of these pathways. DGE analysis based on tag profiling was found to be very useful for detection of minor levels of expression of transcription factors. These two pathways will be discussed in detail in further sections.

4.1.2 Temporal patterns of gene expression: Critical time points

Considerable plasticity in gene expression during seed developmental results in seeds with different qualities. Comprehensive studies have been done to explore developmental stage-specific changes in gene expression, to understand the gene regulatory networks in plants by transcriptome- and proteome-based technologies (Agrawal et al., 2008; Hajduch et al., 2006; Hajduch et al., 2010; Hajduch et al., 2011).

Seed development can be broadly divided into three temporal phases: (i) cell proliferation phase/embryogenesis, (ii) the maturation phase responsible for storage component accumulation, and (iii) the desiccation phase resulting in a viable seed (Obermeier et al., 2009). An earlier proteomics based detailled study of seed development from 2-6 weeks after flowering (WAF) in spring rapeseed variety Reston demonstrated that liquid endosperm dominates the seed portion until 14 daf, while the embryo begins to take up a significant volume of the seed after 21 daf. Subsequently the embryo is occupying a major portion of the seed. IN the latest stages of maturity the seed coat start to change its color as the desiccation

stage approaches. During this intermediate developmental stage the seed weight decreases and the protein content increases dramatically. During maturation the total fatty acid content increases significantly (Hajduch et al., 2006). Obermeier et al. (2009a) used serial analysis of gene expression (SAGE) to analyze gene expression at 23 and 35 dap in winter rapeseed, corresponding to the timepoints before the switch to biosynthesis of seed storage compounds. The 23 dap time point corresponded to the final stages of cell proliferation, and the start of the accumulation of storage proteins. At 35dap the gene expression profile reflected the change towards the maturation phase of seeds (Obermeier et al. 2009a), which ends with the desiccation period. In winter rapeseed the seeds finally have approximately 40 to 50% oil content by dry weight (Wittkop et al., 2009).

Differential expression of genes involved in GSL metabolic pathway and phenylpropanoid pathway directed to lignin biosynthesis was observed in these two selected winter rapeseed genotypes, Express617 & V8, during whole seed developmental period. Critical view of gene expression showed up-regulation of genes involved in lignin biosynthesis in Express617 from 42 dap until 70 dap, which is in fact the maturation phase of seeds in these winter rapeseed genotypes. Previously fine QTL mapping of seed fibre content in a DH population from the cross between Express617 and V8 resulted in co-localization of *Cinnamoyl-CoA Reductase1* (*CCR1*) and *Cinnamyl Alcohol Dehydrogenase2/3* (*CAD2/3*) near the peak of a strong corresponding seed fibre QTL region. Our interest is to observe the temporal variation of these two genes during seed development of these parental genotypes. The key lignin biosynthesis gene *CCR1* was also identified by (Liu et al., 2012b) as a positional candidate in the vicinity of markers which are tightly linked to a major dominant locus for low ADL content in the *B. napus* seed-coat. From this DGE analysis, expression pattern of *CCR1* in the seed developmental period was similar in both genotypes, but showed up-regulation in Express617 relative to V8. *CCR1* and *CCR2* showed up-regulation in the seed maturation phase but down-regulation was observed at 84 dap in Express617. It is reported that *CCR1* has a primary role in constitutive phenylpropanoid biosynthesis, whereas *CCR2* has more activity in of phenolic compound synthesis in response to abiotic and biotic stresses (Lauvergeat et al., 2001).

Multiple members of the *CAD* gene family are also involved in phenylpropanoid biosynthesis. Differential expression of six *CAD* genes was detected during seed development of these two *B. napus* genotypes. *CAD* genes are also reported to be potential candidates for

the alteration of lignin content in rapeseed seeds, and their interaction with *CCR1* was suggested to be involved in the dominant inheritance of low level of seed coat ADL (Liu et al., 2012b; Stein et al., 2013). Similar interactions were also reported previously in tobacco (Chabannes et al., 2001). Higher expression of the *CAD* genes in Express617 in seed maturation phase appeared to be a clue that these genes have role for high lignin content in seeds in this genotype compared to V8, which showed lower expression levels of *CAD* genes at maturation phase through the seed developmental period. Higher levels of *CAD* gene expression has also been reported in final phase of seed development in soybean (Baldoni et al., 2013), and a linear correlation was found between change in lignin content and expression level of *CAD* genes in leaves of *Ginkgo biloba* (Cheng et al., 2013).

Transcription factors controlling the phenylpropanoid pathway also showed differential expression in both genotypes; most of them show their highest expression during the maturation phase at 70dap in Express617. Electrophoretic mobility shift assay (EMSA) and detailed promoter analysis has revealed that activation of monolignol pathway genes is necessarily coordinated to the MYB transcription factor binding motifs corresponding to their AC-rich elements (Patzlaff et al., 2003). AC elements are present in the promoters of most monolignol pathway genes, including *PAL*, *4CL*, *C3H*, *CCoAOMT*, *CCR* and *CAD* (Raes et al., 2003).

Previously, Bhardwaj & Hamama (2003) evaluated rapeseed genotypes to identify the growth stage of seed development which is more suitable for application of environmental conditions or chemicals for the modification of GSL contents. Estimation of total seed GSL from spring *B. napus* genotypes with high and low GSL contents showed similar levels of GSL from 26-35 daf, while variation in GSL content was found to be highly significant in developing seeds from 37 to 52 DAF. The GSL contents started to increase significantly at 26 daf in high GSL lines and continuously increased up to 33 DAF. On the other hand, in the low GSL lines the total GSL content increased only between 33 and 35 DAF. In the present study, the DGE profiles also showed the similar patterns of expression from genes involved in GSL metabolic pathway. In particular, a lower expression of genes responsible for GSL biosynthesis was observed in the 00-quality genotype Express617 relative to V8. The greatest differences were observer in the early seed developmental stage, followed by up-regulation from 42-70 dap and a decrease in expression level till 84 dap during the seed maturation phase.

OBP2/DOF1.1 and MYB transcription factors (MYB34, 28 & 51) were reported previously to be responsible for GSL pathway regulation (Hirai, 2009; Wang et al., 2011). Their expression pattern was also significantly different during early and maturation phases of seed development in Express617 and V8, suggesting their role in regulating final GSL contents in these two genotypes. GSL accumulation in developing seeds was also determined in comparison to other spring and winter rapeseed genotypes. Results showed that spring *B. napus* varieties with low erucic acid but high GSL content (0-quality) accumulate GSL very fast, while 00-quality varieties show GSL accumulation in early developmental stages but a decrease in accumulation during the seed maturation phase. Winter genotypes showed a slower but consistent accumulation of GSL during seed development, whereby 00-quality genotypes accumulated low levels of GSL in the early developing stages, then contents decreased during the maturation phase prior to harvesting (Bloem et al., 2007).

4.1.3 Regulation of phenylpropanoid pathway genes during seed development in relation to anti-nutritive seed fiber compounds

Phenylpropanoids contribute to all aspects of plant responses towards biotic and abiotic stimuli (Vogt, 2010). The phenylpropanoid pathway is a rich source of plants metabolites and essential for the biosynthesis of lignin. Furthermore, it also serves as a starting point for the production of many other important compounds, such as the lignans, flavonoids and coumarins (Fraser, 2011). The genome-wide bioinformatics survey of the Arabidopsis genome provides detail information about genes involved in phenylpropanoid pathway directed to the biosynthetic pathway of lignin and their results revealed the expression of 34 candidate genes from this pathway in different tissues of plants and which belong to the ten enzyme families (Raes et al., 2003). In *B. napus* the phenylpropanoid pathway was explored for genes involved in biosynthesis of lignin compounds by focusing on its role in fungal disease resistance (Obermeier et al., 2013) and for anti-nutritive fibre components of rapeseed meal (Liu et al., 2012b; Stein et al., 2013). High concentrations of the fibre fractions neutral detergent fibre (NDF), acid detergent fibre (ADF) and acid detergent lignin (ADL) in rapeseed meal limit its value in livestock feed (Wittkop et al. 2009).

Genes involved in phenylpropanoid pathway are extensively studied in different plant species. QTL fine mapping and microarray based transcript profiling were used for identification of candidate genes responsible for lignin biosynthesis (Barriere et al., 2008;

Capron et al., 2013; Liu et al., 2012c; Riboulet et al., 2008; Stein et al., 2013). Recently with the advent of high throughput technologies and computational tools, interaction and co-expression of these genes were reported in different plants including *Arabidopsis* (Raes et al., 2003; Ruprecht and Persson, 2012; Vanholme et al., 2012). Disruption of PAL, the first enzyme of the phenylpropanoid pathway, led to transcriptomic adaptation of components of carbohydrate and amino acid metabolism and the phenylpropanoid biosynthesis, revealing complex interactions between these pathways at the gene expression level (Rohde, 2004). Increase in *PAL* transcript levels was observed in lignifying *Pinus taeda* cells when its reaction is furnished with substrate Phe (Anterola et al., 2002). In *B. napus*, differential accumulation and expression of genes related to phenolic compounds were observed between black and yellow seeded genotypes in developing seeds (Qu et al., 2013). Highest expression levesl of *BnPAL* were found at 42dap in the black seeded genotype and at 49dap in the yellow seeded genotype. In the present study we also found higher levels of expression in the maturation phase (from 42 to 70dap). Co-localization of *PAL* with genes for other enzymes of lignin biosynthesis pathway were reported based on QTL mapping (Barriere et al., 2005; Riboulet et al., 2008) and this sassociation was confirmed by new co-expression computational tools in *Arabidopsis*. Similar co-expression networks were found in barley, Medicago, poplar, rice, soybean, and wheat for Arabidopsis *AtPAL1*-orthologs with other downstream gene families of the monolignols pathway, such as *C4H*, *4CL*, *HCT*, *C3H*, *CCoAOMT*, *CCR* and *CAD* (Ruprecht and Persson, 2012).

In spring rapeseed, silencing of the phenylpropanoid pathway genes *COMT*, *F5H-COMT*, and *C3H-C4H* by RNAi resulted in lignin reductions to variable levels. Seeds from transgenic plants were analyzed at 20-25 days post-anthesis. A 40% reduction in lignin content was observed in lines with interrupted *COMT* gene, while 36 and 26% reduction was observed in lines with suppression of *C3H-C4H* and *F5H-COMT*, respectively (Bhinu et al., 2009). In this study, a similar expression pattern of these three cytochromes *C3H*, *C4H* and *F5H* was observed during seed development. Strong up-regulation of these three genes was observed at 42dap in Express617 relative to V8. Over-expression of *F5H* produces lignin highly enriched in S subunits in various plant species, due to diversion of G lignin precursors towards S lignin biosynthesis (Franke et al., 2000). COMT catalyzes the *O*-methylation reaction immediately after F5H and incorporation of unusual monolignol into lignin was reported as a result of *COMT* down-regulation or *F5H* over-expression (Lu et al., 2010). In these *B. napus* genotypes *COMT* is down-regulated while *F5H* is up-regulated at 42dap in Express617. Due

to lack of detailed lignin profiles of seeds from each time point, it was not possible to correlate gene expression with specific lignin subunit composition. Previously, however, Express617 was found to have a higher lignin content compared to V8, and the DH population from their cross showed a significant segregation for seed lignin content (Stein et al., 2013; Wittkop et al., 2012).

Cinnamoyl-CoA reductase (CCR) catalyzes the synthesis of hydroxycinnamaldehydes from the hydroxycinnamoyl-CoA thioesters. Stein et al. (2013) identified strong QTL with very large effects on seed colour, condensed tannin content and seed acid detergent fibre (ADF) which was mapped on chromosome A9 by using highly dense genetic markers map from Express617 x V8 DH population. This QTL was also detected previously in DH-population from cross of black-seeded rapeseed to yellow-seeded rapeseed genotype (Badani et al., 2006), and also confirmed in crosses of yellow seeded and dark seeded Chinese rapeseed varieties by Liu et al. (2012b). The latter study suggested *CCR1* as a potential candidate gene, interacting with *CAD* gene family members to significantly influence the biosynthesis of mono-lignols and other antinutritive phenolic acid derivatives. Stein et al., (2013) reported that a fully functional *CCR1* and *CAD2*/*CAD3* genes were possessed in Express617 which has high ADL contents. While in V8 an impaired *CCR1* sequence was found along with non-functional C-genome sequence and one of the *CAD2*/*CAD3* allele of A-genome is missing, and this double mutation was suggested to be responsible for low level of ADL in V8. In this study we found *CCR1* gene expression patterns were found to be similar in Express617 and V8 during seed developmental stagesm but *CAD* genes showed highly differential expression.

Genes in the lignin biosynthetic pathway need to be coordinately turned on to make lignin. The majority of the lignin biosynthetic genes have a common *cis*-element, namely the AC element, required for their expression in lignifying cells. Important progress has been made in the identification of transcription factors that bind to the AC elements and are potentially involved in the coordinated regulation of lignin biosynthesis (Zhao and Dixon, 2011; Zhong and Ye, 2009; Zhong et al., 2008). *MYB58* and *MYB63* are expressed, specifically, in the cells undergoing secondary wall thickening and are significant regulators of lignin biosynthesis. Their over-expression leads to the ectopic deposition of lignin, while dominant repression resulted in drastic reduction in secondary wall thickening and a deformation of vessel morphology in Arabidopsis (Zhou et al., 2009). In this study we found higher level of expression of *MYB58* and *MYB63* in seed maturation phase in Express617 while in V8,

MYB58 expression was only detectable at 56 and 84 dap and expression of *MYB63* was not detectable.

MYB61 was reported to control multiple processes, including regulation of stomatal aperture, seed coat mucilage deposition and lignifications (Liang et al., 2005; Penfield et al., 2001). *AtMYB61* is expressed, prominently, in the tissues which may be the best and collectively described as sinks – developing vasculature, roots and seeds. In Arabidopsis, its expression was appeared to be uniform throughout the developing seed and did not appear to be confined to any particular cell type (Romano et al., 2012). We also found higher level of expression of *MYB61* in both genotypes throughout seed development. *MYB4* and *MYB32* were investigated in Arabidopsis and reported as closely related factors influencing the pollen development by changing the flux along the phenylpropanoid pathways (Preston et al., 2004). *AtMYB4* was found to repress *C4H* expression. Interestingly, in V8 developing seeds *MYB4* expression was only detectable at 42dap, while C4H showed strong down-regulation at this time point. *CCoAOMT* also showed increased transcript levels while those of *PAL2*, *F5H*, *COMT* and *CAD1* were unaffected by over expression of *AtMYB4*. *4CLI* and *4CL3* are down-regulated by higher activity of *AtMYB4* (Jin et al., 2000). In this study, *MYB32* showed higher levels of expression in early developing pods in both genotypes, while in V8 no expression was detectable in the seed maturation phase. Transcriptional activation of *CAD2* and *CCR* was also investigated in *Eucalyptus gunnii* and conserved *MYB* elements were found to be crucial for the transcriptional activation of *EgCAD2* and *EgCCR* promoters in vascular tissues in planta (Rahantamalala et al., 2010*).*

4.1.4 Regulation of glucosinolate metabolism during seed development

The glucosinolate (GSL) biosynthetic pathway is highly explored in rapeseed due to the anti-nutritive role of GSL in meal, and rapeseed varieties with low levels of GSL were developed via successful breeding programs (Mithen et al., 2000). The broad functionality, physiochemical and genetic studies of GSL have led to a model status for research on secondary metabolites (Sønderby et al., 2010).

As expected, genes involved in the GSL metabolic pathway also showed differential expression during seed development in the low-GSL Express617 and the high-GSL genotype V8. A DH population from the cross of these two genotypes showed two large-effect QTL for

total seed GSL content on chromosomes C07 and C09 (Basunanda et al., 2007). Their results also demonstrated that high-GSL rapeseed genotypes often carry low-GSL alleles at one or more of the major QTL controlling seed GSL accumulation. Bhardwaj and Hamama (2003) demonstrated that differentiation for GSL content in winter rapeseed is initiated after 33 DAF. Here we found that *MAM1* and *BCAT4*, which are responsible for Met-derived aliphatic GSL, showed very low expression in Express617 relative to V8 during seed development. *BCAT4* catalyzes the deamination and transamination in GSL side chain elongation, while *BCAT3* has a dual role in GSL side chain elongation as well as for biosynthesis of branched chain amino acid (Knill et al., 2009). *BCAT3* also showed very low expression during seed development in Express617, with only higher expression at 70dap relative to V8. This is also related to its role for amino acid biosynthesis, because storage protein accumulation is the dominant activity in seeds at the maturation stage. Higher transcription levels of *MAM1* and *MAM3* was found earlier in Arabidopsis to be positively correlated with GSL accumulation in early developmental stages (Redovnikovic et al., 2012). A potential role of *MAM1* in variation for total seed GSL content was also demonstrated in an association study based on simple sequence repeat (SSR) markers in rapeseed (Hasan et al., 2008). The same study also reported SSR markers linked to the genes *CYP83B1* and *CYP79A2*, which are involved in GSL core structure formation. In the DGE profiles, no expression was detected for *CYP79A2* but a similar expression pattern of two other CYP79 enzymes, *CYP79B2* and *CYP79B3* was found in Express617 and V8 during seed development. In Arabidopsis induced expression of *CYP79B2* and *CYP79B3* genes resulted in higher concentrations of indole GSL (Mikkelsen et al., 2003). Lower expression of *CYP83A1* was found in Express617 compared to V8, while *CYP83B1* showed higher expression in Express617. Primarily, *CYP83A1* metabolizes the aliphatic oximes and forms aliphatic GSL, while *CYP83B1* catalyzes aromatic oximesto synthesize corresponding substrates for aromatic and indolic GSL. In *B. rapa*, expression patterns of *CYP83A1* and *CYP83B1* have been studied in leaves, petioles and roots (Zhu et al., 2012). That study found almost two-fold *CYP83A1* transcript abundance than that of *CYP83B1* in leaves and petioles. In contrast, the expression levels of the *CYP83A1* were relatively lower than *CYP83B1* in roots. Direct regulation of *CYP83B1* expression by *OBP2* (DOF type transcription factor) is also reported in Arabidopsis (Malitsky et al., 2008) and in Express617 expression of *OBP2* was also detected through whole seed development while in V8 its expression was detectable only in early time points (from 2-28dap). After the oxidation steps by P450 cytochromes (CYP79 and CYP83), next two reactions are carried out by C-S lyase *SUPERROOT1* (*SUR1*)

and glycosyltransferase (*UGT74B1* and *UGT74C1*). In Arabidopsis, *SUR1* C-S lyase was characterized in a *sur1* mutant and complete abolishment of aliphatic and indole GSL was observed. Expression profile of *SUR1* showed its down regulation during seed development in Express617 relative to V8. *UGT74B1* and *UGT74C1* also showed lower levels of expression in Express617, corresponding to previously insertional *ugt74b1* knockout lines with a significant decrease in aliphatic and indolyl GSL in *Arabidopsis* (Grubb and Abel, 2006)

An overall view of expression profiles of developing seeds showed the down-regulation of genes responsible for side chain elongation and core structure formation in early developmental points, and during maturation phase strong up-regulation these genes was found at 42 and 70dap. Four genes responsible for side chain modification in aliphatic GSL in Arabidopsis were identified by QTL mapping were named as *GS_ELONG*, *GS-OX*, *GS-AOP* and *GS-OH* (Kliebenstein et al., 2001a). Brassicaceae specific falvin mono-oxygenease *FMO GS-OX* genes were identified by phylogenetic analysis. They were named as *FMOGS-OX1-5* and localized within the *GS-OX* locus and their role were found for S-oxygenation based on co-expression with aliphatic glucosinolate genes (Li et al., 2008). Here *FMOGS-OX5* expression was detected and its down regulation was observed in Express617 relative to V8. Their role for S-oxygenation makes them interesting genes, since the cancer preventive properties of cruciferous vegetables are linked to S-oxygenation. GS-AOP is the collective QTL name which was detected by fine mapping in Arabidopsis. GS-AOP1, GS-AOP2 and GS- AOP3 are responsible for second round of binary side chain modification changes methylsulfinyl to alkenyl- and to hydroxyl- aliphatic glucosinolates. The function of *AOP1* is not clear in Arabidopsis but functional characterization of *AOP2* indicates that they are catalyzing the reaction to alkenyl and *AOP3* controls the reaction toward hydroxyalkenyl (Kliebenstein et al., 2001b). In Express617, no expression was detected for *AOP2*, while down regulation of *AOP1* and *AOP3* was detected till 14dap and they were up-regulated in later time points during seed development. Expression of the *AOP2* gene was reported to be light dependent and most abundant in leaf and stem tissue, with a number of light regulatory elements identified in the promoter region of the gene (Neal et al., 2010).

Knowledge of the factors controlling glucosinolate hydrolysis is critical for understanding the ecological roles and human health benefits of these compounds, because it is the hydrolysis products and not the glucosinolates themselves that have been found to be the most active.

From a human health perspective, isothiocyanates are the most important because they are major inducers of carcinogen detoxifying enzymes (Williams, 2010). Final composition of the product mix from glucosinolate-myrosinase system can include isothiocyanates, epithionitriles, nitriles, oxozolidine-2-thiones and thiocyanates, depending on the structure of glucosinolate side chain, chemical conditions such as pH, availability of ferrous ions, the presence or absence of supplementary specifier proteins such as epithiospecifier proteins (ESPs), thiocyanate-forming proteins (TFPs) and nitrile-specifier proteins (NSPs) (Williams, 2010). In this study ten genes were annotated as myrosinase associated proteins in the unigene dataset. Epithiospecifiers (*ESP*), recognized as non-catalytic cofactors of myrosinases, are the major determinant of structural specificity during the formation of epithionitriles and nitriles. The epithiospecifier modifier 1 (*ESM1*) gene encodes a protein shown to inhibit function of ESP, leading to increased isothiocyanate production from GS hydrolysis (Burow et al., 2009). Zhang et al. (2006) identified a myrosinase-associated protein as the *ESM1*QTL in *Arabidopsis* using map-based cloning with recombinant inbred lines, natural variation transcriptomic analysis, and metabolic profiling. *ESM1* knockouts and over-expression lines show that *ESM1* represses nitrile formation and favors isothiocyanate production. *ESP* and *ESM1* showed up-regulation during the seed maturation phase in Express617 compared to V8. Variation in the presence and absence of both *ESP* and *ESM1* in *Brassica* species could potentially lead to unique approaches to simultaneously increase the agronomic value and nutritional content of cruciferous crops and could lead to altered nutritional and flavor qualities, because isothiocyanates are typically more active in anticancer assays as well as more bitter than the corresponding nitriles (Zhang et al., 2006).

Detection of transcription factors (TFs) with very low levels of expression is possible by tag based DGE profiling. GSL biosynthesis is regulated by a complex TF network during biotic and abiotic stress responses. Here we described the detection of the TF genes MYB28, *MYB34* and *MYB51* along with *OBP2*/*DOF1.1* during the seed development in Express617 and V8. *MYB28*, *MYB29*, and *MYB76* are also known as *HAG1*, *HAG3* and *HAG2* (*HIGH ALIPHATIC GLUCOSINOLATE1*, *- 3* and *-2*) are members of the large *R2R3-MYB* transcription factors family in *A. thaliana* and were shown to be involved in the specific regulation of aliphatic methionine-derived glucosinolate biosynthesis (Fig. 4.1). They cluster into subgroup XII together with three other MYB factors *MYB51*/*HIG1*, *MYB122*/*HIG2* (*HIGH INDOLE GLUCOSINOLATE1*, *-2*), and *MYB34*/*ATR1* (*ALTERED TRYPTOPHAN REGULATION 1*.

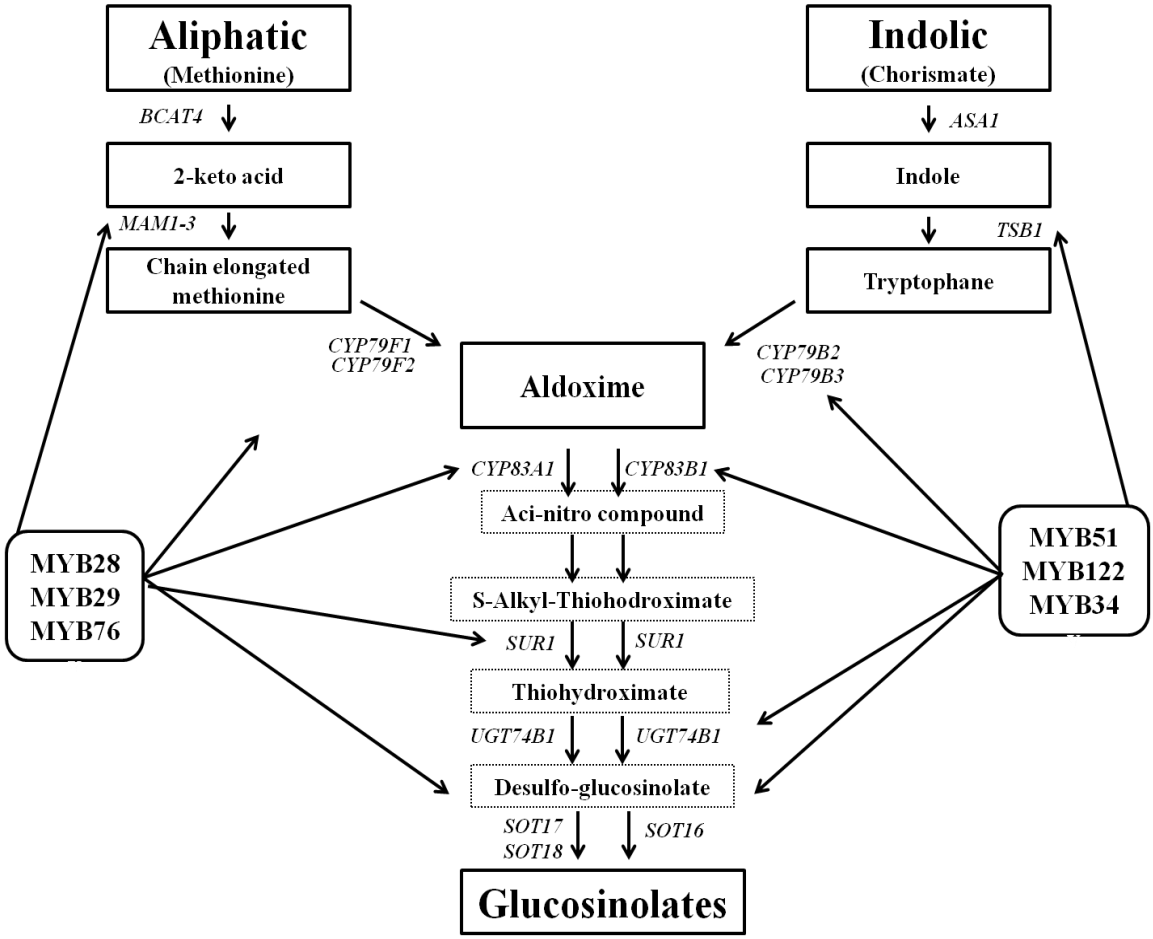

Fig.4.1 Schematic representation of aliphatic and indolic glucosinolate biosynthesis (adopted from Kim et al., 2013). Side-chain elongation; BCAT4, MAM1-3, ASA1, anthranilate synthase alpha 1; TSB1, tryptophan synthase beta 1 Core structure formation; CYP79F1, CYP79F2, CYP79B2, CYP79B3, CYP83A1, CYP83B1, SUR1, UGT7B1, SOT16-18. The key MYB transcription factors involved in aliphatic and indolic glucosinolates are also shown.

MYB28, MYB76, and MYB29 control the biosynthesis of high aliphatic GSLs, while MYB51, MYB122, and MYB34, alternatively called high indolic GSLs, can be manipulated to coordinately control the suite of enzymes that synthesize indolic GSLs (Fig. 4.1) Furthermore, MYB122/HIG2 MYB34/ATR1, and MYB51/HIG1 transcription factors are involved in the homeostasis between auxin (IAA) biosynthesis and indole glucosinolates (Kim et al., 2013).

A transcriptomics and metabolomics study to examine the regulation of glucosinolate (GSL) biosynthesis in *Arabidopsis* transgenic plants over-expressing members of two clades of genes, *MYB28*/*HAG1*-like and *MYB34*/*ATR1*-like, were reported by Malitsky et al. (2008). They found that the activity of these regulators is not restricted to the metabolic space

surrounding GSL biosynthesis but is tightly linked to more distal metabolic networks of primary metabolism. Their results also revealed that expression of *MYB28*-like clade members in terms of downstream gene targets is highly correlated with that of the *ATR1*-like clade members, and *ATR1*/*MYB34* is an important mediator between the gene activities of the two clades. In this study, expression of *MYB28* and *MYB34* was detectable in early seed development points in these winter rapeseed genotypes. Green pods were used to generate the expression libraries in early developmental time points (2-28 dap).

Kim et al. (2013) investigated the expression of MYB transcription factors in young leaves, stem, old leaves, root flower and seeds of *B. rapa*. Higher expression of *MYB28* was detected in stems and flowers, whch contain high levels of aliphatic GSL (Gigolashvili et al., 2007) also reported highest expression of *MYB28* in inflorescences of flowering plants and in old leaves in Arabidopsis. *MYB28*/*HAG1* represents a key component in the regulation of aliphatic methionine-derived GSL biosynthesis in *A. thaliana* (Gigolashvili et al., 2007). *B. napus* genotypes were also explored by associative transcriptomics to define genetic regions and candidate genes controlling total seed GSL contents. Deletion of two copies of *HAG1* (*BnaC.HAG1a* and *BnaA.HAG1c*) from both C2 and A9 in low GS *B. napus* lines disclosed *HAG1* as key player for controlling variation in aliphatic GS synthesis (Harper et al., 2012). Lu et al. (2014) also verified the use of marker trait association for screening of rapeseed germplasm to select low GSL lines based on PCR markers for breeding.

The DOF transcription factor *AtDOF1.1* (*OBP2*) is also reported as part of a regulatory network controlling GSL biosynthesis in Arabidopsis. *DOF1.1* expression is inducible by herbivory and methyl jasmonate Constitutive and inducible over-expression of *DOF1.1* activates expression of *CYP83B1* (Skirycz et al., 2006). In the double zero quality rapeseed genotype Express617, higher expression of *DOF1.1* was observed at early time points and then decreased in descending order till the end of seed maturation. In V8, with high GSL contents expression of *DOF1.1* was only detectable in early time points from 2-28dap. In *B. rapa* higher level of *DOF1.1* isoforms expression was observed in the flowers, stems, and seeds (Kim et al., 2013). The relationship between expression of genes involved in GSL biosynthesis and TFs regulating this pathway along with the metabolomic profile of developing seeds provide a platform to understand the whole mechanism.

4.2 Genetics of root architecture

Root system architecture (RSA) represents an important complex of traits affected by genotype × environment interactions, relevant to survival/performance and showing high variation in many crops. Understanding genetic determinants encoded by the combined effect of multiple loci on root system is a glaring gap in our knowledge. The root system of plants is an ideal place to study the developmental plasticity and determinants of architecture. Acquisition of water and nutrients of plants from the soil is dependable on root systems (Malamy, 2005). Relationships between root growth, development and seed production were explored in *B. napus*. Root development immediately after germination preceding the development of shoot, in seedlings, would be a valuable tool for plant breeders to predict the ability of rapeseed yield potential (Koscielny and Gulden, 2012). Non-destructive phenotyping systems such as rhizotrons have facilitated the direct observation of the roots on a scale involving hundreds of plants. High power, high resolution genome-wide association studies (GWAS) and sequencing methods have far outpaced phenotyping methods necessary for the discovery of regions and underlying genes involved in plant growth and development (Huang et al., 2010; Jung and McCouch, 2013). This project was planned to investigate a large *B. napus* population by GWAS to discover the complex genetic makeup behind root architecture. These investigations have opened the way to the characterization of genes in the polyploid genome of rapeseed encoding components of the complex root architecture trait.

A rhizotron system was optimized to examine the *in vitro* root system growth of rapeseed genotypes 7 days after sowing under controlled conditions. For *B. napus* it was concluded in a growth room study by Koscielny and Gulden (2012) that root length as early as 7 d after imbibition is an excellent measure of seedling vigour and an indicator of seed yield potential of inbred lines. The rhizotron system we used here enabled root system phenotyping of 94 DH lines from the cross Express617 x V8 along with 496 genotypes of a *B. napus* diversity set. High throughput phenotyping data for root traits were analyzed for QTL mapping in the DH population and association mapping was done for the diversity set as an initial step for understanding the genetics of RSA in this polyploid species. Identification of QTL related to interesting phenotypes is the basis for application of genetic markers in plant breeding. Large collections of genetic markers are the key for QTL analysis of complex traits. The power of QTL has proven to be challenging for the identification of genetic and molecular basis of

traits such as in case of rapeseed, selective breeding of genotypes for low glucosinolates and erucic acid (as discussed in the previous section).

Morphological complexity of traits in eukaryotic species could be an outcome of whole-genome duplication coupled with the retention of duplicated genes (Freeling & Thomas, 2006; Martinez-Alberola et al., 2013). Well defined rearrangements and duplication events in the ancestral genome segments of Brassicaceae species have been reported (Parkin, 2005; Parkin et al., 2003; Wang et al., 2011b). These segments facilitate comparative genomics between Brassicaceae species, including other *Brassica* species and the model plant Arabidopsis. Loudet et al. (2005) identified 13 QTLs associated to the root architectural traits in Arabidopsis (Bay0 x Shahdara RIL population). Recently, high-throughput phenotyping of root architectural traits in *Brassica* was also reported by Shi et al. (2013). Thirty eight QTL associated to root traits were detected in *B. napus* DH mapping population Tapidor × Ningyou 7 across nine of the 19 chromosomes. Shi et al. (2013) concluded that assessment of root traits under field conditions can be slow and expensive, and this gel-based high throughput phenotyping of *B. napus* facilitates the screening of large population for root traits. Identification of the genetic elements associated with root traits will provide grounds for the selection of genotypes with potentially improved abiotic stress tolerance and nutrient uptake efficiency.

4.2.1 Phenotypic variation and correlations among root traits

High throughput characterization of a large set of plant populations by phenotyping and genotyping generate a massive amount of information holding potential for quantifying variation in different yield traits. It will be very critical information if altered phenotypes are associated with the presence or absence of a particular gene to determine the function for the thousands of genes present in the genome.

Regardless of the availability of vast genetic resources, little is known about the genes contributing to RSA. The fundamental reason for this knowledge gap is, primarily, the difficulties to image root systems and to identify the relevant quantitative phenotypes from complex topologies (Topp et al., 2013). For the understandings of all architectural possibilities for crop improvement, it is vital to identify the precise nucleotide polymorphisms underling quantitative differences in central RSA traits. The potential exists

to breed for root system architectures that allow to optimize resource acquisition. However, this requires the ability to screen root system development quantitatively, with high resolution, with high throughput.

Rapeseed plants have a tap root system. Root growth is due to cell division and enlargement at the tip of the root. The root system originates from a primary root and continues to develop secondary roots growing outward and downward to the tap root. The root development is relatively invariable with an average of almost 2 cm per day at good soil moisture conditions (http://www.canolacouncil.org/crop-production). Phenotypic investigation of a large set of rapeseed lines in this study showed that there is a large genetic variation for five root traits in four sets of inbred lines, i.e. winter rapeseed, spring rapeseed and swedes together with some other vegetable types. Considerable transgressive segregation of these root traits was observed in the Express617 x V8 DH population, indicating that these traits are quantitatively inherited and controlled by multiple genes which can serve as starting point for genetic improvement (Ding et al., 2012). Loudet et al. (2005) also reported similar pattern of transgressive segregation of lateral root traits in an Arabidopsis RIL population. In *B. napus*, the bi-parental DH mapping population Tapidor × Ningyou 7 was screened for root architectural traits under low and high phosphorous availability. Large variation and strong correlation among root traits and with shoot traits and growth proved their valuable role for crop improvement (Shi et al., 2013).

Wide variation was also observed for these five root traits in three sub-populations of the *B. napus* diversity set. Lateral root number showed significant correlation with primary root length but there was strong negative correlation of lateral root density with primary root length. Based on this genetic variation, identification of QTLs may lead to the discovery of genes concerned in basic processes controlling root architecture. Several QTLs have been reported based on this genetic variation, responsible for important aspects of root architecture in Arabidopsis accessions (Loudet et al., 2005; Mouchel et al., 2004) and also in *B. napus* inbred lines (Shi et al., 2013).

4.2.2 QTL and association mapping of root architecture traits

Quantitative characters are a common feature of variation in populations of crop plants and have been a major area of interest in genetics for over a century. The study of quantitative

traits has involved bioinformatics and statistical tools which provided a conceptual base for partitioning the total phenotypic variance into genetic and environmental variance components. This information can help in analyzing variation in a quantitative trait in congruence with molecular marker data generated in a segregating population. It became feasible to estimate the heritability of the trait from this information and predict the response of the trait to selection. The heritability measures the proportion of the phenotypic variance that is solely due to genetic effects. It is important for QTL mapping because it explains the maximum proportion of phenotypic variance that can be accounted for by QTLs. In this study, broad sense heritability for root traits was 20% and 13% for primary root length and its growth rate, respectively. Lateral root traits showed higher heritabilities of 25%, 26% and 36% for lateral root number, density and length respectively. A range of 13% to 16% of heritability of root traits in a DH mapping population of *B. napus* was reported by Shi et al. (2013).

In modern breeding programmes, QTL mapping is becoming increasingly important for marker assisted selection, as well as for map-based gene discovery. Previously, QTLs associated with seed yield, branch number, pod number and plant height were detected on chromosomes A03, A06 and C03 and co-localized with those involved in root morphology (Yang et al., 2010; Yang et al., 2011). Their results indicated that a developed root system contributes largely to traits that directly or indirectly increase seed yield at maturity. Recently, the response of *B. napus* root system to low and high phosphorous was evaluated by high throughput phenotyping and 38 QTLs were detected for different root and shoot growth traits (Shi et al., 2013). A cluster of highly significant QTL for LRN, LRD and biomass traits at low phosphorous availability were identified on chromosome A03 with association to functional markers named BnPHT3-A3 and BnWRKY-A3. Interestingly, in the present study, lateral root traits LRN, LRL and LRD are also co-localized at 265cM to 275cM on chromosome A03, with the highest genetic variation of 25.5% and also the highest heritability of 36% for LRL. The DH population from Express617 x V8 was extensively analyzed for QTL mapping for several qualitative and quantitative traits. Basunanda et al. (2009) compared QTL regions related to the expression of heterosis for seedling developmental traits, plant height at flowering, seeds per silique, siliques per unit area, thousand seed mass, and seed yield. QTLs associated with root traits co-localized with previously identified QTLs associated with seedling and yield traits presented in Figure 4.2 (Basunanda et al., 2009), and seed glucosinolate content (Basunanda et al., 2007). On A03,

QTL associated with seed yield was co-localized with the QTL region associated with three lateral root traits. In a field and growth room experiments strong relationship between root parameters and seed yield was observed in *B. napus* (Koscielny and Gulden, 2012).

Only one QTL was found here to be associated with PRL at 122.41cM on chromosome C03, with a LOD score of 3.8 and genetic variance of 13.18%. QTLs associated with seed yield, glucosinolates and plant height were also detected on C03 previously. Interestingly, markers linked with the hypocotyl length were co-localized in the QTL region associated to primary root growth rate in this study on C04. QTLs related to lateral root density were reported in *B. napus* on chromosome C04 by Shi et al. (2013). In *B. rapa*, QTLs associated with tap root thickness, length, and weight were also detected on chromosome C04 (Lu et al., 2008). The identification of QTLs which affect the productivity of storage roots, combined with the observation of transgressive segregation of root traits in inbred lines, indicate the effects of positive alleles which could be combined to select lines with an improved root system regarding more efficient water and nutrient acquisition.

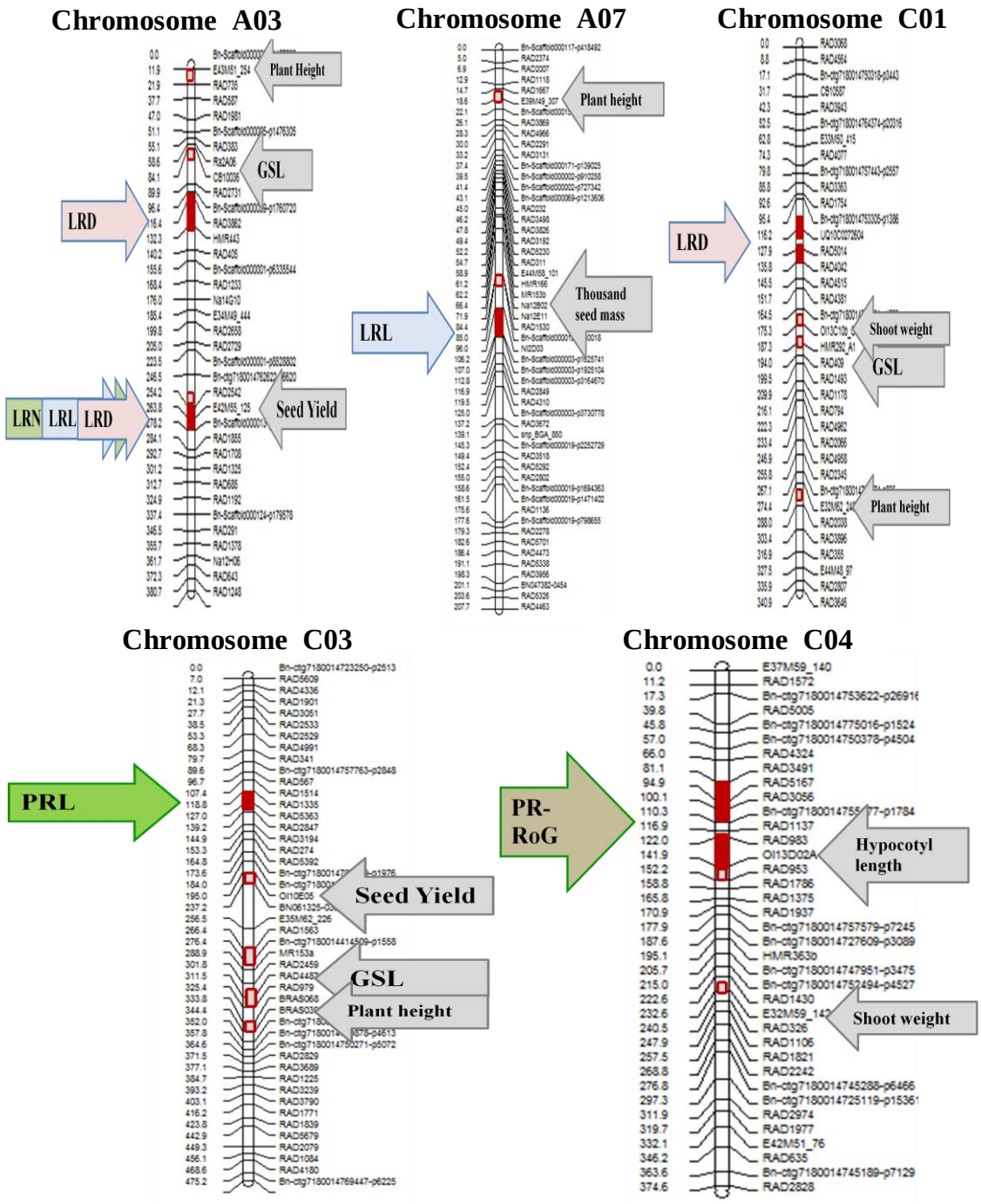

Fig. 4.2 QTLs detected in DH lines from Express617 x V8 for root traits (present study), seedling and yield traits (Basunanda et al., 2009), and seed glucosinolate (GSL) content (Basunanda et al., 2007). QTL positions in cM (2 LOD support interval) are marked as red bar and marker names are presented on chromosomes in respect to their respective distance in cM along each chromosome.

Historically, QTL detection was performed using bi-parental segregating breeding populations with linkage mapping. Breeding populations are different from natural populations in that instead of undergoing natural selection they are subjected to directed selection by the breeder (Würschum, 2012). The genetic basis of breeding populations is generally (much) smaller than that of natural populations. In contrast, association analysis (GWAS) serves as an alternative for QTL mapping using collections of land races, old varieties and breeding lines. Different from conventional QTL mapping, association mapping utilizes the greater number of historical recombination events in (natural) population to map QTL based on linkage disequilibrium (LD) between genome-wide markers and traits. Therefore, a higher resolution of QTL mapping can be achieved with GWAS than by using bi-parental segregating populations (Ersoz et al., 2007). In the present study, three sub-populations separately mainly by their seasonal behavior were found in this diversity set, corresponding to results discriminated by others (Bus et al., 2011; Hasan et al., 2008; Rezaeizad et al., 2010). Allocation of winter and spring rapeseed lines to different groups was attributed to their breeding history. The differentiation into winter and spring forms is governed by a genetic mechanism controlling the requirement for vernalisation to promote the onset of flowering. A clear separation of swede types was possible from the other two identified clusters, which indicated that swedes are most likely derived from different interspecific hybridisation events than those which led to winter and spring oilseed rape forms (Bus et al., 2011).

Based on nonrandom associations of loci in haplotypes, association or LD mapping is a powerful high-resolution tool for genetic analysis of complex quantitative traits. LD arises in structured populations when allelic frequencies differ at two loci across subpopulations irrespective of the linkage status of the loci. Admixed populations formed by the union of previously separate populations into a single panmictic one, can be considered as a case of structured populations where substructuring has recently ceased (Pritchard et al., 2000). Admixture of populations often results in the introduction of chromosomes of different ancestry and allelic frequencies. Admixture of population is one of the major factors that cause spurious associations between marker alleles and the phenotype. High variability was observed regarding the extent of LD across genomes of different species studied to date (Ersoz et al., 2007). Within a given genomic region (specific chromosome) or whole genome-wide patterns of pair-wise LD (based on squared allele frequency correlations (r^2), LD tends to decrease with distance between polymorphic markers. In this study, 496 rapeseed lines

from all over the world were used to estimate the extent of LD. A decrease in LD was observed with distance between SNP markers distributed across nineteen chromosomes. The mean pairwise r^2 (squared allele frequency correlations) value for the whole rapeseed population set was 0.035, which is close to previous estimates of 0.027 (Ecke et al., 2010) 0.0247 (Harper et al., 2012) or 0.037 (Delourme et al., 2013), confirming the low overall level of LD in *B. napus.* The cause for this is thought to be because rapeseed varieties are traditionally bred as an autogamous species with controlled crosses followed by several generations of selfing and testing (Ecke et al., 2010).

Genome wide association analysis between root traits and SNP markers in *B. napus* was done by using GLM and MLM in TASSEL4 software (Bradbury et al., 2007). Inflated distribution of cumulative *P*-values in GLM, observed in quantile-quantile plots, demonstrated that MLM is a more reliable model with smaller number of false positives for association mapping. Stich et al. (2008) also suggested that mixed-model association-mapping approaches based on kinship matrix are more appropriate for association mapping. They also suggested that the 'K+Q' model was not only appropriate for association mapping in humans, maize, and Arabidopsis, but also for rapeseed, potato, and sugar beet, indicating that the 'K+Q' model can be applied widely to various species (Stich et al. 2008).

A total of 38 markers were identified which are significantly associated with five root architecture traits in this diverse population. The associations were tested against a 20% false discovery rate, following the examples of several authors (Cai et al., 2014; Honsdorf et al., 2010; Kraakman et al., 2004), with the argument that in an explorative analysis, the discovery of QTL is more important than stringent avoidance of false positives. The goal of association mapping using rapeseed populations is to identify key genes controlling various traits related to root system architecture, as a basis for incorporation of the best alleles into elite breeding materials. The current study represents a first example of whole genome association analysis of root architecture traits in rapeseed. Previously, Hasan et al. (2008) described association of gene-linked SSR markers to seed glucosinolate content in genetically diverse *B. napus* genotypes. Association mapping for flowering and yield traits along with quality traits including seed oil, protein, GSL, sulfur, oleic and linolenic acid contents in canola quality winter OSR was reported by Honsdorf et al. (2010). Rezaeizad et al. (2010) also identified QTL by association mapping of genome wide SSR markers, finding associations to phenolic

compounds of extraction meal in a population of 49 genetically diverse oilseed rape cultivars of dark-seeded, winter-type OSR accessions.

Harper et al. (2012) developed associative transcriptomics to identify molecular markers associated with trait variation on the basis of gene sequences and global expression patterns. Genomic deletions were identified in two QTLs related to GSL content in seeds. Orthologs of the transcription factor *HAG1* (At5g61420) involved in the GSL biosynthesis pathway were found to be positioned in the deleted region. Genetic architecture of seed weight and seed quality in rapeseed was studied by using the recently developed 60K *Brassica* Infinium® SNP array (Li et al., 2014). Two significant associations on A08 and C03 were detected for erucic acid content, and analysis of markers showed that the peak SNPs were only 233 and 128 kb away from the key genes *BnaA.FAE1* and *BnaC.FAE1*. Four clusters of SNPs associated with glucosinolate content on A09, C02, C07 and C09 were also identified, corresponding to the chromosome regions which contain the previously described *HAG1* orthologues.

Recently, Cai et al. (2014) investigated the yield-related traits plant and first branch height, inflorescence and silique length, seeds per silique and seed weight by genome-wide association analysis in rapeseed. A comparison of this association mapping of yield traits with root traits form the present study showed that markers associated with primary root length (PRL) were located on chromosomes A03, C06 and C08. On C08, two markers significantly associated to PRL and RoG and on the same chromosomes, significant association of markers were detected to plant height and seed weight. In the bi-parental population Express617 x V8, a unique QTL for PRL was detected on chromosome C03, on the same chromosome with markers associated to first branch height and plant height as identified by (Cai et al., 2014). Lateral root traits were clustered to chromosomes A06 and in yield traits association, seeds per siliques and seed weight were found to be associated to the markers located on A06. In our bi-parental population, lateral root traits were clustered on chromosome A03, which was also detected in another study on root traits of a *B. napus* bi-parental population by Shi et al. (2013). This indicates the potential presence of important genes influencing root traits in different B. napus genetic backgrounds. From yield traits, on the other hand, plant height was the only trait found to be associated with markers on chromosome A03.

The variance explained by the mapped QTL or associated markers is one point to consider when discussing the prospects of marker-assisted selection of the QTL. A common observation in QTL mapping is that sometimes QTL for different traits occur at closely linked loci in the genome. Here arises the question whether the clusters represent linked but otherwise independent QTL, or are due to pleiotropic effects of one locus. In some cases plausible arguments for pleiotropy can be derived from metabolic or other relationships between the traits (Honsdorf et al., 2010). Fine mapping of such chromosomal regions would help to determine the candidate genes responsible for natural phenotypic variation of these traits.

4.2.3 Potential candidate genes for root architecture development

The assessment of root traits in plants can be complicated, time consuming and expensive. In this study, gel based high-throughput root phenotyping was employed for screening of *B. napus* large population to characterize the root traits and identify genetic loci controlling these traits. Extensive QTL mapping in many plants was done for identification of chromosomal locations thought to be associated with various root system traits (Kamoshita et al., 2002). Due to lack of information about root system architecture determinants, the possibilities to move from these loci to candidate genes in these systems seem limited, but the identification of genes involved in root architecture development via QTL analysis is by no mean impossible (Zheng et al., 2003). Natural variation in root system size among Arabidopsis ecotypes was explored by Mouchel et al. (2004). Inbred lines were produced from ecotype UK-1 with an extremely short and stunted root system and another ecotype with a more average-sized root system to identify a QTL responsible for 80% of the variation in root length. A novel transcription factor, BREVIS RADIX (BRX) was traced out in this QTL and found to have a strong effect on root system phenotype when transformed to UK-1. These results give basis to use the power of natural mutagenesis to identify new and important genes.

Shi et al. (2013) identified QTL associated with PRL and LRD on chromosome A06 and that QTL region was found to be syntenous with Arabidopsis chromosome 1. Arabidopsis *LPR2* (At1g71040) is involved in the regulation of primary root development under low phosphorous availability, and it is a paralogue of *LPR1* (At1g23010), encoding multicopper oxidases identified in this region of Arabidopsis chromosome 1. In the present study, a single

SNP marker located on chromosome A06 is significantly associated with LRD (*P-value* 0.0007). Mutated INTEGUMENTA-like gene, *PRD* (At1g79700) co-located in the QTL region on chromosome 1 of Arabidopsis, showed decreased primary root-length and lateral root development under low Pi availability compared with the wild-type (Camacho-Cristobal et al., 2008). For traits which have a simple genetic architecture, the number of QTL detected would be strongly influenced by chance, but detection of a certain percentage of the QTL is required for traits with a complex architecture (Ecke et al., 2010). The potential of high-throughput root phenotyping assays and their use to advance the breeding and selection of competent cultivars requires cross validation with root system characteristics and yield determination under challenging field conditions.

4.3 CONCLUSIONS

In this study two complex traits of *B. napus* were investigated:

i) Seed development was studied the rapeseed genotypes Express 617 (00 quality, high lignin) and V8 (high erucic acid, high GSL, high lignin) by digital gene expression (DGE) transcriptome profiling;

ii) QTL mapping and GWAS was applied for the genetic analysis of root architectural traits in a DH population (Express617 x V8) and a large *B. napus* diversity set (n=496), respectively.

Based on the results of these studies the following findings can be demarcated:

- Gene expression throughout the early stages of seed development from 2-28 dap are highly correlated and characterized by a high expression of genes involved in embryonic development, photosynthesis pathway, cell proliferation and seed coat formation.
- Genes involved in lipid and storage protein accumulation showed generally elevated expression during the seed maturation phase.
- Strong differential expression associated with phenylpropanoid and GSL biosynthesis was observed between the two genotypes during the seed maturation phase. A lower expression of genes responsible for GSL biosynthesis was observed in Express617 relative to V8 (high total GSL content).
- A critical view of expression profile showed up-regulation of genes involved in lignin biosynthesis in Express617 (high seed lignin content) during maturation phase of seeds (from 42 dap until 70 dap) relative to V8 (reduced seed lignin content).

- Higher expression of *CAD* genes in Express617 during seed maturation, and a complete loss of CAD gene expression at 42dap in V8, confirmed the importance of *CAD* in regulation of seed lignin content.
- DGE analysis based on tag profiling was found to be very useful for detection of very low levels of expression of transcription factors (TF). Six TF belonging to the MYB family involved in regulation of phenylpropanoid biosynthesis pathway were detected during rapeseed seed development. *MYB58* and *MYB63* are expressed, specifically, in the cells undergoing secondary wall thickening and are significant regulators of lignin-biosynthesis. Higher levels of *MYB58* and *MYB63* expression were observed in the seed maturation phase in Express617 compared to V8. A constitutive expression of *MYB61* was observed in both genotypes throughout seed development.
- Several genes known to be involved in the GSL metabolic pathway have been considered as candidates for controlling GSL contents in rapeseed seeds to reduce total glucosinolates in rapeseed meal. *MAM1* and *BCAT4* which are responsible for Met-derived aliphatic GSL showed very low expression in Express617 relative to V8 during seed development. *CYP83B1* and *CYP79A2* genes which are involved in GSL core structure formation showed a similar expression pattern in Express617 and V8 during seed development. *GS-AOP* genes are responsible for second round of binary side chain modification changes methylsulfinyl to alkenyl- and to hydroxyl- aliphatic glucosinolates. In Express617, no expression was detected for *AOP2*, while down regulation of *AOP1* and *AOP3* was detected till 14 dap and they were up-regulated in later time points during seed development.
- *ESP* and *ESM1*, recognized as non-catalytic cofactors of myrosinase, showed up-regulation during the seed maturation phase in Express617 compared to V8.
- Expression of *MYB28* (*HAG1*), *MYB34* and *MYB51* along with *OBP2*/*DOF1.1* was detected during the seed development in Express617 and V8. Expression of *MYB28* and *MYB34* was observed in early seed development points in these winter rapeseed genotypes. Higher expression of *DOF1.1* was observed in Express617 at early time points and then decreased during seed maturation relative to V8.
- The differential phenotypes of these two winter rapeseed genotypes regarding seed GSL and lignin content are genetically controlled by the interaction of many gene families which showed differential expression during whole seed development. Correlation of DGE profile of seeds from each developmental point with their

metabolome profile along with identification of specific genes would provide more useful and outcome in diverse rapeseed genotypes.

- A non-destructive gel based mini-rhizotrons system for root trait phenotyping in rapeseed was optimized. This system has facilitated the visualization of root system in large *B. napus* genotype collection including 94 DH lines from Express617 x V8 along with 496 inbred lines of a *B. napus* diversity set. A large variation, broad segregation and medium-low heritability of root architectural traits in the biparental population proved that these are quantitatively inherited traits controlled by multiple genes which give intimation to proceed for genetic improvement and selection of rapeseed lines with improved root system.
- In the bi-parental population, 11 QTL regions associated with root architectural traits and in the large *B. napus* diversity set, 38 significant marker-trait associations were detected which is a first step towards marker assisted selection, as well as for map-based gene discovery.
- LD analysis from three sub-populations: winter rapeseed, spring rapeseed, and swede-type with some vegetables confirmed the low overall level of linkage disequilibrium in *B. napus* which is considered to be due to controlled crosses followed by several generations of selfing to develop new varieties with improved seed qualities.

5. SUMMARY

Rapeseed (*Brassica napus* L.) is an important oilseed crop. Its oil is used for human consumption, as green fuel (biodiesel), and in the chemical and pharmaceutical industry. The cake and meal, residues of oil pressing and extraction, are used as valuable components for feeding animals.

Seed metabolism and root traits are two important components of seed quality and yield, respectively, in *B. napus*. Both are controlled by complex genetic mechanisms. The aim of this study was to develop and use novel high throughput DNA sequencing techniques, on one hand, to investigate digital gene expression (DGE) of gene networks responsible for important seed quality traits, and on the other hand to use DGE along with high-throughput phenotyping of root architectural traits in a rapeseed population for marker trait association.

Two *B. napus* black seeded winter genotypes were selected to investigate their transcriptome during seed development by DGE: Express617 which is a 00-quality cultivar with high lignin content and V8, which has high seed erucic acid and glucosinolate (GSL) contents but moderate levels of seed lignin, another antinutritive compound in the seed meal. Early stages of seed development from 2-28 dap showed high correlation and a great variation was observed in later stages and the seed maturation phase in the two genotypes. Based on their previously known differential phenotypes for total GSL and lignin, differential expression of genes involved in GSL metabolic and phenylpropanoid/lignin biosynthesis pathway was observed in the MapMan metabolic pathway annotator during seven seed developmental time points (2-84 days after pollination). A total of 58 genes were annotated to the phenylpropanoid pathway specifically directed to lignin biosynthesis, while 34 genes were detected from the GSL metabolic pathway. Expression pattern of genes involved in lignin biosynthesis showed up-regulation in Express617 during the seed maturation phase from 42 until 70 dap. Expression of six MYB family transcription factors (*MYB4, 32, 58, 61, 63* and *85*) were detected which are responsible for activation of monolignol pathway genes by coordinating binding motifs corresponding to their AC-rich elements. AC elements are present in the promoters of most monolignol pathway genes, including *PAL*, *4CL*, *C3H*, *CCoAOMT*, *CCR* and *CAD*, and many of these genes showed different expression patterns between the two genotypes corresponding to their differences in lignin compounds. Similarly, several genes known to be involved in the GSL metabolic pathway are considered as

candidates for controlling GSL contents in rape seeds to reduce total glucosinolates in rapeseed meal. In this study, expression of 34 genes was observed were involved in GSL amino acid side chain elongation, core structure formation from amino acid moiety, secondary modification and degradation enzymes. Expression of transcription factors *OBP2/DOF1.1* and the MYB family (*MYB34, 28 and 51*) which are known to be responsible for GSL pathway regulation were also detected during seed developmental stages. Further characterization of these genes in developing seeds from each time point and correlation with seed metabolomic profiles for GSL and lignin content will help in validation of their potential role in controlling seed fibre content in black seeded rapeseed genotypes.

In this project, a digital root phenotyping system based on mini-rhizotrons was also optimized for phenotyping root traits in rapeseed. This non-destructive gel based system has facilitated the visualization of the root system in large *B. napus* population. Root architectural traits were studied in two sets of *B. napus* genotypes, Express617 x V8 DH population (94 lines) and 500 inbred lines in the diversity set include winter, spring, vegetable and swede types. Five root traits were investigated for phenotypic analysis, including primary root length (PRL), rate of primary root growth (RoG), lateral root length (LRL), lateral root number (LRN) and lateral root density (LRD).

A large variation, segregation and heritability of root architectural traits in the bi-parental population proved that these are quantitatively traits controlled by multiple genes, which give intimation to proceed for genetic improvement and selection of lines with improved root system. In the bi-parental population Express617 x V8 DH, 11 QTL regions associated with root architectural traits were detected. Some of these are also co-localized with previously detected QTL associated for seedling and yield traits in the same population, and potentially also co-localized with biomass and yield-related traits in other populations. QTL mapping is a first step for marker assisted selection, as well as for map-based gene discovery. In a large *B. napus* diversity set, 38 significant marker-trait associations were detected for root architectural traits. LD analysis confirms the low overall level of linkage disequilibrium in *B. napus* which could be due to controlled crosses followed by several generations of selfing to develop new varieties with improved seed qualities. With the availability of the *B. napus* genome sequence, knowledge of sequence variation in specific genes and cost-effective high-throughput genotyping and phenotyping of qualitative and quantitative traits, it is expected that molecular breeding will play an important role in future breeding of new cultivars.

REFERENCES

Abràmoff MD, Magalhães PJ and Ram SJ. (2004) Image Processing with ImageJ, *Biophotonics International*, **11:** 36-42,

Agrawal GK, Hajduch M, Graham K, Thelen JJ. (2008) In-Depth investigation of the soybean seed-filling proteome and comparison with a parallel study of rapeseed. *Plant Physiol.* **148:** 504-518

Allender CJ, King GJ. (2010) Origins of the amphiploid species *Brassica napus* L. investigated by chloroplast and nuclear molecular markers. *BMC Plant Biol*. **10**

Anterola AM, Jeon JH, Davin LB, Lewis NG. (2002) Transcriptional control of monolignol biosynthesis in Pinus taeda: factors affecting monolignol ratios and carbon allocation in phenylpropanoid metabolism. *J Biol Chem* **277:** 18272-18280

Badani AG, Snowdon RJ, Wittkop B, Lipsa FD, Baetzel R, Horn R, De Haro A, Font R, Luehs W, Friedt W. (2006) Colocalization of a partially dominant gene for yellow seed colour with a major QTL influencing acid detergent fibre (ADF) content in different crosses of oilseed rape (*Brassica napus*). *Genome* **49:** 1499-1509

Baldoni A, Von Pinho EV, Fernandes JS, Abreu VM, Carvalho ML (2013) Gene expression in the lignin biosynthesis pathway during soybean seed development. *Genet Mol Res* **12**

Bancroft I, Morgan C, Fraser F, Higgins J, Wells R, Clissold L, Baker D, Long Y, Meng J, Wang X, Liu S, Trick M (2011) Dissecting the genome of the polyploid crop oilseed rape by transcriptome sequencing. *Nat Biotech* **29:** 762-766

Barriere Y, Laperche A, Barrot L, Aurel G, Briand M, Jouanin L. (2005) QTL analysis of lignification and cell wall digestibility in the Bay-0 x Shahdara RIL progeny of Arabidopsis thaliana as a model system for forage plant. *Plant Sci.* **168:** 1235-1245

Barriere Y, Thomas J, Denoue D. (2008) QTL mapping for lignin content, lignin monomeric composition, p-hydroxycinnamate content, and cell wall digestibility in the maize recombinant inbred line progeny F838 x F286. *Plant Sci.* **175:** 585-595

Basunanda P, Radoev M, Ecke W, Friedt W, Becker HC, Snowdon RJ. (2010) Comparative mapping of quantitative trait loci involved in heterosis for seedling and yield traits in oilseed rape (*Brassica napus* L.). *Theor Appl Genet* **120:** 271-281

Basunanda P, Radoev M, Ecke W, Friedt W, Becker HC, Snowdon RJ. (2009) Comparative mapping of quantitative trait loci involved in heterosis for seedling and yield traits in oilseed rape (*Brassica napus* L.). *Theor Appl Genet* **120:** 271-281

Basunanda P, Spiller TH, Hasan M, Gehringer A, Schondelmaier J, Luhs W, Friedt W, Snowdon RJ (2007) Marker-assisted increase of genetic diversity in a double-low seed quality winter oilseed rape genetic background. *Plant Breed.* **126:** 581-587

Benjamini Y, Hochberg Y. (1995) Controlling the False Discovery Rate: A Practical and Powerful Approach to Multiple Testing. *J Royal Stat Society Series B (Method.)* **57:** 289-300

Bhardwaj HL, Hamama AA. (2003) Accumulation of glucosinolate, oil, and erucic acid in developing Brassica seeds. *Indust Crops Products* **17:** 47-51

Bhinu VS, Li R, Huang J, Kaminskyj S, Sharpe A, Hannoufa A. (2009) Perturbation of lignin biosynthesis pathway in *Brassica napus* (canola) plants using RNAi. *Can J Plant Sci.* **89:** 441-453

Blake J., Spink J., Bingham I. 2006. Management of oilseed rape to balance root and canopy growth. Hereford, UK, 22 p.

Bloem E, Haneklaus S, Schnug E. (2007) Changes in the sulphur and glucosinolate content of developing pods and seeds of oilseed rape (*Brassica napus* L.) in relation to different cultivars. *Landbauforsch Volk* **57:** 297-306

Bouteille M, Rolland G, Balsera C, Loudet O, Muller B. (2012) Disentangling the intertwined genetic bases of root and shoot growth in Arabidopsis. *PLoS ONE* **7:** e32319

Bradbury PJ, Zhang Z, Kroon DE, Casstevens TM, Ramdoss Y, Buckler ES. (2007) TASSEL: software for association mapping of complex traits in diverse samples. *Bioinformatics* **23:** 2633-2635

Brenner S, Johnson M, Bridgham J, Golda G, Lloyd DH, Johnson D, Luo SJ, McCurdy S, Foy M, Ewan M, Roth R, George D, Eletr S, Albrecht G, Vermaas E, Williams SR, Moon K, Burcham T, Pallas M, DuBridge RB, Kirchner J, Fearon K, Mao J, Corcoran K. (2000) Gene expression analysis by massively parallel signature sequencing (MPSS) on microbead arrays. *Nat Biotechnol* **18:** 630-634

Buckler ESt, Thornsberry JM. (2002) Plant molecular diversity and applications to genomics. *Curr Opin Plant Biol* **5:** 107-111

Burow M, Losansky A, Müller R, Plock A, Kliebenstein DJ, Wittstock U. (2009) The Genetic Basis of Constitutive and Herbivore-Induced ESP-Independent Nitrile Formation in Arabidopsis. *Pl Physiol***149:** 561-574

Bus A, Körber N, Snowdon RJ, Stich B (2011) Patterns of molecular variation in a species-wide germplasm set of Brassica napus. *Theor. Appl. Genet.* **123:** 1413-1423

Butruille DV, Guries RP, Osborn TC (1999) Increasing yield of spring oilseed rape hybrids through introgression of winter germplasm. *Crop Sci.* **39:** 1491-1496

Cai D, Xiao Y, Yang W, Ye W, Wang B, Younas M, Wu J, Liu K (2014) Association mapping of six yieldrelated traits in rapeseed (*Brassica napus* L.). *Theor Appl Genet* **127:** 85-96

Camacho-Cristobal JJ, Rexach J, Conejero G, Al-Ghazi Y, Nacry P, Doumas P. (2008) PRD, an Arabidopsis AINTEGUMENTA-like gene, is involved in root architectural changes in response to phosphate starvation. *Planta* **228:** 511-522

Capron A, Chang XF, Hall H, Ellis B, Beatson RP, Berleth T. (2013) Identification of quantitative trait loci controlling fibre length and lignin content in Arabidopsis thaliana stems. *J Exp Bot* **64:** 185-197

Cardon LR, Bell JI. (2001) Association study designs for complex diseases. *Nat Rev Genet* **2:** 91-99

Cardone M, Prati MV, Rocco V, Seggiani M, Senatore A, Vitoloi S. (2002) Brassica carinata as an alternative oil crop for the production of biodiesel in Italy: engine performance and regulated and unregulated exhaust emissions. *Environ Sci Technol* **36:** 4656-4662

Chabannes M, Barakate A, Lapierre C, Marita JM, Ralph J, Pean M, Danoun S, Halpin C, Grima-Pettenati J, Boudet AM. (2001) Strong decrease in lignin content without significant alteration of plant development is induced by simultaneous down-regulation of cinnamoyl CoA reductase (CCR) and cinnamyl alcohol dehydrogenase (CAD) in tobacco plants. *Plant J* **28:** 257-270

Chagné D, Batley J, Edwards D, Forster JW. (2007) Single Nucleotide Polymorphisms genotyping in plants, in: NC Oraguzie, et al. (Eds.), Association mapping in plants, Springer, New York. pp 77-94.

Chagne D, Crowhurst RN, Troggio M, Davey MW, Gilmore B, Lawley C, Vanderzande S, Hellens RP, Kumar S, Cestaro A, Velasco R, Main D, Rees JD, Iezzoni A, Mockler T, Wilhelm L, Van de Weg E, Gardiner SE, Bassil N, Peace C (2012) Genome-Wide SNP Detection, Validation, and Development of an 8K SNP Array for Apple. *PLoS One* **7**

Chalhoub B, Denoeud F, Liu S, Parkin IAP et al., (2014) Early allopolyploid evolution in the post-Neolithic Brassica napus oilseed genome. *Science* 345: 950-953

Cheng H, Li L, Xu F, Cheng S, Cao F, Wang Y, Yuan H, Jiang D, Wu C. (2013) Expression patterns of a cinnamyl alcohol dehydrogenase gene involved in lignin biosynthesis and environmental stress in *Ginkgo biloba*. *Mol Biol Rep* **40:** 707-721

Churchill GA, Doerge RW. (1994) Empirical threshold values for quantitative trait mapping. *Genetics* **138:** 963-971

Clark RT, MacCurdy RB, Jung JK, Shaff JE, McCouch SR, Aneshansley DJ, Kochian LV. (2011) Three-Dimensional Root Phenotyping with a Novel Imaging and Software Platform. *Plant Physiol* **156:** 455-465

Corder EH, Saunders AM, Risch NJ, Strittmatter WJ, Schmechel DE, Gaskell PC, Jr., Rimmler JB, Locke PA, Conneally PM, Schmader KE, et al. (1994) Protective effect of apolipoprotein E type 2 allele for late onset Alzheimer disease. *Nat Genet* **7:** 180-184

De Deyn GB, Cornelissen JH, Bardgett RD (2008) Plant functional traits and soil carbon sequestration in contrasting biomes. *Ecol Lett* **11:** 516-531

de Dorlodot S, Forster B, Pages L, Price A, Tuberosa R, Draye X. (2007) Root system architecture: opportunities and constraints for genetic improvement of crops. *Trends Plant Sci* **12:** 474-481

Delourme R, Falentin C, Fomeju BF, Boillot M, Lassalle G, Andre I, Duarte J, Gauthier V, Lucante N, Marty A, Pauchon M, Pichon JP, Ribiere N, Trotoux G, Blanchard P, Riviere N, Martinant JP, Pauquet J. (2013) High-density SNP-based genetic map development and linkage disequilibrium assessment in *Brassica napus* L. *BMC Genomics* **14:** 120

Ding G, Zhao Z, Liao Y, Hu Y, Shi L, Long Y, Xu F. (2012) Quantitative trait loci for seed yield and yield-related traits, and their responses to reduced phosphorus supply in Brassica napus. *Ann Bot* **109:** 747-759

Dong J, Keller WA, Yan W, Georges F. (2004) Gene expression at early stages of *Brassica napus* seed development as revealed by transcript profiling of seed-abundant cDNAs. *Planta* **218:** 483-491

Downey RK. (1990) Brassica oilseed breeding: achievements and opportunities. *Plant Breed Abstr* **60:** 1165–1170

Downey RK, Röbbelen G. (1989) Brassica species. In: Röbbelen G, Downey R, Ashri A (eds) Oil Crops of the World. McGraw-Hill, New York, pp 339-382

Duran C, Eales D, Marshall D, Imelfort M, Stiller J, Berkman PJ, Clark T, McKenzie M, Appleby N, Batley J, Basford K, Edwards D. (2010) Future tools for association mapping in crop plants. *Genome* **53:** 1017-1023

Earl D, vonHoldt B. (2012) STRUCTURE HARVESTER: a website and program for visualizing STRUCTURE output and implementing the Evanno method. *Conserv Genet Resources* **4:** 359-361

Ecke W, Clemens R, Honsdorf N, Becker HC. (2010) Extent and structure of linkage disequilibrium in canola quality winter rapeseed (*Brassica napus* L.). *Theor Appl Genet* **120:** 921-931

Edwards D, Batley J, Cogan NOI, Forster JW, Chagné D. (2007) Single Nucleotide Polymorphism discovery, in: NC Oraguzie, et al. (Eds.), Association mapping in plants, Springer, New York. pp 53-76.

Edwards D, Batley J, Snowdon RJ. (2013) Accessing complex crop genomes with next-generation sequencing. *Theor Appl Genet* **126:** 1-11

Edwards D, Batley J. (2010) Plant genome sequencing: applications for crop improvement. *Plant Biotech J* **8:** 2-9

Ehrenreich IM, Hanzawa Y, Chou L, Roe JL, Kover PX, Purugganan MD. (2009) Candidate gene association mapping of Arabidopsis flowering time. *Genetics* **183:** 325-335

Emrani SN, Arzani A, Saeidi G. (2011) Seed viability, germination and seedling growth of canola (*Brassica napus* L.) as influenced by chemical mutagens. *Afr J Biotechnol* **10:** 12602-12613

Enami, H. R.; Safafar, H. (2010) Evaluation of Adding Canola Meal to Diet on Growth Performance of Male Wistar Rats. *J Animal Vet Advan.* **6**:1073-1076.

Ersoz E, Yu J, Buckler E. (2007) Applications of Linkage Disequilibrium and Association Mapping in Crop Plants. In *Genomics-Assisted Crop Improvement*, Varshney R, Tuberosa R (eds), 5, pp 97-119. Springer Netherlands

Evanno G, Regnaut S, Goudet J. (2005) Detecting the number of clusters of individuals using the software structure: a simulation study. *Mol Eco* **14:** 2611-2620

Eveland AL, McCarty DR, Koch KE. (2008) Transcript Profiling by 3'-Untranslated Region Sequencing Resolves Expression of Gene Families. *Plant Physiol* **146:** 32-44

Fiedler K, Bekele WA, Friedt W, Snowdon R, Stutzel H, Zacharias A, Uptmoor R. (2012) Genetic dissection of the temperature dependent emergence processes in sorghum using a cumulative emergence model and stability parameters. *Theor Appl Genet* **125:** 1647-1661

Fitz Gerald JN, Lehti-Shiu MD, Ingram PA, Deak KI, Biesiada T, Malamy JE. (2006) Identification of quantitative trait loci that regulate arabidopsis root system size and plasticity. *Genetics* **172:** 485-498

Flint-Garcia SA, Thornsberry JM, Buckler ES. (2003) Structure of linkage disequilibrium in plants. *Ann Rev Plant Biol* **54:** 357-374

Fourmann M, Barret P, Froger N, Baron C, Charlot F, Delourme R, Brunel D. (2002) From *Arabidopsis thaliana* to *Brassica napus*: development of amplified consensus genetic markers (ACGM) for construction of a gene map. *TAG Theor Appl Genet* **105:** 1196-1206

Franke R, McMichael CM, Meyer K, Shirley AM, Cusumano JC, Chapple C. (2000) Modified lignin in tobacco and poplar plants over-expressing the Arabidopsis gene encoding ferulate 5-hydroxylase. *Plant J* **22:** 223-234

Fraser. (2011) The Phenylpropanoid Pathway in Arabidopsis. *The Arabidopsis Book*

Frazer KA, Ballinger DG, Cox DR, Hinds DA, Stuve LL et al., (2007) A second generation human haplotype map of over 3.1 million SNPs. *Nature* **449:** 851-U853

Freeling M, Thomas BC. (2006) Gene-balanced duplications, like tetraploidy, provide predictable drive to increase morphological complexity. *Genome Res* **16:** 805-814

Friedman M. (1996) Nutritional Value of Proteins from Different Food Sources. A Review. *J Agricult Food Chem* **44:** 6-29

Friedt W, Snowdon R, Ordon F, Ahlemeyer J. (2007) Plant Breeding: Assessment of Genetic Diversity in Crop Plants and its Exploitation in Breeding. In *Progress in Botany*, Esser K, Löttge U, Beyschlag W, Murata J (eds), Vol. 68, 7, pp 151-178. Springer Berlin Heidelberg

Friedt W, Snowdon R. (2009) Oilseed Rape. In: *Handbook of Plant Breeding*, vol. 4. Oil Crops, Vollman, J. & Rajcan, J. (eds.), Springer-Verlag, Dordrecht, Heidelberg, London, New York, 91-126

Ghasemi-Golezani K, Sheikhzadeh-Mosaddegh P, Shakiba MR, Mohamadi A, Nasrollahzadeh S. (2011) Development of Seed Physiological Quality in Winter Oilseed Rape (*Brassica napus* L.) Cultivars. *Not Bot Horti Agrobo* **39:** 208-212

Gigolashvili T, Yatusevich R, Berger B, Müller C, Flügge U-I. (2007) The R2R3-MYB transcription factor HAG1/MYB28 is a regulator of methionine-derived glucosinolate biosynthesis in *Arabidopsis thaliana*. *The Plant Journal* **51:** 247-261

Grubb CD, Abel S. (2006) Glucosinolate metabolism and its control. *Trends Plant Sci* **11:** 89-100

Hajduch M, Casteel JE, Hurrelmeyer KE, Song Z, Agrawal GK, Thelen JJ. (2006) Proteomic analysis of seed filling in *Brassica napus*. developmental characterization of metabolic isozymes using high-resolution two-dimensional gel electrophoresis. *Plant Physiol* **141:** 32-46

Hajduch M, Hearne LB, Miernyk JA, Casteel JE, Joshi T, Agrawal GK, Song Z, Zhou M, Xu D, Thelen JJ. (2010) Systems analysis of seed filling in arabidopsis: using general linear modeling to assess concordance of transcript and protein expression. *Plant Physiol* **152:** 2078-2087

Hajduch M, Matusova R, Houston NL, Thelen JJ. (2011) Comparative proteomics of seed maturation in oilseeds reveals differences in intermediary metabolism. *Proteomics* **11:** 1619-1629

Harper AL, Trick M, Higgins J, Fraser F, Clissold L, Wells R, Hattori C, Werner P, Bancroft I. (2012) Associative transcriptomics of traits in the polyploid crop species *Brassica napus*. *Nat Biotechnol* **30:** 798-802

Hasan M, Friedt W, Pons-Kuehnemann J, Freitag NM, Link K, Snowdon RJ. (2008) Association of gene-linked SSR markers to seed glucosinolate content in oilseed rape (*Brassica napus* ssp. napus). *Theor Appl Genet* **116:** 1035-1049

Hasan M, Seyis F, Badani AG, Pons-Kuhnemann J, Friedt W, Luhs W, Snowdon RJ. (2006) Analysis of genetic diversity in the *Brassica napus* L. gene pool using SSR markers. *Genet Resources Crop Evol* **53:** 793-802

Hawthorne F, Feng S, Metlapally R, Li YJ, Tran-Viet KN, Guggenheim JA, Malecaze F, Calvas P, Rosenberg T, Mackey DA, Venturini C, Hysi PG, Hammond CJ, Young TL. (2013) Association Mapping of the High-Grade Myopia MYP3 Locus Reveals Novel Candidates UHRF1BP1L, PTPRR, and PPFIA2. *Invest Ophthalmol Vis Sci* **54:** 2076-2086

Hirai MY. (2009) A robust omics-based approach for the identification of glucosinolate biosynthetic genes. *Phytochem Rev* **8:** 15-23

Hochholdinger F, Tuberosa R. (2009) Genetic and genomic dissection of maize root development and architecture. *Curr Opin Plant Biol* **12:** 172-177

Hong CP, Kwon S-J, Kim JS, Yang T-J, Park B-S, Lim YP. (2008) Progress in understanding and sequencing the genome of *Brassica rapa*. *Int J Plant genomics* **2008:** 582837

Honsdorf N, Becker HC, Ecke W. (2010) Association mapping for phenological, morphological, and quality traits in canola quality winter rapeseed (*Brassica napus* L.). *Genome* **53:** 899-907

Hu Y, Wu G, Cao Y, Wu Y, Xiao L, Li X, Lu C. (2009) Breeding response of transcript profiling in developing seeds of *Brassica napus*. *BMC Mol Biol* **10:** 49

Hua W, Li RJ, Zhan GM, Liu J, Li J, Wang XF, Liu GH, Wang HZ. (2012) Maternal control of seed oil content in *Brassica napus*: the role of silique wall photosynthesis. *The Plant J* **69:** 432-444

Huang X, Wei X, Sang T, Zhao Q, Feng Q, Zhao Y, Li C, Zhu C, Lu T, Zhang Z, Li M, Fan D, Guo Y, Wang A, Wang L, Deng L, Li W, Lu Y, Weng Q, Liu K, Huang T, Zhou T, Jing Y, Lin Z, Buckler ES, Qian Q, Zhang QF, Li J, Han B. (2010) Genome-wide association studies of 14 agronomic traits in rice landraces. *Nat Genet* **42:** 961-967

Hund A, Trachsel S, Stamp P (2009) Growth of axile and lateral roots of maize: I development of a phenotying platform. *Plant Soil* **325:** 335-349

Hyten DL, Cannon SB, Song QJ, Weeks N, Fickus EW, Shoemaker RC, Specht JE, Farmer AD, May GD, Cregan PB. (2010) High-throughput SNP discovery through deep resequencing of a reduced representation library to anchor and orient scaffolds in the soybean whole genome sequence. *BMC Genomics* **11**

Jain M. (2012) Next-generation sequencing technologies for gene expression profiling in plants. *Brief Func Genomics* **11:** 63-70

Jin H, Cominelli E, Bailey P, Parr A, Mehrtens F, Jones J, Tonelli C, Weisshaar B, Martin C. (2000) Transcriptional repression by AtMYB4 controls production of UV-protecting sunscreens in Arabidopsis. *Embo J* **19:** 6150-6161

Jung JK, McCouch S. (2013) Getting to the roots of it: Genetic and hormonal control of root architecture. *Front Plant Sci* **4:** 186

Kamoshita A, Wade J, Ali L, Pathan S, Zhang J, Sarkarung S, Nguyen T. (2002) Mapping QTLs for root morphology of a rice population adapted to rainfed lowland conditions. *Theor Appl Genet* **104:** 880-893

Kaul S, Koo HL, Jenkins J, Rizzo M, Rooney T, Tallon LJ, Feldblyum T et al., (2000) Analysis of the genome sequence of the flowering plant Arabidopsis thaliana. *Nature* **408:** 796-815

Kim YB, Li X, Kim SJ, Kim HH, Lee J, Kim H, Park SU. (2013) MYB transcription factors regulate glucosinolate biosynthesis in different organs of Chinese cabbage (*Brassica rapa* ssp. pekinensis). *Molecules* **18:** 8682-8695

Kliebenstein DJ, Kroymann J, Brown P, Figuth A, Pedersen D, Gershenzon J, Mitchell-Olds T. (2001a) Genetic control of natural variation in Arabidopsis glucosinolate accumulation. *Plant Physiol* **126:** 811-825

Kliebenstein DJ, Lambrix VM, Reichelt M, Gershenzon J, Mitchell-Olds T. (2001b) Gene duplication in the diversification of secondary metabolism: tandem 2-oxoglutarate-dependent dioxygenases control glucosinolate biosynthesis in Arabidopsis. *Plant Cell* **13:** 681-693

Knill T, Reichelt M, Paetz C, Gershenzon J, Binder S. (2009) Arabidopsis thaliana encodes a bacterial-type heterodimeric isopropylmalate isomerase involved in both Leu biosynthesis and the Met chain elongation pathway of glucosinolate formation. *Plant Mol Biology* **71:** 227-239

Koch MA, Kiefer C. (2006) Molecules and migration: biogeographical studies in cruciferous plants. *Plant Systematics Evol* **259:** 121-142

Koscielny CB, Gulden RH. (2012) Seedling root length in *Brassica napus* L. is indicative of seed yield. *Can J Plant Sci* **92:** 1229-1237

Kraakman AT, Niks RE, Van den Berg PM, Stam P, Van Eeuwijk FA. (2004) Linkage disequilibrium mapping of yield and yield stability in modern spring barley cultivars. *Genetics* **168:** 435-446

Kumar S, You FM, Cloutier S. (2012) Genome wide SNP discovery in flax through next generation sequencing of reduced representation libraries. *BMC Genomics* **13**

Lagercrantz U, Lydiate DJ. (1996) Comparative Genome Mapping in Brassica. *Genetics* **144:** 1903-1910

Lauvergeat V, Lacomme C, Lacombe E, Lasserre E, Roby D, Grima-Pettenati J. (2001) Two cinnamoyl-CoA reductase (CCR) genes from *Arabidopsis thaliana* are differentially expressed during development and in response to infection with pathogenic bacteria. *Phytochemistry* **57:** 1187-1195

Li F, Chen B, Xu K, Wu J, Song W, Bancroft I, Harper AL, Trick M, Liu S, Gao G, Wang N, Yan G, Qiao J, Li J, Li H, Xiao X, Zhang T, Wu X. (2014) Genome-Wide Association Study Dissects the Genetic Architecture of Seed Weight and Seed Quality in Rapeseed (*Brassica napus* L.). *DNA Res*

Li J, Hansen BG, Ober JA, Kliebenstein DJ, Halkier BA. (2008) Subclade of flavin-monooxygenases involved in aliphatic glucosinolate biosynthesis. *Plant Physiol* **148:** 1721-1733

Liang YK, Dubos C, Dodd IC, Holroyd GH, Hetherington AM, Campbell MM. (2005) AtMYB61, an R2R3-MYB transcription factor controlling stomatal aperture in Arabidopsis thaliana. *Curr Biol* **15:** 1201-1206

Lim GAC, Jewell EG, Li X, Erwin TA, Love C, Batley J, Spangenberg G, Edwards D. (2007) A comparative map viewer integrating genetic maps for Brassica and Arabidopsis. *BMC Plant Biol* **7**

Lisson, S.N., J.A. Kirkegaard, M.J. Robertson, and A. Zwart. 2007: What is limiting canola yield in southern New South wales; A diagnosis of casual factors. *Aust. J. Expl. Agric*. **47:** 1435-1445

Liu L, Li YH, Li SL, Hu N, He YM, Pong R, Lin DN, Lu LH, Law M. (2012a) Comparison of Next-Generation Sequencing Systems. *J Biomed Biotechnol*

Liu LZ, Stein A, Wittkop B, Sarvari P, Li JN, Yan XY, Dreyer F, Frauen M, Friedt W, Snowdon RJ. (2012c) A knockout mutation in the lignin biosynthesis gene CCR1 explains a major QTL for acid detergent lignin content in *Brassica napus* seeds. *Theor Appl Genet* **124:** 1573-1586

Loudet O, Gaudon V, Trubuil A, Daniel-Vedele Fo. (2005) Quantitative trait loci controlling root growth and architecture in *Arabidopsis thaliana* confirmed by heterogeneous inbred family. *Theor Appl Genet* **110:** 742-753

Lu F, Marita JM, Lapierre C, Jouanin L, Morreel K, Boerjan W, Ralph J. (2010) Sequencing around 5-hydroxyconiferyl alcohol-derived units in caffeic acid O-methyltransferase-deficient poplar lignins. *Plant Physiol***153:** 569-579

Lu G, Cao J, Yu X, Xiang X, Chen H. (2008) Mapping QTLs for root morphological traits in *Brassica rapa* L. based on AFLP and RAPD markers. *J Appl Genet* **49:** 23-31

Lu G, Harper AL, Trick M, Morgan C, Fraser F, O'Neill C, Bancroft I. (2014) Associative transcriptomics study dissects the genetic architecture of seed glucosinolate content in *Brassica napus*. *DNA Res*1-13

Lynch JP. (1995) Root Architecture and Plant Productivity. *Plant Physiol***109:** 7-13

Lynch JP. (2007) Roots of the second green revolution. *Aust J Bot* **55:** 493-512

Mackay TFC, Stone EA, Ayroles JF. (2009) The genetics of quantitative traits: challenges and prospects. *Nat Rev Genet* **10:**565–577

Malamy JE. (2005) Intrinsic and environmental response pathways that regulate root system architecture. *Plant, Cell Env* **28:** 67-77

Malitsky S, Blum E, Less H, Venger I, Elbaz M, Morin S, Eshed Y, Aharoni A. (2008) The transcript and metabolite networks affected by the two clades of Arabidopsis glucosinolate biosynthesis regulators. *Plant Physiol* **148:** 2021-2049

Manschadi AM, Hammer GL, Christopher JT, deVoil P. (2008) Genotypic variation in seedling root architectural traits and implications for drought adaptation in wheat (*Triticum aestivum* L.). *Plant Soil* **303:** 115-129

Marioni JC, Mason CE, Mane SM, Stephens M, Gilad Y. (2008) RNA-seq: An assessment of technical reproducibility and comparison with gene expression arrays. *Genome Res* **18:** 1509-1517

Martinez-Alberola F, Del Campo EM, Lazaro-Gimeno D, Mezquita-Claramonte S, Molins A, Mateu-Andres I, Pedrola-Monfort J, Casano LM, Barreno E. (2013) Balanced gene losses, duplications and intensive rearrangements led to an unusual regularly sized genome in Arbutus unedo chloroplasts. *PLoS ONE* **8:** 679-685

Mitchell-Olds T. (2010) Complex-trait analysis in plants. *Genome Biol*. **11:**113.

Mikkelsen MD, Petersen BL, Glawischnig E, Jensen AB, Andreasson E, Halkier BA. (2003) Modulation of CYP79 genes and glucosinolate profiles in Arabidopsis by defense signaling pathways. *Plant Physiol* **131:** 298-308

Mithen RF, Dekker M, Verkerk R, Rabot S, Johnson IT. (2000) The nutritional significance, biosynthesis and bioavailability of glucosinolates in human foods. *J Sci Food Agri* **80:** 967-984

Morris GP, Ramu P, Deshpande SP, Hash CT, Shah T, Upadhyaya HD, Riera-Lizarazu O, Brown PJ, Acharya CB, Mitchell SE, Harriman J, Glaubitz JC, Buckler ES, Kresovich S. (2013) Population genomic and genome-wide association studies of agroclimatic traits in sorghum. *Proc Natl Acad Sci U S A* **110:** 453-458

Morrissy S, Zhao Y, Delaney A, Asano J, Dhalla N, Li I, McDonald H, Pandoh P, Prabhu A-L, Tam A, Hirst M, Marra M. (2001) Digital Gene Expression by Tag Sequencing on the Illumina Genome Analyzer. In *Curr Protocols Human Genetics*. John Wiley & Sons, Inc.

Morrissy S, Zhao Y, Delaney A, Asano J, Dhalla N, Li I, McDonald H, Pandoh P, Prabhu A-L, Tam A, Hirst M, Marra M (2010) Digital Gene Expression by Tag Sequencing on the Illumina Genome Analyzer. In *Curr Protocols Human Genetics* 11.11.1-11.11.36,

Mouchel CF, Briggs GC, Hardtke CS. (2004) Natural genetic variation in Arabidopsis identifies BREVIS RADIX, a novel regulator of cell proliferation and elongation in the root. *Genes Dev* **18:** 700-714

Murashige T, Skoog F. (1962) A Revised Medium for Rapid Growth and Bio Assays with Tobacco Tissue Cultures. *Physiologia Plantarum* **15:** 473-497

Mwachireya, Beames, Higgs, Dosanjh. (1999) Digestibility of canola protein products derived from the physical, enzymatic and chemical processing of commercial canola meal in rainbow trout *Oncorhynchus mykiss* (Walbaum) held in fresh water. *Aquaculture Nutri* **5:** 73-82

Neal C, Fredericks D, Griffiths C, Neale A. (2010) The characterisation of AOP2: a gene associated with the biosynthesis of aliphatic alkenyl glucosinolates in *Arabidopsis thaliana*. *BMC Plant Biol* **10:** 170

Niu Y, Wu G-Z, Ye R, Lin WH, Shi QM, Xue LJ, Xu XD, Li Y, Du YG, Xue HW. (2009a) Global Analysis of Gene Expression Profiles in *Brassica napus* Developing Seeds Reveals a Conserved Lipid Metabolism Regulation with *Arabidopsis thaliana*. *Mol Plant* **2:** 1107-1122

Nobuta K, Venu RC, Lu C, Belo A, Vemaraju K, Kulkarni K, Wang W, Pillay M, Green PJ, Wang G-l, Meyers BC. (2007) An expression atlas of rice mRNAs and small RNAs. *Nat Biotech* **25:** 473-477

Obermeier C, Hossain M, Snowdon R, Knüfer J, Tiedemann A, Friedt W. (2013) Genetic analysis of phenylpropanoid metabolites associated with resistance against *Verticillium longisporum* in *Brassica napus*. *Mol Breed* **31:** 347-361

Obermeier C, Hosseini B, Friedt W, Snowdon R. (2009) Gene expression profiling via LongSAGE in a non-model plant species: a case study in seeds of *Brassica napus*. *BMC Genomics* **10**

Ochoa IE, Blair MW, Lynch JP. (2006) QTL analysis of adventitious root formation in common bean under contrasting phosphorus availability. *Crop Sci* **46:** 1609-1621

Ozsolak F, Milos PM. (2011) RNA sequencing: advances, challenges and opportunities. *Nat Rev Genet* **12:** 87-98

Palaisa KA, Morgante M, Williams M, Rafalski A. (2003) Contrasting effects of selection on sequence diversity and linkage disequilibrium at two phytoene synthase loci. *The Plant Cell* **15:** 1795-1806

Panjabi P, Jagannath A, Bisht NC, Padmaja KL, Sharma S, Gupta V, Pradhan AK, Pental D. (2008) Comparative mapping of *Brassica juncea* and *Arabidopsis* thailiana using Intron Polymorphism (IP) markers: homoeologous relationships, diversification and evolution of the A, B and C Brassica genomes. *BMC Genomics* **9**

Parkin IAP, Gulden SM, Sharpe AG, Lukens L, Trick M, Osborn TC, Lydiate DJ. (2005) Segmental structure of the *Brassica napus* genome based on comparative analysis with *Arabidopsis thaliana*. *Genetics* **171:** 765-781

Parkin IAP, Sharpe AG, Lydiate DJ. (2003) Patterns of genome duplication within the *Brassica napus* genome. *Genome* **46:** 291-303

Parkin IAP. (2005) Segmental Structure of the *Brassica napus* Genome Based on Comparative Analysis With *Arabidopsis thaliana*. *Genetics* **171:** 765-781

Patzlaff A, Newman LJ, Dubos C, Whetten RW, Smith C, McInnis S, Bevan MW, Sederoff RR, Campbell MM. (2003) Characterisation of Pt MYB1, an R2R3-MYB from pine xylem. *Plant Mol Biol* **53:** 597-608

Peltonen-Sainio P, Jauhiainen L, Laitinen P, Salopelto J, Saastamoinen M, Hannukkala A. (2011) Identifying difficulties in rapeseed root penetration in farmers' fields in northern European conditions. *Soil Use Manage* **27:** 229-237

Penfield S, Meissner RC, Shoue DA, Carpita NC, Bevan MW. (2001) MYB61 is required for mucilage deposition and extrusion in the Arabidopsis seed coat. *Plant Cell* **13:** 2777-2791

Preston J, Wheeler J, Heazlewood J, Li SF, Parish RW (2004) AtMYB32 is required for normal pollen development in *Arabidopsis thaliana*. *Plant J* **40:** 979-995

Pritchard J, Stephens M, Rosenberg N, Donnelly P. (2000) Association Mapping in Structured Populations. *The American J Human Genet* **67:** 170-181

Qu C, Fu F, Lu K, Zhang K, Wang R, Xu X, Wang M, Lu J, Wan H, Zhanglin T, Li J .(2013) Differential accumulation of phenolic compounds and expression of related genes in black- and yellow-seeded Brassica napus. *J Exp Bot* **64:** 2885-2898

Raes J, Rohde A, Christensen JH, Van de Peer Y, Boerjan W. (2003) Genome-wide characterization of the lignification toolbox in Arabidopsis. *Plant Physiol***133:** 1051-1071

Rahantamalala A, Rech P, Martinez Y, Chaubet-Gigot N, Grima-Pettenati J, Pacquit V. (2010) Coordinated transcriptional regulation of two key genes in the lignin branch pathway CAD and CCR is mediated through MYB- binding sites. *BMC Plant Biology* **10:** 130

Redovnikovic IR, Textor S, Lisnic B, Gershenzon J. (2012) Expression pattern of the glucosinolate side chain biosynthetic genes MAM1 and MAM3 of *Arabidopsis thaliana* in different organs and developmental stages. *Plant Physiol Biochem* **53:** 77-83

Reymond M, Svistoonoff S, Loudet O, Nussaume L, Desnos T. (2006) Identification of QTL controlling root growth response to phosphate starvation in *Arabidopsis thaliana*. *Plant Cell Environ* **29:** 115-125

Rezaeizad A, Wittkop B, Snowdon R, Hasan M, Mohammadi V, Zali A, Friedt W. (2010) Identification of QTLs for phenolic compounds in oilseed rape (*Brassica napus* L.) by association mapping using SSR markers. *Euphytica* **177:** 335-342

Riboulet C, Fabre F, Denoue D, Martinant JP, Lefevre B, Barriere Y (2008) QTL mapping and candidate gene research from lignin content and cell wall digestibility in a top-cross of a flint maize recombinant inbred line progeny harvested at silage stage. *Maydica* **53:** 1-9

Rohde A. (2004) Molecular Phenotyping of the pal1 and pal2 Mutants of *Arabidopsis thaliana* Reveals Far-Reaching Consequences on Phenylpropanoid, Amino Acid, and Carbohydrate Metabolism. *The Plant Cell Online* **16:** 2749-2771

Romano JM, Dubos C, Prouse MB, Wilkins O, Hong H, Poole M, Kang K-Y, Li E, Douglas CJ, Western TL, Mansfield SD, Campbell MM. (2012) AtMYB61, an R2R3-MYB transcription factor, functions as a pleiotropic regulator via a small gene network. *New Phytologist* **195:** 774-786

Ruprecht C, Persson S. (2012) Co-expression of cell-wall related genes: new tools and insights. *Front Plant Sci* **3:** 83

Schmidt R, Acarkan A, Boivin K. (2001) Comparative structural genomics in the Brassicaceae family. *Plant Physiol Biochem* **39:** 253-262

Schwender J, Goffman F, Ohlrogge JB, Shachar-Hill Y. (2004) Rubisco without the Calvin cycle improves the carbon efficiency of developing green seeds. *Nature* **432:** 779-782

Schwender J, Ohlrogge J, Shachar-Hill Y. (2004) Understanding flux in plant metabolic networks. *Curr Opin Plant Biol* **7:** 309-317

Sharpe AG, Lydiate DJ. (2003) Mapping the mosaic of ancestral genotypes in a cultivar of oilseed rape (*Brassica napus*) selected via pedigree breeding. *Genome* **46:** 461-468

Shi L, Shi T, Broadley MR, White PJ, Long Y, Meng J, Xu F, Hammond JP. (2013) High-throughput root phenotyping screens identify genetic loci associated with root architectural traits in *Brassica napus* under contrasting phosphate availabilities. *Ann Bot* **112:** 381-389

Sim SC, Durstewitz G, Plieske J, Wieseke R, Ganal MW, Van Deynze A, Hamilton JP, Buell CR, Causse M, Wijeratne S, Francis DM. (2012) Development of a Large SNP Genotyping Array and Generation of High-Density Genetic Maps in Tomato. *PLoS One* **7**

Skirycz A, Reichelt M, Burow M, Birkemeyer C, Rolcik J, Kopka J, Zanor MI, Gershenzon J, Strnad M, Szopa J, Mueller-Roeber B, Witt I. (2006) DOF transcription factor AtDof1.1 (OBP2) is part of a regulatory network controlling glucosinolate biosynthesis in Arabidopsis. *The Plant J* **47:** 10-24

Snowdon RJ, Friedrich T, Friedt W, Köhler W. (2002) Identifying the chromosomes of the A- and C-genome diploid Brassica species *B. rapa* (syn. campestris) and *B. oleracea* in their amphidiploid *B. napus*. *Theor Appl Genet* **104:** 533-538

Snowdon RJ. (2007) Cytogenetics and genome analysis in Brassica crops. *Chromosome Res* **15:** 85-95

Sønderby IE, Geu-Flores F, Halkier BA. (2010) Biosynthesis of glucosinolates – gene discovery and beyond. *Trends Plant Scie* **15:** 283-290

Stefansson BR Hougen FW. (1964) Selection of rape plants (*Brassica napus*) with seed oil practically free of erucic acid. *Can J Plant Sci* **44:** 359–364

Stefansson BR. (1983) In: Kramer JKG, Sauer FD, Pigden WJ (eds) High and low erucic acid rapeseed oils. Academic, New York, pp 143-160

Stein A, Wittkop B, Liu L, Obermeier C, Friedt W, Snowdon RJ. (2013) Dissection of a major QTL for seed colour and fibre content in *Brassica napus* reveals colocalization with candidate genes for phenylpropanoid biosynthesis and flavonoid deposition. *Plant Breed* **132:** 382-389

Stich B, Mohring J, Piepho HP, Heckenberger M, Buckler ES, Melchinger AE. (2008) Comparison of mixed-model approaches for association mapping. *Genetics* **178:** 1745-1754

Stracke S, Haseneyer G, Veyrieras JB, Geiger HH, Sauer S, Graner A, Piepho HP. (2009) Association mapping reveals gene action and interactions in the determination of flowering time in barley. *Theor Appl Genet* **118:** 259-273

t Hoen PAC, Ariyurek Y, Thygesen HH, Vreugdenhil E, Vossen RHAM, de Menezes RX, Boer JM, van Ommen GJB, den Dunnen JT. (2008) Deep sequencing-based expression analysis shows major advances in robustness, resolution and inter-lab portability over five microarray platforms. *Nucl Acids Res* **36:** 6934-43

Tan H, Yang X, Zhang F, Zheng X, Qu C, Mu J, Fu F, Li J, Guan R, Zhang H, Wang G, Zuo J. (2011) Enhanced seed oil production in canola by conditional expression of *Brassica napus* LEAFY COTYLEDON1 and LEC1-LIKE in Developing Seeds. *Pl Physiol***156:** 1577-1588

Thimm O, Blasing O, Gibon Y, Nagel A, Meyer S, Kruger P, Selbig J, Muller LA, Rhee SY, Stitt M. (2004) MAPMAN: a user-driven tool to display genomics data sets onto diagrams of metabolic pathways and other biological processes. *Plant J* **37:** 914-939

Thorup-Kristensen, K. 2006. Root growth and nitrogen uptake of carrot, early cabbage, onion and lettuce following a range of green manures. *Soil Use Manag*, **22:** 29–38.

Topp CN, Iyer-Pascuzzi AS, Anderson JT, Lee CR, Zurek PR, Symonova O, Zheng Y, Bucksch A, Mileyko Y, Galkovskyi T, Moore BT, Harer J, Edelsbrunner H, Mitchell-Olds T, Weitz JS, Benfey PN. (2013) 3D phenotyping and quantitative trait locus mapping identify core regions of the rice genome controlling root architecture. *Proc Natl Acad Sci U S A* **110:** 1695-1704

Trebbi D, Maccaferri M, de Heer P, Sorensen A, Giuliani S, Salvi S, Sanguineti MC, Massi A, van der Vossen EAG, Tuberosa R. (2011) High-throughput SNP discovery and genotyping in durum wheat (*Triticum durum* Desf.). *Theor Appl Genet* **123:** 555-569

Trick M, Long Y, Meng J, Bancroft I. (2009) Single nucleotide polymorphism (SNP) discovery in the polyploid *Brassica napus* using Solexa transcriptome sequencing. *Plant Biotech J* **7:** 334-346

Usadel B, Poree F, Nagel A, Lohse M, Czedik-Eysenberg A, Stitt M. (2009) A guide to using MapMan to visualize and compare Omics data in plants: a case study in the crop species, Maize. *Plant, Cell & Environment* **32:** 1211-1229

Vanholme R, Storme V, Vanholme B, Sundin L, Christensen JH, Goeminne G, Halpin C, Rohde A, Morreel K, Boerjan W. (2012) A systems biology view of responses to lignin biosynthesis perturbations in Arabidopsis. *The Plant Cell* **24:** 3506-3529

Velculescu VE, Zhang L, Vogelstein B, Kinzler KW. (1995) Serial Analysis of Gene Expression. *Science* **270:** 484-487

Venglat P, Xiang D, Yang H, Wan L, Tibiche C, Ross A, Wang E, Selvaraj G, Datla R. (2013) Gene expression profiles during embryo development in *Brassica napus*. *Plant Breeding***: 5:** 514-522

Vicente-Carbajosa J, Carbonero P. (2005) Seed maturation: developing an intrusive phase to accomplish a quiescent state. *Int J Dev Biol* **49:** 645-651

Vogt T. (2010) Phenylpropanoid Biosynthesis. *Mol Plant* **3:** 2-20

Wang H, Wu J, Sun SL, Liu B, Cheng F, Sun RF, Wang XW. (2011a) Glucosinolate biosynthetic genes in *Brassica rapa*. *Gene* **487:** 135-142

Wang J, Kroon H, Wang L, Caluwe H, Bögemann G, Weerden G, Kang S, Smits AM. (2009) Root foraging and yield components underlying limited effects of partial root-zone drying on oilseed rape, a crop with an indeterminate growth habit. *Plant Soil* **323:** 163-176

Wang S, Peatman E, Abernathy J, Waldbieser G, Lindquist E, Richardson P, Lucas S, Wang M, Li P, Thimmapuram J. (2010) Assembly of 500,000 inter-specific catfish expressed sequence tags and large scale gene-associated marker development for whole genome association studies. *Genome Biol* **11:** R8

Wang S., Basten C.J, and Zeng ZB. (2012) Windows QTL Cartographer 2.5. Department of Statistics,NorthCarolinaState University, Raleigh, NC. (http://statgen.ncsu.edu/qtlcart/WQTLCart.htm)

Wang X, Wang H, Wang J, Sun R, Wu J, Liu S, Bai Y, Mun J-H, Bancroft I, et al., (2011) The genome of the mesopolyploid crop species *Brassica rapa*. *Nat Genetics* **43:** 1035-1039

White JA, Todd J, Newman T, Focks N, Girke T, de Ilarduya OM, Jaworski JG, Ohlrogge JB, Benning C. (2000a) A new set of Arabidopsis expressed sequence tags from developing seeds. The metabolic pathway from carbohydrates to seed oil. *Plant Physiol* **124:** 1582-1594

White JA, Todd J, Newman T, Focks N, Girke T, de Ilárduya OMn, Jaworski JG, Ohlrogge JB, Benning C. (2000b) A new set of arabidopsis expressed sequence tags from developing seeds. the metabolic pathway from carbohydrates to seed oil. *Plant Physiol***124:** 1582-1594

Williams D. (2010) The role of epithiospecifier protein (ESP) in plant metabolism and its impact on the regulation of anti-cancer isothiocyanates in Brassica crops. *PhD Thesis*, School of Biological Sciences, The University of Queensland.

Wittkop B, Snowdon RJ, Friedt W. (2009) Status and perspectives of breeding for enhanced yield and quality of oilseed crops for Europe. *Euphytica* **170:** 131-140

Wittkop B, Snowdon RJ, Friedt W. (2012) New NIRS calibrations for fiber fractions reveal broad genetic variation in *Brassica napus* seed quality. *J Agricul Food Chem* **60:** 2248-2256

Würschum T. (2012) Mapping QTL for agronomic traits in breeding populations. *Theor Appl Genet* **125:** 201-210

Yang M, Ding G, Shi L, Feng J, Xu F, Meng J. (2010) Quantitative trait loci for root morphology in response to low phosphorus stress in *Brassica napus*. *Theor Appl Genet* **121:** 181-193

Yang M, Ding G, Shi L, Xu F, Meng J. (2011) Detection of QTL for phosphorus efficiency at vegetative stage in *Brassica napus*. *Plant Soil* **339:** 97-111

Zhang WP, Shen XY, Wu P, Hu B, Liao CY. (2001) QTLs and epistasis for seminal root length under a different water supply in rice (*Oryza sativa* L.). *Theor Appl Genet* **103:** 118-123

Zhang Z, Ober JA, Kliebenstein DJ. (2006) The gene controlling the quantitative trait locus EPITHIOSPECIFIER MODIFIER1 ALTERS GLUCOSINOLATE HYDROLYSIS AND INSECT RESISTANCE in Arabidopsis. *The Plant Cell Online* **18:** 1524-1536

Zhang ZW, Ersoz E, Lai CQ, Todhunter RJ, Tiwari HK, Gore MA, Bradbury PJ, Yu JM, Arnett DK, Ordovas JM, Buckler ES. (2010) Mixed linear model approach adapted for genome-wide association studies. *Nat Genetics* **42:** 355-U118

Zhao K, Aranzana MJ, Kim S, Lister C, Shindo C, Tang C, Toomajian C, Zheng H, Dean C, Marjoram P, Nordborg M. (2007) An Arabidopsis example of association mapping in structured samples. *PLoS Genet* **3:** e4

Zhao Q, Dixon RA. (2011) Transcriptional networks for lignin biosynthesis: more complex than we thought? *Trends Plant Sci* **16:** 227-233

Zheng BS, Yang L, Zhang WP, Mao CZ, Wu YR, Yi KK, Liu FY, Wu P. (2003) Mapping QTLs and candidate genes for rice root traits under different water-supply conditions and comparative analysis across three populations. *Theor Appl Genet* **107:** 1505-1515

Zhong R, Ye ZH. (2009) Transcriptional regulation of lignin biosynthesis. *Plant Signaling Behavior* **4:** 1028-1034

Zhong RQ, Lee CH, Zhou JL, McCarthy RL, Ye ZH. (2008) A battery of transcription factors involved in the regulation of secondary cell wall biosynthesis in Arabidopsis. *Plant Cell* **20:** 2763-2782

Zhou J, Lee C, Zhong R, Ye ZH. (2009) MYB58 and MYB63 are transcriptional activators of the lignin biosynthetic pathway during secondary cell wall formation in arabidopsis. *The Plant Cell Online* **21:** 248-266

Zhu B, Wang Z, Yang J, Zhu Z, Wang H. (2012) Isolation and expression of glucosinolate synthesis genes cyp83a1 and cyp83b1 in pak choi (*Brassica rapa* L. ssp. chinensis var. communis (N. Tsen & S.H. Lee) Hanelt. *Int J Mol Sci* **13:** 5832-5843

Zhu J, Ingram PA, Benfey PN, Elich T. (2011) From lab to field, new approaches to phenotyping root system architecture. *Curr Opin Plant Biol.* **14:** 310-177.

APPENDIX

Appendix A. Genetic map. Genetic map of the *B. napus* doubled haploid (DH) population "Express 617"× "V8" showed distribution of containing 1199 markers along 19 chromosomes which includes SSR, RAD and SNPs based markers

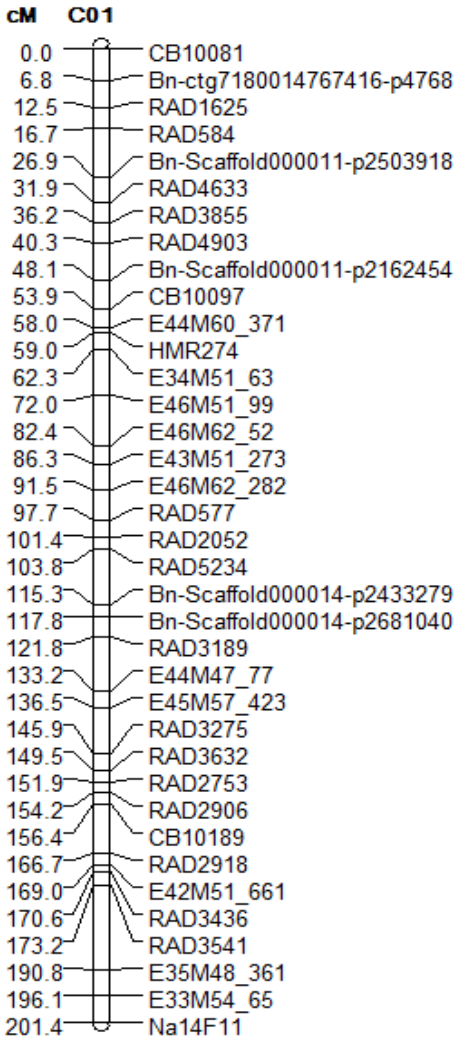

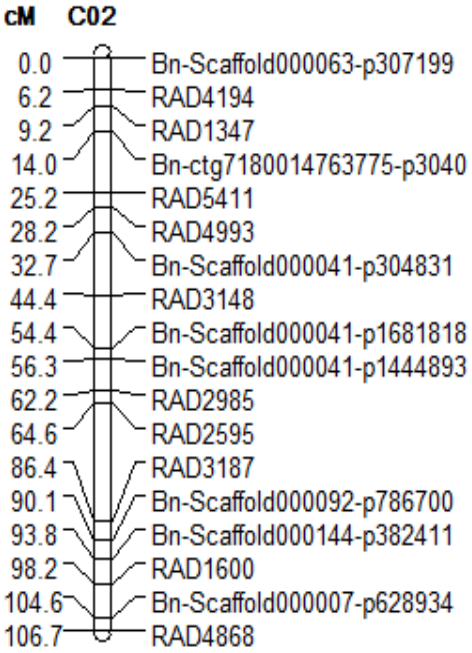

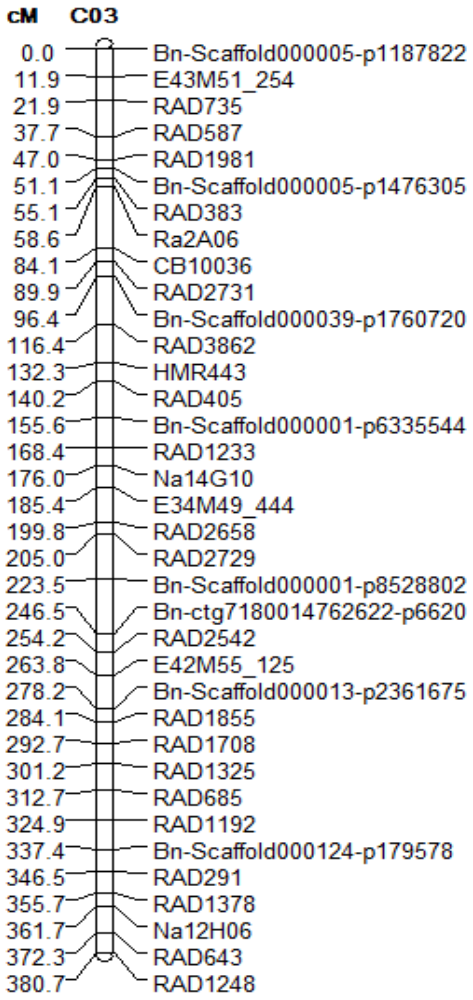

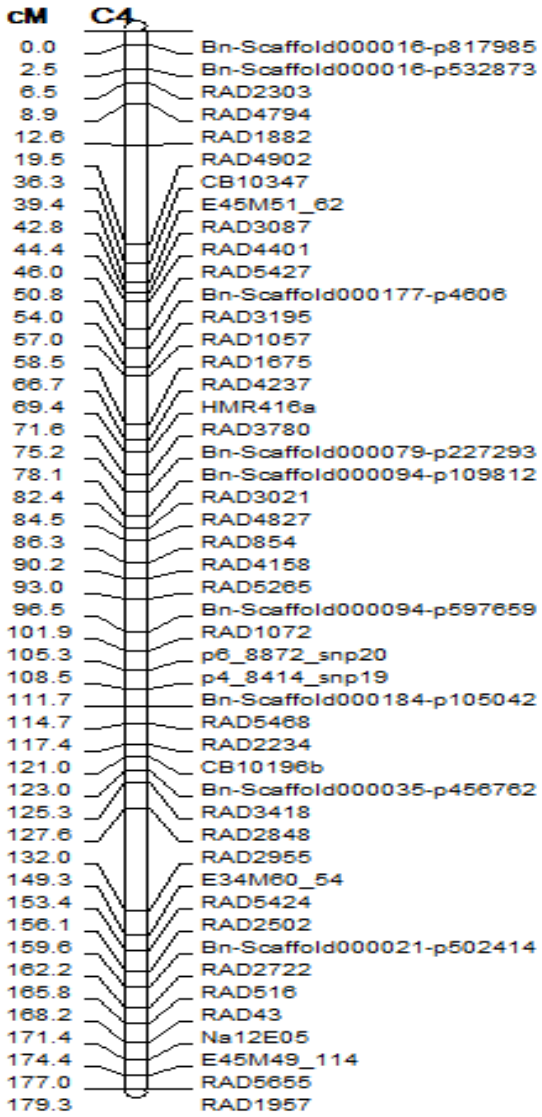
cM
C4
0.0 Bn-Scaffold000016-p817985
2.5 Bn-Scaffold000016-p532873
6.5 RAD2303
8.9 RAD4794
12.6 RAD1882
19.5 RAD4902
36.3 CB10347
39.4 E45M51_62
42.8 RAD3087
44.4 RAD4401
46.0 RAD5427
50.8 Bn-Scaffold000177-p4606
54.0 RAD3195
57.0 RAD1057
58.5 RAD1675
66.7 RAD4237
69.4 HMR416a
71.6 RAD3780
75.2 Bn-Scaffold000079-p227293
78.1 Bn-Scaffold000094-p109812
82.4 RAD3021
84.5 RAD4827
86.3 RAD854
90.2 RAD4158
93.0 RAD5265
96.5 Bn-Scaffold000094-p597659
101.9 RAD1072
105.3 p6_8872_snp20
108.5 p4_8414_snp19
111.7 Bn-Scaffold000184-p105042
114.7 RAD5468
117.4 RAD2234
121.0 CB10196b
123.0 Bn-Scaffold000035-p456762
125.3 RAD3418
127.6 RAD2848
132.0 RAD2955
149.3 E34M60_54
153.4 RAD5424
156.1 RAD2502
159.6 Bn-Scaffold000021-p502414
162.2 RAD2722
165.8 RAD516
168.2 RAD43
171.4 Na12E05
174.4 E45M49_114
177.0 RAD5655
179.3 RAD1957

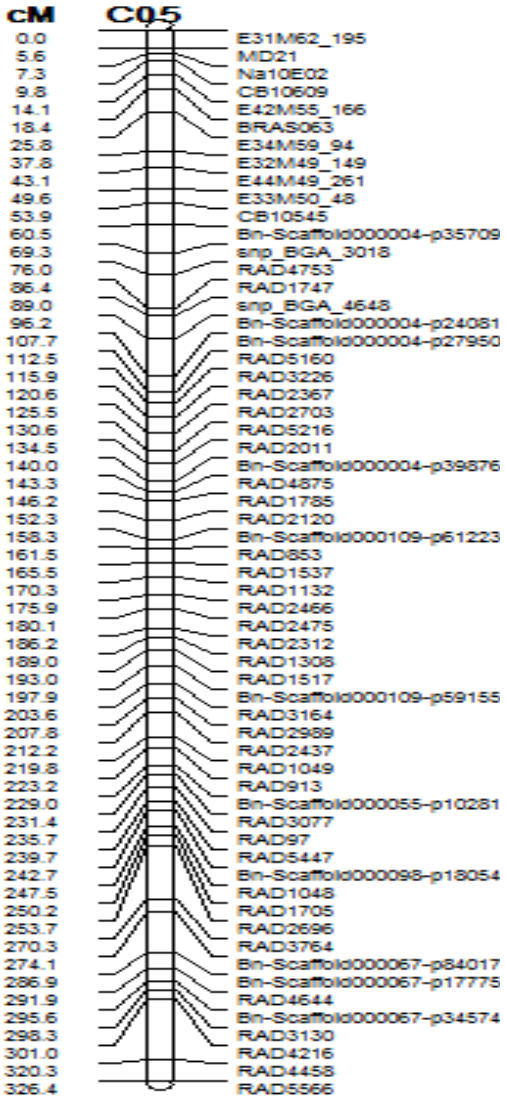
cM
C05
0.0 E31M62_195
5.6 MD21
7.3 Na10E02
9.8 CB10609
14.1 E42M55_166
18.4 BRAS063
25.8 E34M59_94
37.8 E32M49_149
43.1 E44M49_261
49.6 E33M50_48
53.9 CB10545
60.5 Bn-Scaffold000004-p35709
69.3 snp_BGA_3018
76.0 RAD4753
86.4 RAD1747
89.0 snp_BGA_4648
96.2 Bn-Scaffold000004-p24081
107.7 Bn-Scaffold000004-p27950
112.5 RAD5160
115.9 RAD3226
120.6 RAD2367
125.5 RAD2703
130.6 RAD5216
134.5 RAD2011
140.0 Bn-Scaffold000004-p39876
143.3 RAD4875
146.2 RAD1785
152.3 RAD2120
158.3 Bn-Scaffold000109-p61223
161.5 RAD853
165.5 RAD1537
170.3 RAD1132
175.9 RAD2466
180.1 RAD2475
186.2 RAD2312
189.0 RAD1308
193.0 RAD1517
197.9 Bn-Scaffold000109-p59155
203.6 RAD3164
207.8 RAD2989
212.2 RAD2437
219.8 RAD1049
223.2 RAD913
229.0 Bn-Scaffold000055-p10281
231.4 RAD3077
235.7 RAD97
239.7 RAD5447
242.7 Bn-Scaffold000098-p18054
247.5 RAD1048
250.2 RAD1705
253.7 RAD2696
270.3 RAD3764
274.1 Bn-Scaffold000067-p84017
286.9 Bn-Scaffold000067-p17775
291.9 RAD4644
295.6 Bn-Scaffold000067-p34574
298.3 RAD3130
301.0 RAD4216
320.3 RAD4458
326.4 RAD5566

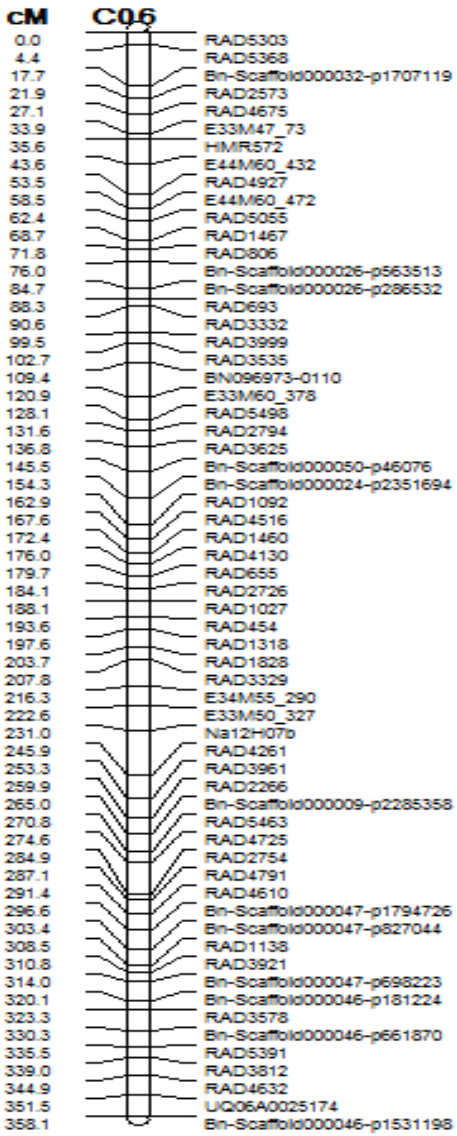
cM
C06
0.0 RAD5303
4.4 RAD5368
17.7 Bn-Scaffold000032-p1707119
21.9 RAD2573
27.1 RAD4675
33.9 E33M47_73
35.6 HMR572
43.6 E44M60_432
53.5 RAD4927
58.5 E44M60_472
62.4 RAD5055
68.7 RAD1467
71.8 RAD806
76.0 Bn-Scaffold000026-p563513
84.7 Bn-Scaffold000026-p286532
88.3 RAD693
90.6 RAD3332
99.5 RAD3999
102.7 RAD3535
109.4 BN096973-0110
120.9 E33M60_378
128.1 RAD5498
131.6 RAD2794
136.8 RAD3625
145.5 Bn-Scaffold000050-p46076
154.3 Bn-Scaffold000024-p2351694
162.9 RAD1092
167.6 RAD4516
172.4 RAD1460
176.0 RAD4130
179.7 RAD655
184.1 RAD2726
188.1 RAD1027
193.6 RAD454
197.6 RAD1318
203.7 RAD1828
207.8 RAD3329
216.3 E34M55_290
222.6 E33M50_327
231.0 Na12H07b
245.9 RAD4261
253.3 RAD3961
259.9 RAD2266
265.0 Bn-Scaffold000009-p2285358
270.8 RAD5463
274.6 RAD4725
284.9 RAD2754
287.1 RAD4791
291.4 RAD4610
296.6 Bn-Scaffold000047-p1794726
303.4 Bn-Scaffold000047-p827044
308.5 RAD1138
310.8 RAD3921
314.0 Bn-Scaffold000047-p698223
320.1 Bn-Scaffold000046-p181224
323.3 RAD3578
330.3 Bn-Scaffold000046-p661870
335.5 RAD5391
339.0 RAD3812
344.9 RAD4632
351.5 UQ06A0025174
358.1 Bn-Scaffold000046-p1531198

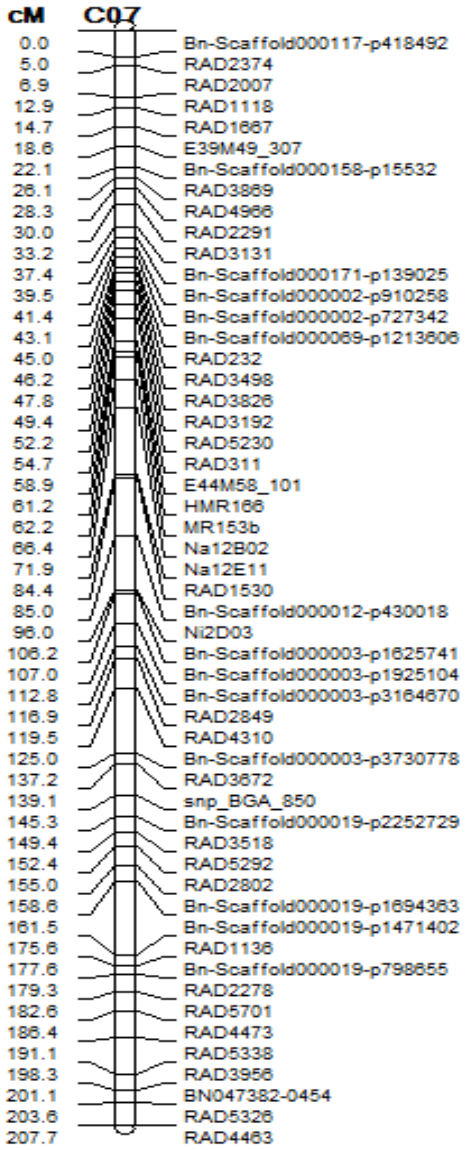
cM C07
0.0 Bn-Scaffold000117-p418492
5.0 RAD2374
6.9 RAD2007
12.9 RAD1118
14.7 RAD1667
18.6 E39M49_307
22.1 Bn-Scaffold000158-p15532
26.1 RAD3869
28.3 RAD4966
30.0 RAD2291
33.2 RAD3131
37.4 Bn-Scaffold000171-p139025
39.5 Bn-Scaffold000002-p910258
41.4 Bn-Scaffold000002-p727342
43.1 Bn-Scaffold000069-p1213606
45.0 RAD232
46.2 RAD3498
47.8 RAD3826
49.4 RAD3192
52.2 RAD5230
54.7 RAD311
58.9 E44M58_101
61.2 HMR166
62.2 MR153b
66.4 Na12B02
71.9 Na12E11
84.4 RAD1530
85.0 Bn-Scaffold000012-p430018
96.0 Ni2D03
106.2 Bn-Scaffold000003-p1625741
107.0 Bn-Scaffold000003-p1925104
112.8 Bn-Scaffold000003-p3164670
116.9 RAD2849
119.5 RAD4310
125.0 Bn-Scaffold000003-p3730778
137.2 RAD3672
139.1 snp_BGA_850
145.3 Bn-Scaffold000019-p2252729
149.4 RAD3518
152.4 RAD5292
155.0 RAD2802
158.6 Bn-Scaffold000019-p1694363
161.5 Bn-Scaffold000019-p1471402
175.6 RAD1136
177.6 Bn-Scaffold000019-p798655
179.3 RAD2278
182.6 RAD5701
186.4 RAD4473
191.1 RAD5338
198.3 RAD3956
201.1 BN047382-0454
203.6 RAD5326
207.7 RAD4463

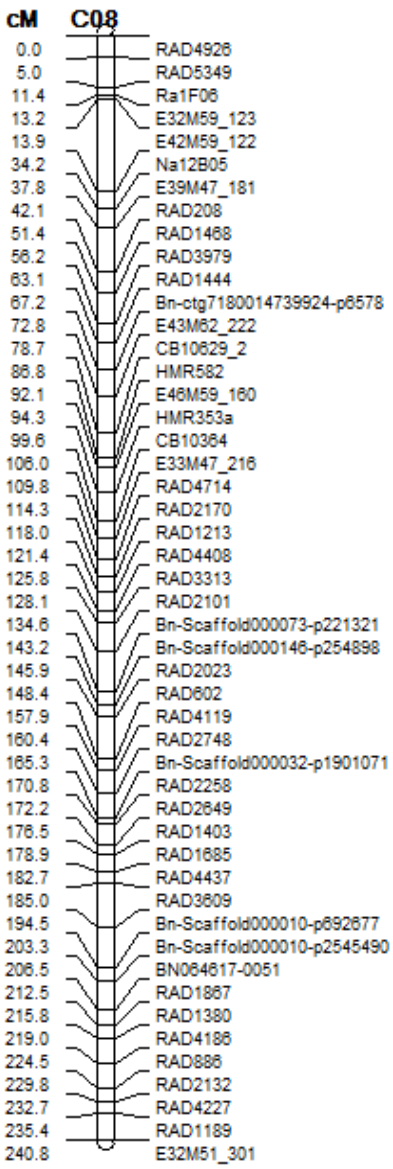
cM C08
0.0 RAD4926
5.0 RAD5349
11.4 Ra1F06
13.2 E32M59_123
13.9 E42M59_122
34.2 Na12B05
37.8 E39M47_181
42.1 RAD208
51.4 RAD1468
56.2 RAD3979
63.1 RAD1444
67.2 Bn-ctg7180014739924-p6578
72.8 E43M62_222
78.7 CB10629_2
86.8 HMR582
92.1 E46M59_160
94.3 HMR353a
99.6 CB10364
106.0 E33M47_216
109.8 RAD4714
114.3 RAD2170
118.0 RAD1213
121.4 RAD4408
125.8 RAD3313
128.1 RAD2101
134.6 Bn-Scaffold000073-p221321
143.2 Bn-Scaffold000146-p254898
145.9 RAD2023
148.4 RAD602
157.9 RAD4119
160.4 RAD2748
165.3 Bn-Scaffold000032-p1901071
170.8 RAD2258
172.2 RAD2649
176.5 RAD1403
178.9 RAD1685
182.7 RAD4437
185.0 RAD3609
194.5 Bn-Scaffold000010-p692677
203.3 Bn-Scaffold000010-p2545490
206.5 BN064617-0051
212.5 RAD1867
215.8 RAD1380
219.0 RAD4186
224.5 RAD886
229.8 RAD2132
232.7 RAD4227
235.4 RAD1189
240.8 E32M51_301

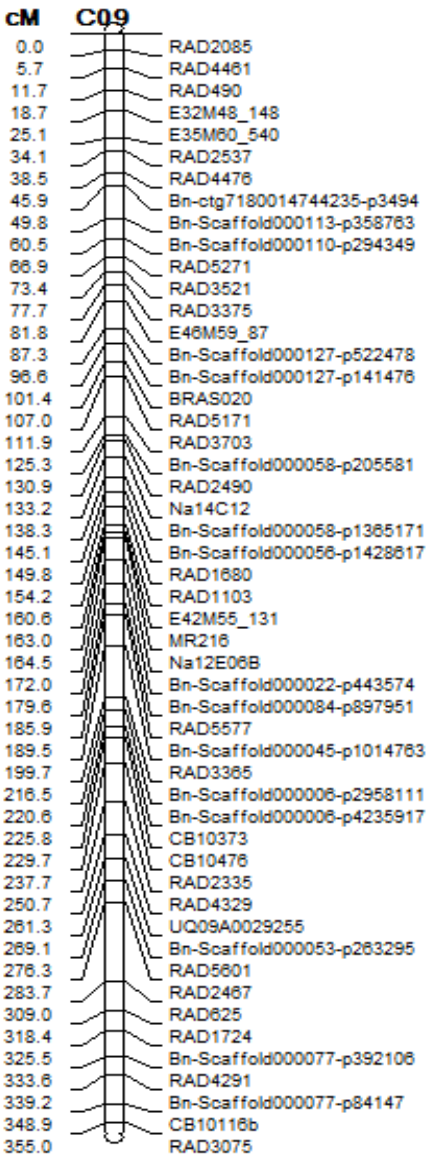
cM C09
0.0 RAD2085
5.7 RAD4461
11.7 RAD490
18.7 E32M48_148
25.1 E35M60_540
34.1 RAD2537
38.5 RAD4476
45.9 Bn-ctg7180014744235-p3494
49.8 Bn-Scaffold000113-p358763
60.5 Bn-Scaffold000110-p294349
66.9 RAD5271
73.4 RAD3521
77.7 RAD3375
81.8 E46M59_87
87.3 Bn-Scaffold000127-p522478
96.6 Bn-Scaffold000127-p141476
101.4 BRAS020
107.0 RAD5171
111.9 RAD3703
125.3 Bn-Scaffold000058-p205581
130.9 RAD2490
133.2 Na14C12
138.3 Bn-Scaffold000058-p1365171
145.1 Bn-Scaffold000056-p1428617
149.8 RAD1680
154.2 RAD1103
160.6 E42M55_131
163.0 MR216
164.5 Na12E06B
172.0 Bn-Scaffold000022-p443574
179.6 Bn-Scaffold000084-p897951
185.9 RAD5577
189.5 Bn-Scaffold000045-p1014763
199.7 RAD3365
216.5 Bn-Scaffold000006-p2958111
220.6 Bn-Scaffold000006-p4235917
225.8 CB10373
229.7 CB10476
237.7 RAD2335
250.7 RAD4329
261.3 UQ09A0029255
269.1 Bn-Scaffold000053-p263295
276.3 RAD5601
283.7 RAD2467
309.0 RAD625
318.4 RAD1724
325.5 Bn-Scaffold000077-p392106
333.6 RAD4291
339.2 Bn-Scaffold000077-p84147
348.9 CB10116b
355.0 RAD3075

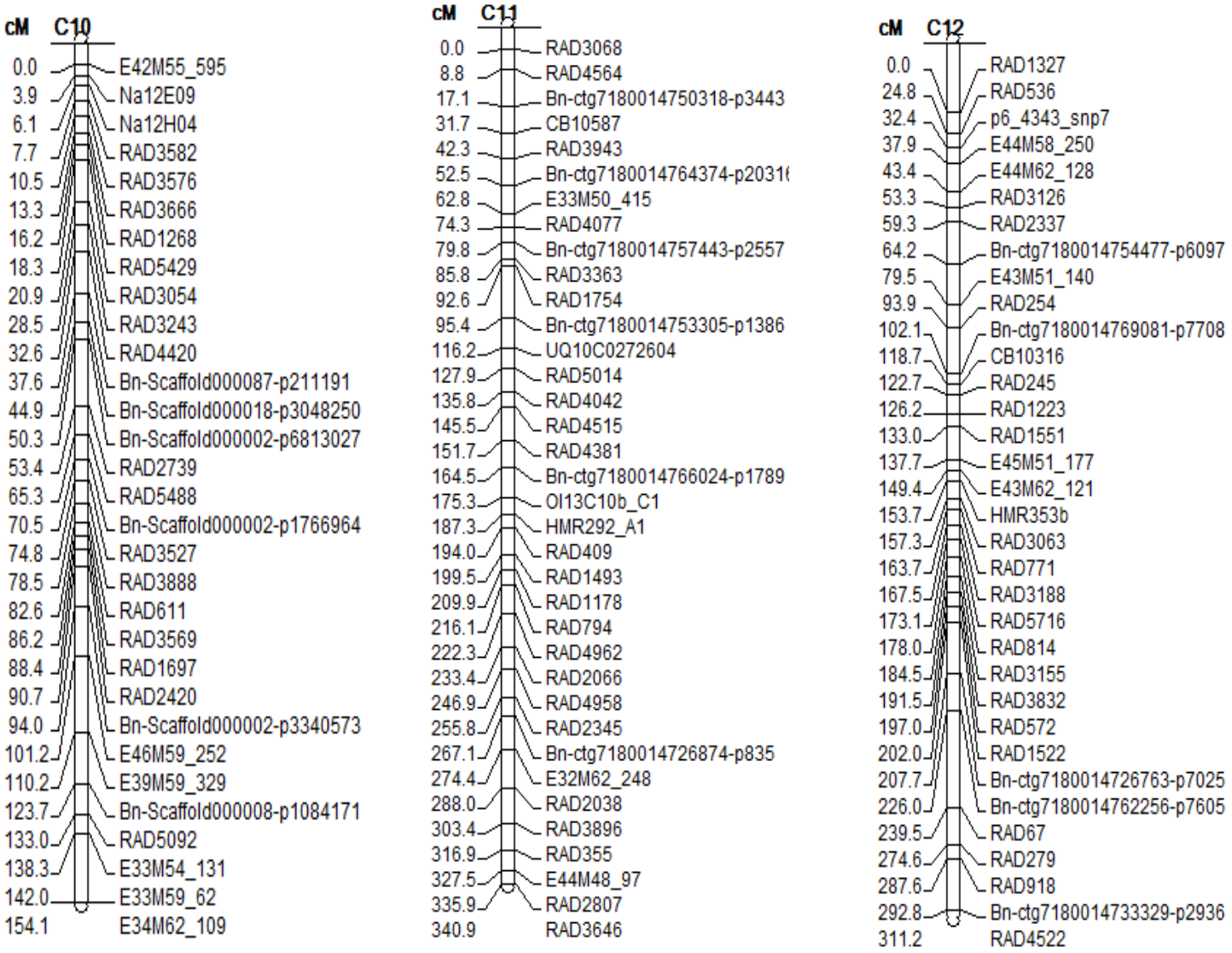
cM C10
0.0 E42M55_595
3.9 Na12E09
6.1 Na12H04
7.7 RAD3582
10.5 RAD3576
13.3 RAD3666
16.2 RAD1268
18.3 RAD5429
20.9 RAD3054
28.5 RAD3243
32.6 RAD4420
37.6 Bn-Scaffold000087-p211191
44.9 Bn-Scaffold000018-p3048250
50.3 Bn-Scaffold000002-p6813027
53.4 RAD2739
65.3 RAD5488
70.5 Bn-Scaffold000002-p1766964
74.8 RAD3527
78.5 RAD3888
82.6 RAD611
86.2 RAD3569
88.4 RAD1697
90.7 RAD2420
94.0 Bn-Scaffold000002-p3340573
101.2 E46M59_252
110.2 E39M59_329
123.7 Bn-Scaffold000008-p1084171
133.0 RAD5092
138.3 E33M54_131
142.0 E33M59_62
154.1 E34M62_109
cM C11
0.0 RAD3068
8.8 RAD4564
17.1 Bn-ctg7180014750318-p3443
31.7 CB10587
42.3 RAD3943
52.5 Bn-ctg7180014764374-p2031
62.8 E33M50_415
74.3 RAD4077
79.8 Bn-ctg7180014757443-p2557
85.8 RAD3363
92.6 RAD1754
95.4 Bn-ctg7180014753305-p1386
116.2 UQ10C0272604
127.9 RAD5014
135.8 RAD4042
145.5 RAD4515
151.7 RAD4381
164.5 Bn-ctg7180014766024-p1789
175.3 OI13C10b_C1
187.3 HMR292_A1
194.0 RAD409
199.5 RAD1493
209.9 RAD1178
216.1 RAD794
222.3 RAD4962
233.4 RAD2066
246.9 RAD4958
255.8 RAD2345
267.1 Bn-ctg7180014726874-p835
274.4 E32M62_248
288.0 RAD2038
303.4 RAD3896
316.9 RAD355
327.5 E44M48_97
335.9 RAD2807
340.9 RAD3646
cM C12
0.0 RAD1327
24.8 RAD536
32.4 p6_4343_snp7
37.9 E44M58_250
43.4 E44M62_128
53.3 RAD3126
59.3 RAD2337
64.2 Bn-ctg7180014754477-p6097
79.5 E43M51_140
93.9 RAD254
102.1 Bn-ctg7180014769081-p7708
118.7 CB10316
122.7 RAD245
126.2 RAD1223
133.0 RAD1551
137.7 E45M51_177
149.4 E43M62_121
153.7 HMR353b
157.3 RAD3063
163.7 RAD771
167.5 RAD3188
173.1 RAD5716
178.0 RAD814
184.5 RAD3155
191.5 RAD3832
197.0 RAD572
202.0 RAD1522
207.7 Bn-ctg7180014726763-p7025
226.0 Bn-ctg7180014762256-p7605
239.5 RAD67
274.6 RAD279
287.6 RAD918
292.8 Bn-ctg7180014733329-p2936
311.2 RAD4522

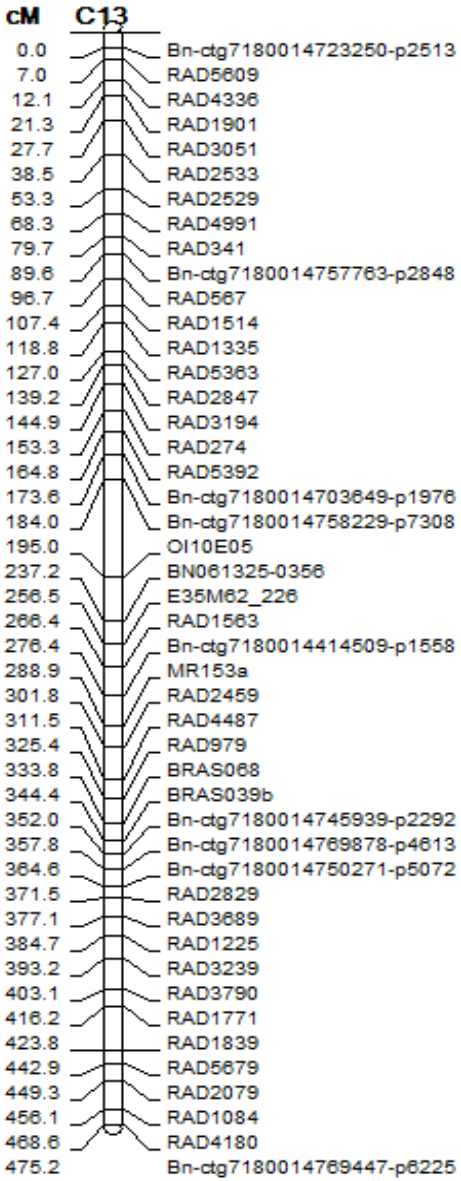
cM C13
0.0 Bn-ctg7180014723250-p2513
7.0 RAD5609
12.1 RAD4336
21.3 RAD1901
27.7 RAD3051
38.5 RAD2533
53.3 RAD2529
68.3 RAD4991
79.7 RAD341
89.6 Bn-ctg7180014757763-p2848
96.7 RAD567
107.4 RAD1514
118.8 RAD1335
127.0 RAD5363
139.2 RAD2847
144.9 RAD3194
153.3 RAD274
164.8 RAD5392
173.6 Bn-ctg7180014703649-p1976
184.0 Bn-ctg7180014758229-p7308
195.0 OI10E05
237.2 BN061325-0356
256.5 E35M62_226
266.4 RAD1563
276.4 Bn-ctg7180014414509-p1558
288.9 MR153a
301.8 RAD2459
311.5 RAD4487
325.4 RAD979
333.8 BRAS068
344.4 BRAS039b
352.0 Bn-ctg7180014745939-p2292
357.8 Bn-ctg7180014769878-p4613
364.6 Bn-ctg7180014750271-p5072
371.5 RAD2829
377.1 RAD3689
384.7 RAD1225
393.2 RAD3239
403.1 RAD3790
416.2 RAD1771
423.8 RAD1839
442.9 RAD5679
449.3 RAD2079
456.1 RAD1084
468.6 RAD4180
475.2 Bn-ctg7180014769447-p6225

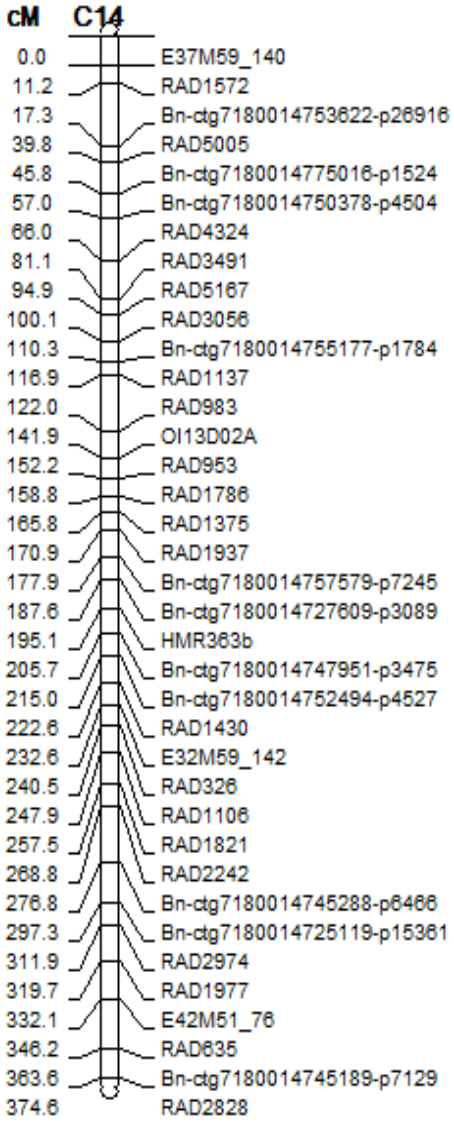
cM C14
0.0 E37M59_140
11.2 RAD1572
17.3 Bn-ctg7180014753622-p26916
39.8 RAD5005
45.8 Bn-ctg7180014775016-p1524
57.0 Bn-ctg7180014750378-p4504
66.0 RAD4324
81.1 RAD3491
94.9 RAD5167
100.1 RAD3056
110.3 Bn-ctg7180014755177-p1784
116.9 RAD1137
122.0 RAD983
141.9 OI13D02A
152.2 RAD953
158.8 RAD1786
165.8 RAD1375
170.9 RAD1937
177.9 Bn-ctg7180014757579-p7245
187.6 Bn-ctg7180014727609-p3089
195.1 HMR363b
205.7 Bn-ctg7180014747951-p3475
215.0 Bn-ctg7180014752494-p4527
222.6 RAD1430
232.6 E32M59_142
240.5 RAD326
247.9 RAD1106
257.5 RAD1821
268.8 RAD2242
276.8 Bn-ctg7180014745288-p6466
297.3 Bn-ctg7180014725119-p15361
311.9 RAD2974
319.7 RAD1977
332.1 E42M51_76
346.2 RAD635
363.6 Bn-ctg7180014745189-p7129
374.6 RAD2828

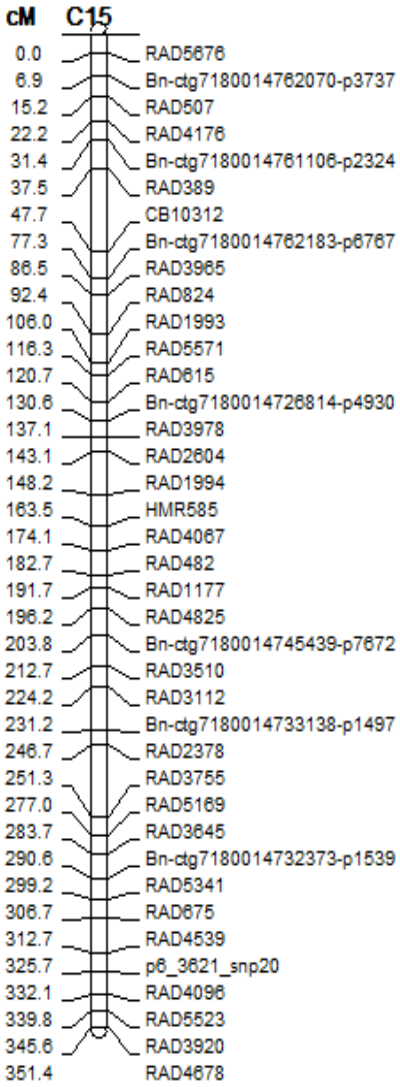
cM C15
0.0 RAD5676
6.9 Bn-ctg7180014762070-p3737
15.2 RAD507
22.2 RAD4176
31.4 Bn-ctg7180014761106-p2324
37.5 RAD389
47.7 CB10312
77.3 Bn-ctg7180014762183-p6767
86.5 RAD3965
92.4 RAD824
106.0 RAD1993
116.3 RAD5571
120.7 RAD615
130.6 Bn-ctg7180014726814-p4930
137.1 RAD3978
143.1 RAD2604
148.2 RAD1994
163.5 HMR585
174.1 RAD4067
182.7 RAD482
191.7 RAD1177
196.2 RAD4825
203.8 Bn-ctg7180014745439-p7672
212.7 RAD3510
224.2 RAD3112
231.2 Bn-ctg7180014733138-p1497
246.7 RAD2378
251.3 RAD3755
277.0 RAD5169
283.7 RAD3645
290.6 Bn-ctg7180014732373-p1539
299.2 RAD5341
306.7 RAD675
312.7 RAD4539
325.7 p6_3621_snp20
332.1 RAD4096
339.8 RAD5523
345.6 RAD3920
351.4 RAD4678

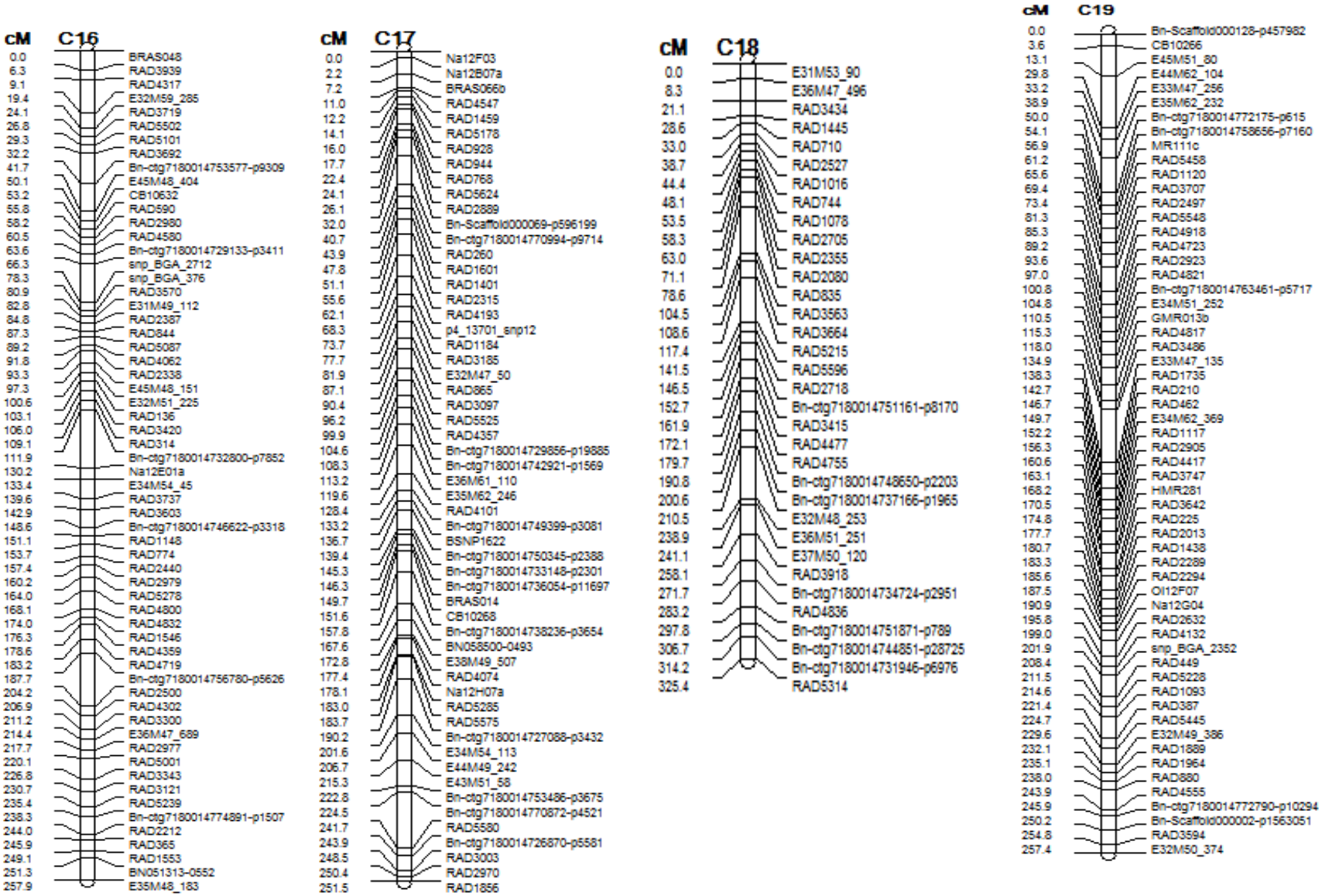
cM C16
0.0 BRAS048
6.3 RAD3939
9.1 RAD4317
19.4 E32M59_285
24.1 RAD3719
26.8 RAD5502
29.3 RAD5101
32.2 RAD3692
41.7 Bn-ctg7180014753577-p9309
50.1 E45M48_404
53.2 CB10632
55.8 RAD590
58.2 RAD2980
60.5 RAD4580
63.6 Bn-ctg7180014729133-p3411
66.3 snp_BGA_2712
78.3 snp_BGA_376
80.9 RAD3570
82.8 E31M49_112
84.8 RAD2387
87.3 RAD844
89.2 RAD5087
91.8 RAD4062
93.3 RAD2338
97.3 E45M48_151
100.6 E32M51_225
103.1 RAD136
106.0 RAD3420
109.1 RAD314
111.9 Bn-ctg7180014732800-p7852
130.2 Na12E01a
133.4 E34M54_45
139.6 RAD3737
142.9 RAD3603
148.6 Bn-ctg7180014746622-p3318
151.1 RAD1148
153.7 RAD774
157.4 RAD2440
160.2 RAD2979
164.0 RAD5278
168.1 RAD4800
174.0 RAD4832
176.3 RAD1546
178.6 RAD4359
183.2 RAD4719
187.7 Bn-ctg7180014756780-p5626
204.2 RAD2500
206.9 RAD4302
211.2 RAD3300
214.4 E36M47_689
217.7 RAD2977
220.1 RAD5001
226.8 RAD3343
230.7 RAD3121
235.4 RAD5239
238.3 Bn-ctg7180014774891-p1507
244.0 RAD2212
245.9 RAD365
249.1 RAD1553
251.3 BN051313-0552
257.9 E35M48_183
cM C17
0.0 Na12F03
2.2 Na12B07a
7.2 BRAS066b
11.0 RAD4547
12.2 RAD1459
14.1 RAD5178
16.0 RAD928
17.7 RAD944
22.4 RAD768
24.1 RAD5624
26.1 RAD2889
32.0 Bn-Scaffold000069-p596199
40.7 Bn-ctg7180014770994-p9714
43.9 RAD260
47.8 RAD1601
51.1 RAD1401
55.6 RAD2315
62.1 RAD4193
68.3 p4_13701_snp12
73.7 RAD1184
77.7 RAD3185
81.9 E32M47_50
87.1 RAD865
90.4 RAD3097
96.2 RAD5525
99.9 RAD4357
104.6 Bn-ctg7180014729856-p19885
108.3 Bn-ctg7180014742921-p1569
113.2 E36M61_110
119.6 E35M62_246
128.4 RAD4101
133.2 Bn-ctg7180014749399-p3081
136.7 BSNP1622
139.4 Bn-ctg7180014750345-p2388
145.3 Bn-ctg7180014733148-p2301
146.3 Bn-ctg7180014736054-p11697
149.7 BRAS014
151.6 CB10268
157.8 Bn-ctg7180014738236-p3654
167.6 BN058500-0493
172.8 E38M49_507
177.4 RAD4074
178.1 Na12H07a
183.0 RAD5285
183.7 RAD5575
190.2 Bn-ctg7180014727088-p3432
201.6 E34M54_113
206.7 E44M49_242
215.3 E43M51_58
222.8 Bn-ctg7180014753486-p3675
224.5 Bn-ctg7180014770872-p4521
241.7 RAD5580
243.9 Bn-ctg7180014726870-p5581
248.5 RAD3003
250.4 RAD2970
251.5 RAD1856
cM C18
0.0 E31M53_90
8.3 E36M47_496
21.1 RAD3434
28.6 RAD1445
33.0 RAD710
38.7 RAD2527
44.4 RAD1016
48.1 RAD744
53.5 RAD1078
58.3 RAD2705
63.0 RAD2355
71.1 RAD2080
78.6 RAD835
104.5 RAD3563
108.6 RAD3664
117.4 RAD5215
141.5 RAD5596
146.5 RAD2718
152.7 Bn-ctg7180014751161-p8170
161.9 RAD3415
172.1 RAD4477
179.7 RAD4755
190.8 Bn-ctg7180014748650-p2203
200.6 Bn-ctg7180014737166-p1965
210.5 E32M48_253
238.9 E36M51_251
241.1 E37M50_120
258.1 RAD3918
271.7 Bn-ctg7180014734724-p2951
283.2 RAD4836
297.8 Bn-ctg7180014751871-p789
306.7 Bn-ctg7180014744851-p28725
314.2 Bn-ctg7180014731946-p6976
325.4 RAD5314
cM C19
0.0 Bn-Scaffold000128-p457982
3.6 CB10266
13.1 E45M51_80
29.8 E44M62_104
33.2 E33M47_256
38.9 E35M62_232
50.0 Bn-ctg7180014772175-p615
54.1 Bn-ctg7180014758656-p7160
56.9 MR111c
61.2 RAD5458
65.6 RAD1120
69.4 RAD3707
73.4 RAD2497
81.3 RAD5548
85.3 RAD4918
89.2 RAD4723
93.6 RAD2923
97.0 RAD4821
100.8 Bn-ctg7180014763461-p5717
104.8 E34M51_252
110.5 GMR013b
115.3 RAD4817
118.0 RAD3486
134.9 E33M47_135
138.3 RAD1735
142.7 RAD210
146.7 RAD462
149.7 E34M62_369
152.2 RAD1117
156.3 RAD2905
160.6 RAD4417
163.1 RAD3747
168.2 HMR281
170.5 RAD3642
174.8 RAD225
177.7 RAD2013
180.7 RAD1438
183.3 RAD2289
185.6 RAD2294
187.5 OI12F07
190.9 Na12G04
195.8 RAD2632
199.0 RAD4132
201.9 snp_BGA_2352
208.4 RAD449
211.5 RAD5228
214.6 RAD1093
221.4 RAD387
224.7 RAD5445
229.6 E32M49_386
232.1 RAD1889
235.1 RAD1964
238.0 RAD880
243.9 RAD4555
245.9 Bn-ctg7180014772790-p10294
250.2 Bn-Scaffold000002-p1563051
254.8 RAD3594
257.4 E32M50_374

Erklärung

„Ich erkläre: Ich habe die vorgelegte Dissertation selbständig und ohne unerlaubte fremde Hilfe und nur mit den Hilfen angefertigt, die ich in der Dissertation angegeben habe. Alle Textstellen, die wörtlich oder sinngemäß aus veröffentlichten Schriften entnommen sind, und alle Angaben, die auf mündlichen Auskünften beruhen, sind als solche kenntlich gemacht. Bei den von mir durchgeführten und in der Dissertation erwähnten Untersuchungen habe ich die Grundsätze guter wissenschaftlicher Praxis, wie sie in der „Satzung der Justus-Liebig-Universität Gießen zur Sicherung guter wissenschaftlicher Praxis“ niedergelegt sind, eingehalten.“

Gießen, 10.11.2014 **Aysha Kiran**

ACKNOWLEDGMENTS

All praise and thanks for "**Almighty Allah**" Lord of splendid throne, Holder of sovereignty, Rule of the day of repayment, The merciful who split the seeds and kernel, who bring living from dead and dead from living, who has placed the stars to guide us through darkness on land and sea, who bestowed upon me the health, thoughts, sources, talented teachers and nice colleagues.

I also offer my humblest thanks to the glittering star of knowledge and guidance, the **Holy Prophet Muhammad (PBUH)** from the deepest core of my heart who leads our lives to success and destiny and who is forever a model of guidance and knowledge for humanity.

Being an ordinary human, initially this task seems uphill, turned downhill but with the encouragement, keen interest, nice behavior, admirable guidance, his valuable suggestions to improve the manuscript and constant help of my supervisor **Prof. Dr. Dr. h.c. Wolfgang Friedt** who took valuable time for me from his busiest time.

It is great honor for me to record the sincerest gratitude to **Prof. Dr. Volker Wissemann** Acting Director, Institute of Systematic Botany, Justus Liebig University, Giessen, Germany for his valuable comments and advices as co-supervisor.

I would like to offer my cordial thanks to **Prof. Dr. Rod Snowdon** for his dynamic supervision, valid counseling and valuable suggestions during conduct of research. It was because of his inspiring guidance and sympathetic attitude during the entire study that I could prepare this manuscript.

I wish to express my sincere thanks to **Dr. Christian Obermeier** and **Dr. Birgit Saman** for their constructive thought and help in bioinformatics. I am very thankful to **Dr. Benjamin, Dr. Wubishet, Stavros, Birgit, Annete, Ulrika, Swetlana, Nelly, Lidia** and **Liane** for providing me required research facilities and guidance, and also to all colleagues of Department of Plant Breeding for their extreme cooperation and unbelievable help during the whole research work.

My heartful appreciation is due to my husband **Dr. Abdul Wakeel** for his encouragements and understanding, and to my loving sons **Muhammad Anas** & **Zayed Ahmad** for their patience, sacrifice, and prayers. I express my deepest gratitude to my **parents**, **sisters, sister in laws** and **brothers** who always encouraged and prayed for my success.

My heartiest regards and thanks to ever-affectionate friends **QumQum Noshad, Tayyaba Shaheen, Iram Farooq, Mahwish, Asma, Ammara, Shazia, Kiran, Sabiha, Sidra, Razia, Sumera, Shamaila, Hannan, Madiha, Douniya** and **Soumaiyas**. Their good wishes are always a source of inspiration for me.

Special thanks should also be extended to all Muslim and Pakistani community for their possible assistance and nice company during my stay in Germany

This work is funded by the Deutsche Forschungsgemeinschaft (DFG) as part of the tri-national ERANET Plant Genomics project "ASSYST: Associative expression and systems analysis of complex traits in oilseed rape/canola."

I am also thankful to higher education commission (HEC) Pakistan for their support.

AYSHA KIRAN

Der Lebenslauf wurde aus der elektronischen Version der Arbeit entfernt.

The curriculum vitae was removed from the electronic version of the paper.

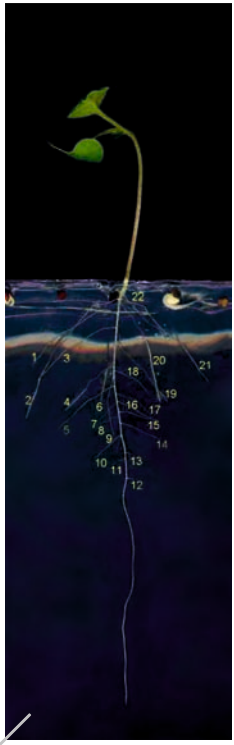

édition scientifique
VVB LAUFERSWEILER VERLAG

VVB LAUFERSWEILER VERLAG
STAUFENBERGRING 15
D-35396 GIESSEN

Tel: 0641-5599888 Fax: -5599890
redaktion@doktorverlag.de
www.doktorverlag.de

ISBN: 978-3-8359-6257-6